

# Therapeutic systems for Insulin-like growth factor-I

Dissertation zur Erlangung des naturwissenschaftlichen Doktorgrades der  
Julius-Maximilians-Universität Würzburg

vorgelegt von

Isabel Schultz  
aus Dahn

Würzburg 2015





Eingereicht bei der Fakultät für Chemie und Pharmazie am

\_\_\_\_\_

Gutachter der schriftlichen Arbeit

1. Gutachter: \_\_\_\_\_

2. Gutachter: \_\_\_\_\_

Prüfer des öffentlichen Promotionskolloquiums

1. Prüfer: \_\_\_\_\_

2. Prüfer: \_\_\_\_\_

3. Prüfer: \_\_\_\_\_

Datum des öffentlichen Promotionskolloquiums

\_\_\_\_\_

Doktorurkunde ausgehändigt am



**TABLE OF CONTENTS**

SUMMARY ..... 1

ZUSAMMEMFASSUNG ..... 5

CHAPTER I ..... 9

*DRUG DELIVERY OF INSULIN-LIKE GROWTH FACTOR I*

CHAPTER II ..... 45

*INSULIN-LIKE GROWTH FACTOR-I AEROSOL FORMULATIONS FOR PULMONARY DELIVERY*

CHAPTER III ..... 73

*PULMONARY INSULIN-LIKE GROWTH FACTOR I DELIVERY FROM TREHALOSE AND SILK-FIBROIN MICROPARTICLES*

CHAPTER IV ..... 113

*EXPRESSION OF IGF-I MUTANTS*

CONCLUSION AND OUTLOOK..... 147

DOCUMENTATION OF AUTHORSHIP ..... 159

CURRICULUM VITAE..... 163

ACKNOWLEDGMENTS ..... 167









## SUMMARY

Insulin-like growth factor I (IGF-I) is a polypeptide with a molecular weight of 7.649 kDa and an anabolic potential. Thereby, IGF-I has a promising therapeutic value e.g. in muscle wasting diseases such as sarcopenia. IGF-I is mainly secreted by the liver in response to growth hormone (GH) stimulation and is rather ubiquitously found within all tissues. The effects of IGF-I are mediated by its respective IGF-I transmembrane tyrosine kinase receptor triggering the stimulation of protein synthesis, glucose uptake and the regulation of cell growth. The actions of IGF-I are modulated by six IGF binding proteins binding and transporting IGF-I in a binary or ternary complex to tissues and receptors and modulating the binding of IGF-I to its receptor. The nature of the formed complexes impacts IGF-I's half-life, modulating the half-life between 10 minutes (free IGF-I) to 12 - 15 hours when presented in a ternary complex with IGF binding protein 3 and an acid labile subunit (ALS). Therefore, sustained drug delivery systems of free IGF-I are superficially seen as interesting for the development of controlled release profiles, as the rate of absorption is apparently and easily set slower by simple formulation as compared to the rapid rate of elimination. Thereby, one would conclude, the formulation scientist can rapidly develop systems for which the pharmacokinetics of IGF-I are dominated by the formulation release kinetics. However, the *in vivo* situation is more complex and as mentioned (*vide supra*), the half-life may easily be prolonged up to hours providing proper IGF-I complexation takes place upon systemic uptake. These and other aspects are reviewed in **Chapter I**, within which we introduce IGF-I as a promising therapeutic agent detailing its structure and involved receptors along with the resulting signaling pathways. We summarize the control of IGF-I pharmacokinetics in nature within the context of its complex system of 6 binding proteins to control half-life and tissue distribution. Furthermore, we describe IGF-I variants with modulated properties *in vivo* and originated from alternative splicing. These insights were translated into sophisticated IGF-I delivery systems for therapeutic use. Aside from safety aspects, the challenges and requirements of an effective IGF-I therapy are discussed. Localized and systemic IGF-I delivery strategies, different routes of administration as well as liquid and solid IGF-I formulations are reviewed. Effective targeting of IGF-I by protein decoration is outlined and consequently this chapter provides an interesting guidance for successful IGF-I-delivery. In **Chapter II**, we firstly outline the stability of IGF-I in liquid formulations with the intention to

## SUMMARY

---

deliver the biologic through the lung and the impact of buffer type, sodium chloride concentration and pH value on IGF-I stability is presented. IGF-I integrity was preserved in histidine buffer over 4 months at room temperature, but methionine 59 oxidation (Met(o)) along with reducible dimer and trimer formation was observed in an acidic environment (pH 4.5) and using acetate buffer. Strong aggregation resulted in a complete loss of IGF-I bioactivity, whereas the potency was partly maintained in samples showing a slight aggregation and complete IGF-I oxidation. Atomization by air-jet or vibrating-mesh nebulizers yielded in limited Met(o) formation and no aggregation. The results of IGF-I nebulization experiments regarding aerosol output rate, mass median aerodynamic diameter and fine particle fraction were comparable with 0.9% sodium chloride reference, approving the applicability of liquid IGF-I formulations for pulmonary delivery. In **Chapter III** we escalated the development to solid delivery systems designed for alveolar landing upon inhalation and by deploying trehalose and the newly introduced for pulmonary application silk-fibroin as carriers. Microparticles were produced using nano spray drying following analyses including IGF-I integrity, IGF-I release profiles and aerodynamic properties. *In vitro* transport kinetics of IGF-I across pulmonary Calu-3 epithelia were suggesting similar permeability as compared to IGF-I's cognate protein, insulin that has already been successfully administered pulmonary in clinical settings. These *in vivo* results were translated to an *ex vivo* human lung lobe model. This work showed the feasibility of pulmonary IGF-I delivery and the advantageous diversification of excipients for pulmonary formulations using silk-fibroin. **Chapter IV** focuses on an innovative strategy for safe and controllable IGF-I delivery. In that chapter we escalated the development to novel IGF-I analogues. The intention was to provide a versatile biologic into which galenical properties can be engineered through chemical synthesis, e.g. by site directed coupling of polymers to IGF-I. For this purpose we genetically engineered two IGF-I variants containing an unnatural amino acid at two positions, respectively, thereby integrating alkyne functions into the primary sequence of the protein. These allowed linking IGF-I with other molecules in a site specific manner, i.e. via a copper catalyzed azide-alkyne Huisgen cycloaddition (click reaction). In this chapter we mainly introduce the two IGF-I variants, detail the delivery concept and describe the optimization of the expression conditions of the IGF-I variants.

In conclusion, we span from simple liquid formulations for aerolization through solid systems for tailored for maximal alveolar landing to novel engineered IGF-I analogues. Thereby, three

strategies for advanced IGF-I delivery were addressed and opportunities and limitations of each were outlined. Evidence was provided that sufficiently stable and easy to manufacture formulations can be developed as typically required for first in man studies. Interestingly, solid systems – typically introduced in later stages of pharmaceutical development – were quite promising. By use of silk-fibroin as a new IGF-I carrier for pulmonary administration, a new application was established for this excipient. The demonstrated success using the *ex vivo* human lung lobe model provided substantial confidence that pulmonary IGF-I delivery is possible in man. Finally, this work describes the expression of two IGF-I variants containing two unnatural amino acids to implement an innovative strategy for IGF-I delivery. This genetic engineering approach was providing the fundament for novel IGF-I analogues. Ideally, the biologic is structurally modified by covalently linked moieties for the control of pharmacokinetics or for targeted delivery, e.g. into sarcopenic muscles. One future scenario is discussed in the ‘conclusion and outlook’ section for which IGF-I is tagged to a protease sensitive linker peptide and this linker peptide in return is coupled to a polyethylenglykole (PEG) polymer (required to prolong the half-life). Some proteases may serve as proxy for sarcopenia such that protease upregulation in compromised muscle tissues drives cleavage of IGF-I from the PEG. Thereby, IGF-I is released at the seat of the disease while systemic side effects are minimized.



## ZUSAMMEMFASSUNG

Insulin-like growth factor I (IGF-I) ist ein 7.6 kDa großes Polypeptid, das eine anabole Wirkung besitzt und dadurch ein vielversprechendes Therapeutikum in Muskelerkrankungen wie z.B. Sarkopenie darstellt. IGF-I wird hauptsächlich von der Leber gebildet und infolge der Stimulation des Wachstumshormons Somatotropin sezerniert. In fast jedem Gewebe des Körpers kommt IGF-I vor. Die Wirkungen von IGF-I werden über eigene Rezeptoren, die an die Zellmembran gebunden sind, die Rezeptor-Tyrosinkinasen, ausgeführt. Zu den Wirkungen gehören unter anderem die Stimulation der Proteinsynthese, die Aufnahme von Glucose in die Zellen und die Regulierung des Zellwachstums. Die Effekte von IGF-I werden von 6 IGF-Bindungsproteinen (IGFBP 1-6) gesteuert, indem IGF-I in einem binären oder ternären Komplex zu den Geweben transportiert oder auch die Bindung von IGF-I an den Rezeptor verhindert werden kann. Die sich bildenden Komplexe haben auch einen Einfluss auf die Halbwertszeit (HWZ) von IGF-I, da für ungebundenes IGF-I eine HWZ von ca. 10 Minuten festgestellt werden konnte, aber IGF-I, gebunden in einem ternären Komplex mit dem Bindungsprotein 3 und der säurelabilen Untereinheit (ALS) eine erhöhte HWZ von 12 – 15 Stunden aufweist. Deswegen sind „sustained drug delivery“ Systeme von ungebundenem IGF-I auf den ersten Blick interessant für die Entwicklung von kontrollierten Freisetzungprofilen, da die Absorptionsgeschwindigkeit offensichtlich und problemlos durch triviale Formulierung verlangsamt werden kann im Vergleich zu der schnellen Eliminationsgeschwindigkeit. Deshalb könnte man daraus schließen, dass ein Formulierungsexperte recht schnell Systeme entwickeln kann, in denen die Freisetzungskinetik der Formulierung über die pharmakokinetischen Eigenschaften von IGF-I dominiert. Jedoch ist die *in vivo* Situation wesentlich komplexer und wie oben bereits erwähnt, könnte die Halbwertszeit problemlos bis zu mehreren Stunden verlängert werden, sofern geeignete Komplexbildung von IGF-I nach systemischer Aufnahme erfolgt. Diese und weitere Aspekte werden in **Kapitel I** beschrieben. Außerdem stellen wir IGF-I als wertvolles Therapeutikum vor, beschreiben dessen Struktur, die beteiligten Rezeptoren und die daraus resultierenden Signalwege. Wir fassen die Kontrolle der Pharmakokinetik von IGF-I in der Natur zusammen, im Rahmen von einem komplexen System aus 6 Bindungsproteinen, die die Halbwertszeit und die Gewebeverteilung steuern. Außerdem beschreiben wir IGF-I Varianten, die veränderte Eigenschaften *in vivo* aufweisen und durch alternatives Spleißen

entstanden sind. Diese Erkenntnisse werden in hochentwickelte „IGF-I delivery“ Systeme für den therapeutischen Gebrauch umgesetzt. Neben Sicherheitsaspekten werden die Herausforderungen und Anforderungen einer effektiven IGF-I Therapie diskutiert. Darüber hinaus wird über lokale und systemische „IGF-I delivery“ Strategien, verschiedene Verabreichungswege sowie flüssige und feste IGF-I Formulierungen berichtet. Ebenso wird die wirkungsvolle IGF-I Freisetzung am Zielort durch Ausschmückung des Proteins beschrieben und dementsprechend liefert dieses Kapitel eine interessante Orientierungshilfe für eine erfolgreiche IGF-I Therapie. Im **Kapitel II** untersuchen wir die Stabilität von IGF-I in flüssigen Formulierungen zur pulmonalen Anwendung bezüglich Puffersystem, Natriumchlorid Konzentration und pH Wert. Die IGF-I Integrität wurde im Histidin Puffer über 4 Monate bei Raumtemperatur aufrechterhalten. Allerdings wurde bei Verwendung eines Acetat Puffers pH 4.5, Oxidation am Methionin 59 (Met(o)) sowie die Entstehung von reduzierbaren Dimeren und Trimeren beobachtet. Starke Aggregation führte zum vollständigen Verlust der IGF-I Bioaktivität, während die Wirkung in Proben aufrechterhalten werden konnte, in denen eine geringe Aggregation, aber deutliche Oxidation festgestellt wurde. Nach der Verneblung der flüssigen IGF-I Formulierung im Histidin-Puffer pH 6.5 mit einem Druckluftvernebler und einem Schwingmembranvernebler wurde jeweils eine leichte Bildung von Met(o), aber keine Aggregatbildung ermittelt. Die Ergebnisse der IGF-I Verneblungsexperimente waren vergleichbar mit den Referenzwerten einer isotonischen Kochsalzlösung bezüglich der Abgabeleistung, dem massenbezogenen medianen aerodynamischen Durchmesser und dem Feinpartikel Anteil. Hierdurch wurde gezeigt, dass sich flüssige IGF-I Formulierungen zur pulmonalen Anwendung eignen. Im **Kapitel III** berichten wir von einer Weiterentwicklung zu festen IGF-I Formulierungen für die pulmonale Route unter Verwendung von Trehalose und Seidenfibroin als neues Trägermaterial für die pulmonale Applikation. Mikropartikel wurden durch Nanosprühtrocknung hergestellt und anschließend auf IGF-I Integrität, IGF-I Freisetzung und dem aerodynamischen Durchmesser untersucht. Die Kinetik des *in vitro* Transportes von IGF-I durch Calu-3 Lungenepithelzellen war vergleichbar zur Durchgängigkeit von Insulin, das bereits erfolgreich pulmonal verabreicht wurde. Dieser Erfolg wurde auch *ex vivo* in einem menschlichen Lungenlappen Model bestätigt. In der Arbeit wird somit gezeigt, dass IGF-I zur pulmonalen Anwendung geeignet ist und die Verwendung von Seidenfibroin eine nützliche Erweiterung zu den bisher eingesetzten Trägermaterialien darstellt. Das **Kapitel IV** konzentriert

sich auf eine innovative Strategie, um IGF-I sicher und kontrollierbar zu verabreichen. In diesem Kapitel erweitern wir die Entwicklung zu neuartigen IGF-I Varianten. Wir streben damit an ein vielseitiges Biologikum zu entwickeln, dessen Eigenschaften durch chemische Reaktionen verändert werden können wie zum Beispiel die spezifische Verknüpfung mit Polymeren. Zu diesem Zweck erzeugten wir gentechnisch zwei IGF-I Varianten, die jeweils an zwei Positionen eine unnatürliche Aminosäure aufweisen und führten dadurch Alkine Gruppen in die Primärstruktur der Proteine ein. Diese Vorgehensweise ermöglicht es nun IGF-I mit anderen Molekülen positionsspezifisch zu verbinden wie zum Beispiel durch die kupferkatalysierte Azid-Alkin-Cycloaddition (Click – Reaktion). In diesem Kapitel stellen wir hauptsächlich die zwei IGF-I Varianten vor, beschreiben ausführlich das Konzept der IGF-I Zustellung und erklären die Vorgehensweise zur Optimierung der Expressionsbedingungen der IGF-I Varianten. Abschließend lässt sich sagen, dass sich diese Arbeit über einfach flüssige Formulierungen zur Verneblung, feste Formulierung mit guten aerodynamischen Eigenschaften zur Erreichung der Alveolen und neuartig entwickelte IGF-I Varianten erstreckt. Hierzu werden drei Strategien zur modernen IGF-I Gabe thematisiert und sowohl die Möglichkeiten als auch die Grenzen der jeweiligen Therapie erörtert. Wir haben den Nachweis erbracht, dass ausreichend stabile und leicht herzustellende Formulierungen entwickelt werden können, die üblicherweise für „First-In-Man“ Studien benötigt werden. Interessanterweise stellten sich die festen Formulierungen, die eigentlich in den späteren Phasen der pharmazeutischen Entwicklung eingeführt werden, als sehr vielversprechend heraus. Durch den Einsatz von Seidenfibroin als neuen Träger zur pulmonalen Anwendung haben wir einen neuen Verwendungszweck für Seidenfibroin etabliert. Der erfolgreiche Versuch *ex vivo* am menschlichen Lungenlappen Model liefert die feste Überzeugung, dass es möglich ist, IGF-I im Menschen pulmonal anzuwenden. Letztendlich, beschreibt die Arbeit die Expression von zwei IGF-I Varianten, die zwei unnatürliche Aminosäuren aufweisen, um eine neuartige Strategie zur IGF-I Verabreichung umzusetzen. Dieser gentechnische Ansatz liefert die Grundlage für neue IGF-I Varianten. Idealerweise, wird das Biopharmazeutikum strukturell durch kovalent gebundene Reste verändert, um die pharmakokinetischen Eigenschaften zu steuern oder um zielgenaue Wirkstoffabgabe zu erreichen zum Beispiel in den sarkopenischen Muskeln. Ein Zukunftsszenarium wird im Abschnitt „Conclusion and Outlook“ diskutiert, in dem IGF-I mit einem Protease empfindlichen Linker versehen wird, der wiederum mit einem Polyethylenglykol (PEG) Polymer verknüpft ist.

## ZUSAMMEMFASSUNG

---

Der PEG Rest wird benötigt, um die Halbwertszeit von IGF-I zu erhöhen. Einige Proteasen könnten als Stellvertreter für Sarkopenie dienen, so dass die Hochregulierung der Proteasen in gefährdeten Muskelgeweben zur Spaltung von IGF-I und dem PEG Rest führt. Dadurch wird IGF-I am Ursprung der Erkrankungen freigesetzt, während die systemischen Nebenwirkungen weitgehend vermindert sind.



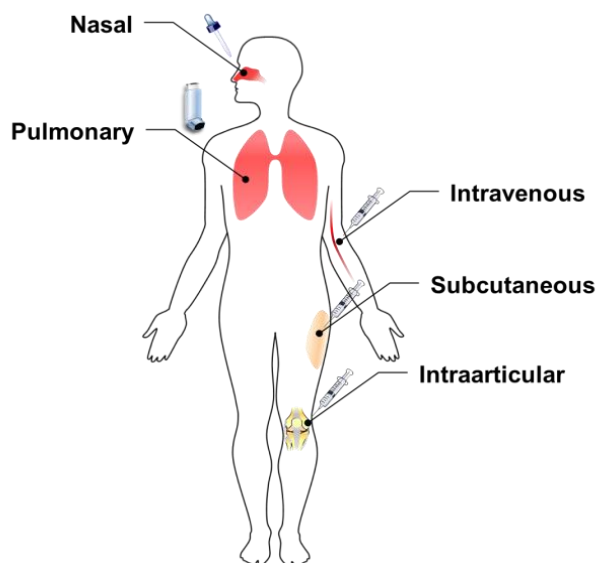
# CHAPTER I

## DRUG DELIVERY OF INSULIN-LIKE GROWTH FACTOR I

Isabel Schultz, Joel Wurzel, Lorenz Meinel\*

Institute for Pharmacy and Food Chemistry, University of Wuerzburg,

Am Hubland, DE-97074 Wuerzburg, Germany



*European Journal of Pharmaceutics and Biopharmaceutics*, 2015, in press,  
*doi:10.1016/j.ejpb.2015.04.026.*

### ABSTRACT

This review starts off outlining the control of Insulin-like growth factor I (IGF-I) kinetics in Nature and by virtue of a complex system of 6 binding proteins controlling half-life and tissue distribution of this strong anabolic peptide. In addition, alternative splicing is known to result in IGF-I variants with modulated properties *in vivo* and this insight is currently translated into advanced IGF-I variants for therapeutic use. Insights into these natural processes resulted in biomimetic strategies with the ultimate goal to control pharmacokinetics and have recently propelled new developments leading to optimized pharmaceutical performance of this protein *in vivo*. Aside from parenteral administration routes, IGF-I was successfully delivered across various epithelial barriers from liquid as well as from solid pharmaceutical forms opening novel and more convenient delivery modalities. IGF-I decoration yielded effective targeting upon systemic administration expanding the options for optimally deploying the growth factor for therapy. This review summarizes the exciting biotechnological and pharmaceutical progress seen for IGF-I delivery in recent years and critically discusses outcome in light of translational application for future IGF-I therapeutics.

---

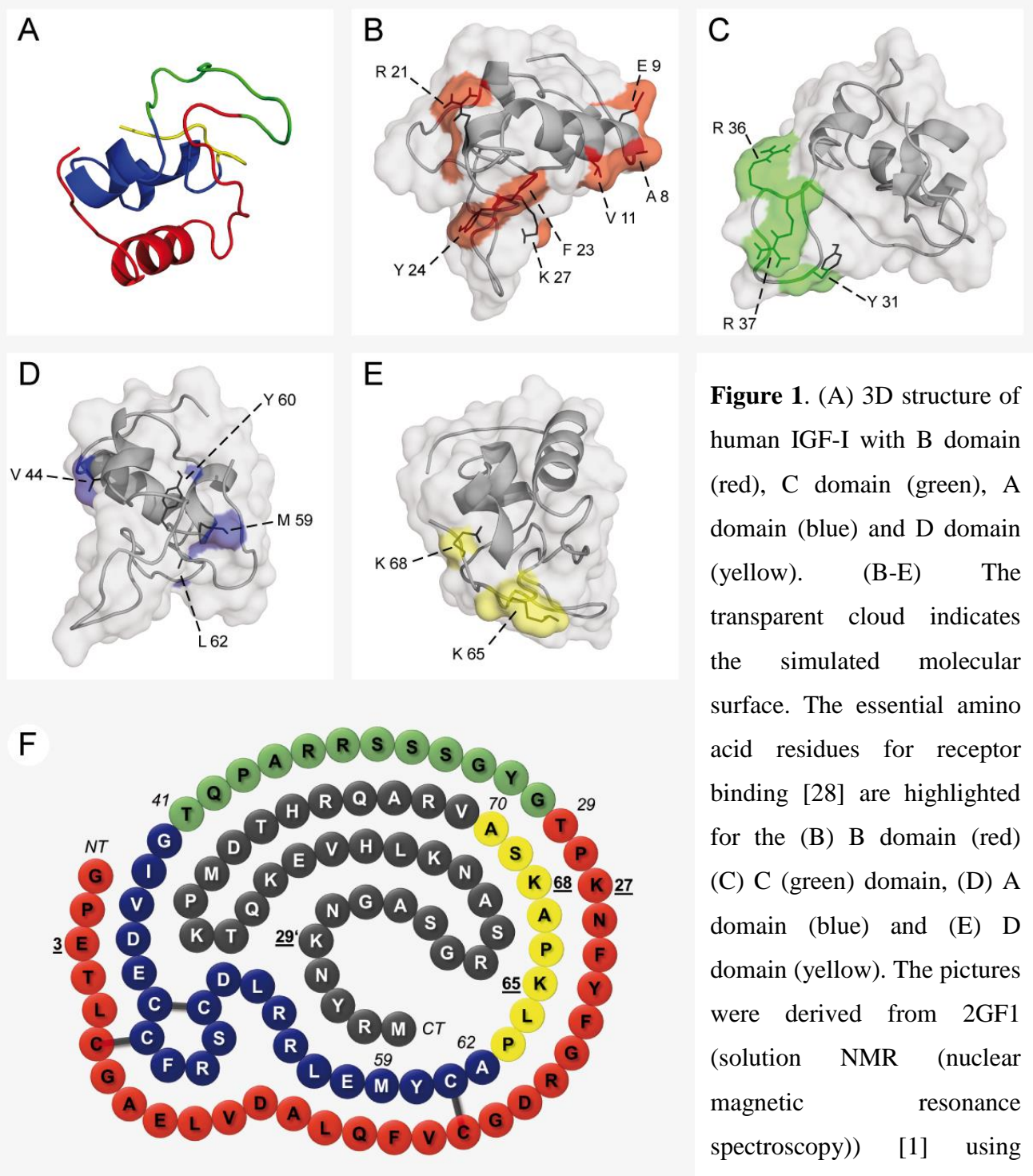
## INTRODUCTION

Insulin-like growth factor-I (IGF-I) is a polypeptide with a molecular weight of 7.649 kDa playing a key role in the regulation of cellular growth and metabolism. The growth factor was discovered in 1957 [2] and renamed as Somatomedin in 1972 [3]. Complete structural characterization was in 1978 [4]. IGF-I is a 70 amino acid peptide in a single chain with three disulfide bonds and classified into four domains (A, B, C, D; **Figure 1**). The “insulin-like” characteristics of IGF-I are structurally reflected by the homology of its A and B chains with those of Insulin [5]. In spite of these structural similarities, Insulin binds the Insulin receptor with 100 fold better affinity as compared to IGF-I [6-8]. The specific IGF-I transmembrane tyrosine kinase receptor is composed of two extracellular  $\alpha$  – subunits (~ 130 kDa), containing a cysteine-rich domain for ligand specificity with two transmembrane  $\beta$ -subunits (~ 95 kDa) [9, 10]. IGF-I binding to its receptor activates PI3K (phosphatidylinositol-3kinase) and MAP (mitogen-activated protein) kinase pathway [6]. IGF-I receptors are found nearly ubiquitously including cells of the immune system (T-cells, human monocytes and B-cells), musculoskeletal tissues (chondrocytes, osteoblasts, osteocytes, osteoclasts, myocytes) the reproductive system (e.g. uterus, ovaria, placenta, testis), endocrine cells (thyroid cells and adrenal cells) as well as in neural cells, fibroblasts, endothelial cells, hepatocytes, or keratinocytes [11, 12]. The extent to which IGF-I receptors are found in tissues has been correlated with systemic IGF-I levels [13]. Approximately 80% of the IGF-I in blood are produced in the liver (endocrine) and 20% by local production (autocrine/paracrine) both of which resulting in quite distinguishable pharmacological roles [5, 14]. IGF-I activity is further modulated by six IGF--binding proteins (IGFBP-1-6) modulating the pharmacokinetics including tissue distribution, transport across biological barriers, and IGF-I pharmacodynamics [15]. IGF-I stimulates the cellular activity increasing glucose uptake, oxidation and incorporation into glycogen, as well as protein synthesis [12, 16]. It is for these anabolic activities that IGF-I has been suggested for the treatment of atrophic musculoskeletal diseases, including sarcopenia, cachexia, osteoporosis, growth failure, treatment of cartilage lesions, or for fracture repair [17-25]. Other potential applications include the treatment after myocardial infarction [26], or neurodegenerative diseases [14]. The delicate control of IGF-I activity *in vivo* is translating into diverse delivery modalities, driven by the intended pharmacological intervention. This article reviews localized delivery

strategies and systemic delivery approaches with the ultimate goal to provide guidance for effective IGF-I delivery.

### ***Pharmacokinetics and safety of IGF-I***

IGF-I pharmacokinetics are modulated by six IGF-binding proteins [27]. Approximately 99% of plasma IGF-I is bound to IGFBPs, particularly to IGFBP-3 [7, 13, 16, 28, 29], forming a ternary complex consisting of IGF-I, IGFBP-3 (46-53 kDa protein) and the acid labile subunit (ALS; 88 kDa glycoprotein). This ternary 150-kDa complex increases the plasma half-life of IGF-I from 10 minutes in free form [6, 30] to 12-15 hours [6, 30]. These insights were therapeutically translated by administering IGF-I together with IGFBP-3 (*vide infra*) in an effort to address the challenge of the short plasma half-life of free IGF-I. The formation of a ternary complex is known for IGF-I, ALS and IGFBP-5, but not for IGFBP-1, -2, -4, or -6 [31]. The A domain and B domain of IGF-I (**Figure 1**) are mainly responsible for interactions with all IGFBPs [28, 32]. For example, the affinity of IGF-I to its binding proteins was strongly decreased by substitution of the B domain or the mutation of amino acids such as Phe49, Arg50, Ser51 (located on A domain). IGFBPs participate with their N-terminal and C-terminal domain in IGF-I binding [33]. It was previously demonstrated that Leu<sup>77</sup>, Leu<sup>80</sup> and Leu<sup>81</sup> as well as Gly<sup>217</sup> and Gln<sup>223</sup> of IGFBP-3 were critically involved in interactions with IGF-I [34]. Apart from IGFBP binding forming a sink for administered IGF-I as do cell surfaces, pharmacokinetics (PK) are impacted by the route of administration. For example, a half-life of about 6 hours has been reported in patients with primary IGF deficiency (IGFD) when IGF-I alone was given subcutaneously [35]. Consequently, the dose of IGF-I, its site of administration (e.g. subcutaneous versus intravenous) and other parameters will impact PK and clinical development programs must detail the specific profiles for novel formulations. This delicate control of IGF-I is further modulated by the responsiveness of its binding partners to other proteins. For example, IGFBP-3 and ALS concentrations are responsive to growth hormone (GH) or IGF-I levels themselves modulate the concentrations of these [6]. IGF-I is mainly metabolized in the liver and kidneys or degraded locally by proteases [35]. By virtue of its Insulin receptor binding activity, therapeutic intervention with IGF-I is challenged by hypoglycemia and the risk has been assessed at about 10% of that following Insulin administration [36]. Other reported adverse events are related to GH suppression, lipohypertrophy and pain at the injection site following subcutaneous



system (Version 1.7.4 Schrödinger, LLC). (F) Amino acid sequence of human IGF-I [4] with E-peptide [107] (dark-grey). Disulfide bonds are represented as bold lines between cysteine residues.

administration, headache and tonsillar hypertrophy in patients with severe primary IGF deficiency [35]. Anti-IGF-I antibodies were found within the first year of subcutaneous IGF-I administration to IGFD patients, but these antibodies did not impact the growth promoting effect of IGF-I [35]. Similar findings regarding antibody formation were reported for Insulin, for which stronger antibody responses were discussed after pulmonary as compared to subcutaneous administration, respectively [37]. One study linked a need for increasing Insulin doses with rising insulin-antibody levels following intraperitoneal Insulin administration [38]. In general, these findings on immunity raise concerns associated to any replacement therapy, including other growth factors or enzymes [39]. Another concern related to this anabolic protein is its possible neoplastic potential. Chronic toxicity studies in Sprague Dawley rats exposed to different doses of subcutaneous IGF-I (0, 0.25, 1, 4 and 10 mg/kg/day) for up to two years resulted in observations of adrenal medullary hyperplasia and pheochromocytoma at doses  $\geq 1$  mg/kg/day and at all doses for male and female rats, respectively [35, 36, 40]. Mammary gland carcinoma was found in male and female rats at (excessively high doses of) 10 mg/kg/day. Although IGF-I plasma levels are elevated in several cancers a causal relationship such that increased IGF-I plasma concentrations predispose subjects to the development of cancers cannot be justified to date [36]. For a safe, systemic intervention in rather benign and chronic diseases such as sarcopenia one may translate these insights into the conservative goal to reach plasma levels not exceeding what is found for the upper 95<sup>th</sup> percentile of the respective gender and age group in normal subjects [41]. Safety concerns may be adequately mitigated by this strategy, particularly when addressing chronic treatment regimens as required for sarcopenia or other therapies benefitting from the anabolic activity of IGF-I. However, future studies must demonstrate if this careful adaptation of IGF-I levels is sufficient to yield clinical responses. Alternatively, one may consider 95<sup>th</sup> percentiles of other age groups, as IGF-I levels fluctuate strongly throughout age with peaks during puberty [41]. A safe and successful therapy also includes a strict control of the manufacturing process. High quality and reliability of the outcome products has to be ensured and low levels of degradation products and missfolded proteins must be specified along with various other parameters which are standard to any biomanufacturing process for biologics (e.g. host cell proteins, etc).

## ***IGF-I delivery***

Pharmacokinetic and pharmacodynamic properties of therapeutic IGF-I are impacted by the route of administration and the dosage form (**Figure 2**). A successful application is linked with several requirements driven by poor bioavailability and potential side effects (*vide supra*). The most convenient route of administration - the oral route - is challenged by rapid proteolytic degradation, hence poor bioavailability [42]. In spite of the general challenge for oral peptide delivery, IGF-I's close relative – Insulin – has been subject to various attempts targeting the oral route [43-48]. By virtue of the homology of IGF-I and Insulin primary structures (*vide supra*), one may arguably assume that previous successes for Insulin delivery may serve as a guiding starting point for defining a galenic strategy for IGF-I. Tablets or capsules with functional excipients protecting Insulin from enzymatic degradation and different nanoparticulate carrier systems (e.g. solid nanoparticles, liposomes or polymeric-based nanoparticles) were described [46] but the outcome has not justified an industrial development to date. Furthermore, nasal and rectal applications of Insulin have been discussed [49-51]. A buccal spray is marketed in India and Ecuador (Oral-lyn) [47] and one may speculate that in light of IGF-I's similarity to Insulin, buccal IGF-I delivery may translate into convenient use of this growth factor e.g. in sarcopenia, although this has not been explored to date. Similarly, pulmonary Insulin delivery proved successful and market entry of Afrezza is expected for 2015 following the previous entry and withdrawal of Exubera [52, 53]. In the following sections we outline IGF-I dosage forms, routes of administration, IGF-I modifications and other reported strategies and we also extrapolate to possible yet unexplored delivery modalities (**Figure 2**).

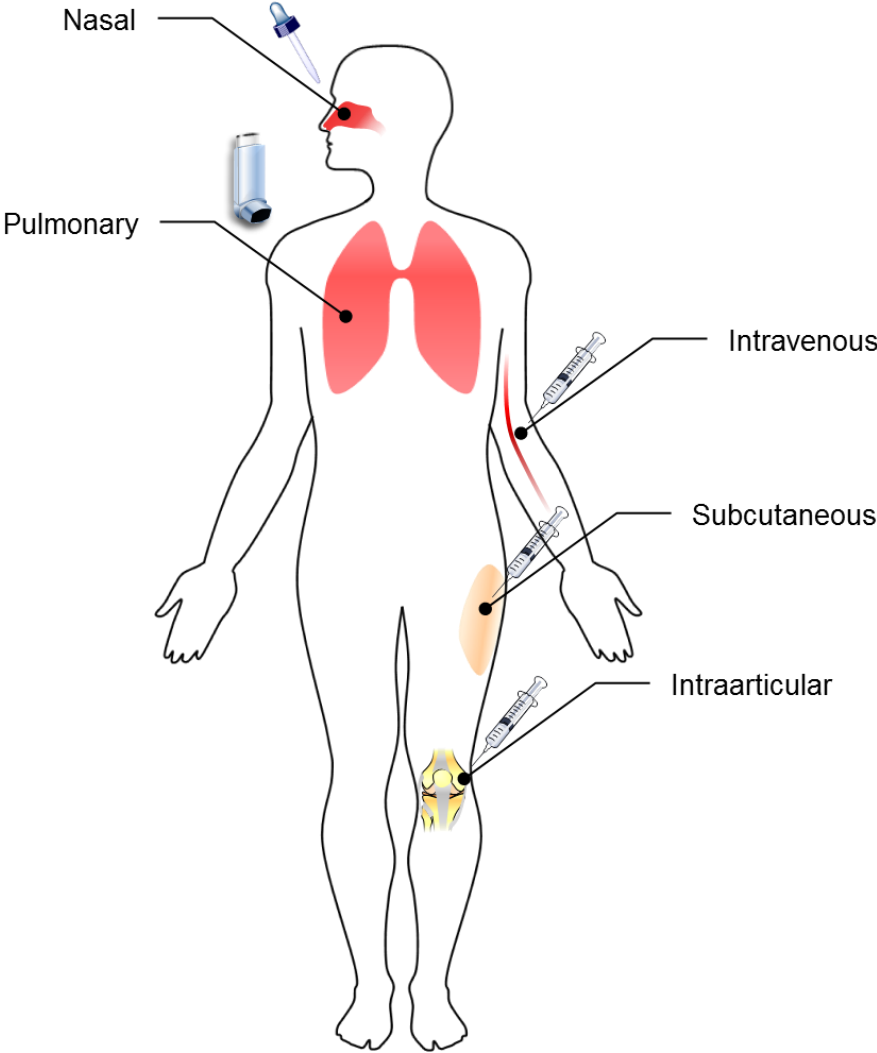


**Figure 2.** Cartoon outlining the different administration routes for IGF-I.



## *Liquid formulations for IGF-I delivery*

Liquid formulations for injection are the common route for the administration of protein therapeutics. Stable IGF-I formulations require a precise adaptation of pH, buffer strength and type [18]. IGF-I is susceptible to oxidation, preferential at its methionine at position 59 (Met(o)-IGF-I, **Figure 1 D, F**), induced for example by light, oxygen, ferric ions or phosphate [18, 24, 25, 54, 55]. Supplementing formulations with methionine prevented Met59 oxidation, yielding stable formulations for months when formulated at pH 6.5 [18]. A liquid formulation of IGF-I for subcutaneous application (Mecasermin, Increlex<sup>®</sup>) is formulated at pH 5.4 [35]. Nebulization of a stable liquid IGF-I formulation resulted in aerosols with a mass median diameter of either 2.7  $\mu\text{m}$  or 4.9  $\mu\text{m}$  using a standard air jet nebulizer or a new generation vibrating-mesh nebulizer, respectively [18]. IGF-I integrity was maintained throughout manufacture, and the formation of covalent aggregates was prevented during storage and after nebulization. The results of this study along with the finding that IGF-I passed through the lung [56] suggested a promising potential of liquid IGF-I formulations for pulmonary IGF-I delivery. Nasal administration is an alternative route for systemic peptide delivery and favorable due to a relatively large surface area, higher permeability as compared to other sites, vascularization and bypass of the first-pass effect [57, 58]. Consequently, nasal IGF-I delivery has been subject to various studies [59-66]. Interestingly, a study reported on IGF-I delivery into the brain (bypassing the blood-brain barrier) after intranasal administration [59]. Higher concentrations of <sup>125</sup>I-labeled IGF-I were detected in the central nervous system (CNS) after intranasal compared to intravenous administration. Subsequently, CNS availability following intranasal administration was linked to the peripheral olfactory system and the peripheral trigeminal system [61]. The pharmacodynamic potential of intra-nasally delivered IGF-I was demonstrated for the treatment of brain stroke using a rat model of middle cerebral artery occlusion (MCAO), in which IGF-I administration decreased the infarct volume and enhanced neurological functions [60]. A dose of 50  $\mu\text{L}$  solution per rat (150  $\mu\text{g}$  IGF-I, 10 mM sodium succinate buffer, 140 mM sodium chloride, pH 6.0) was applied over a period of 20 minutes by dropping solutions into the nostrils (5  $\mu\text{L}$ /drop). The efficacy upon intranasal administration was corroborated in a cerebral hypoxia-ischemia model in rat pups, in which IGF-I administration up to 1 hour after injury reduced the size of the lesion, enhanced neurobehavioral performance, reduced apoptotic cell death and improved the proliferation of neuronal and oligodendroglial progenitor cells [62]. A

dose of 5  $\mu\text{L}$  solution per rat (50  $\mu\text{g}$  IGF-I, 0.1% BSA in 5  $\mu\text{L}$  PBS) was applied into the right nostril. Subsequent studies detailed the time of intranasal administration following injury, with benefits being demonstrated for administrations up to 6 hours after cerebral ischemia following whole body hypothermia [63]. Other studies demonstrated efficacy in a rat model of lipopolysaccharide-induced brain injury and positive impact was reported on behavioral deficits [64]. In these studies, a dose of 5  $\mu\text{L}$  solution per rat (50  $\mu\text{g}$  IGF-I, 0.1% BSA in 5  $\mu\text{L}$  PBS) was applied into the left nostril at 1 or 2 h after the intracerebral injection of lipopolysaccharide. Other studies reported benefits of intra-nasally administered IGF-I for neurodegenerative disorders including relevant animal model systems for Huntington`s disease [65] and spinocerebella ataxia type I [67]. These studies demonstrated, that stable, liquid formulations of IGF-I can be formulated. They also detailed, that apart from obvious administration schemes (s.c., i.v., etc), trans-epithelial transport is feasible for buccal delivery and – upon aerosolization from liquid formulations – for pulmonary delivery (**Figure 2**).

### ***Solid formulations for immediate IGF-I delivery***

The lung is a well-studied administration route for protein delivery and offers advantageous conditions for drug absorption by means of a large surface area, thin alveolar epithelium and circumvention of the first-pass metabolism [68]. The pulmonary route is well established for Insulin [69] and inhalable Insulin (Afrezza<sup>®</sup>) has been reported to enter the market in the United State [70]. Pulmonary Insulin resulted in a rapid absorption and improved postprandial metabolic control, reduced events of hypoglycemia [71, 72] and the variability of pharmacodynamic parameters was comparable to subcutaneous administration [69]. These studies on Insulin were expanded to IGF-I following the hypothesis that what is found for Insulin may be successfully extrapolated to IGF-I and by means of the structural similarity of both peptides [56]. IGF-I was spray-dried in two formulations deploying trehalose or silk-fibroin as carriers with trehalose being a commonly used, non-reducing disaccharide and silk-fibroin (SF) being a larger protein, with reported stabilizing impact on sensitive biologicals [73]. *In vitro* studies demonstrated immediate release of IGF-I from trehalose and within three hours from SF particles. Released IGF-I was bioactive and degradation was minimal and comparable for both carriers, with IGF-I oxidation (oxidation did not impact overall potency) being more pronounced in the SF formulation. This was linked to the lack of methionine as reducing agent in the SF formulation,

which was present in trehalose. Both formulations resulted in comparable IGF-I uptake upon inhalation from a dust gun and as demonstrated in an *ex vivo* perfused human lung lobe model, with about 6% IGF-I of the applied dose being recovered from the perfusion fluid [56]. This study concluded, that pulmonary IGF-I delivery is a suitable approach to compensate for reduced systemic levels e.g. as present in the elderly and within this age group for the treatment of sarcopenia. However, the limited bioavailability challenges this administration route for indications requiring larger doses, e.g. as needed for IGF-I deficiencies.

### ***Solid formulations for controlled IGF-I delivery***

As pointed out before, the plasma half-life of IGF-I is a function of several parameters, with plasma half-life reported as short as 10 and 12 minutes for *free* IGF-I [30] to several hours when bound to IGFBP [30]. Based on these findings, several drug delivery platforms were developed releasing IGF-I with slow and rate limiting kinetics for controlled drug delivery. For example, IGF-I was encapsulated into multivesicular liposomes of a diameter of 18 – 20  $\mu\text{m}$  and resulting in elevated and stable IGF-I plasma levels for up to 5-7 days after subcutaneous injection in rats [74]. Other spherical systems were described based on poly(D,L-lactide-co-glycolide) (PLGA) and prepared by solvent extraction. These IGF-I microspheres were successfully prepared in presence of stabilizing excipients such as albumin [17, 19, 24, 25, 75, 76]. IGF-I loaded microparticles demonstrated a burst release followed by a sustained release with pulsatile features for up to 13 days *in vitro* [25]. IGF-I delivered from these PLGA microspheres were implanted into bone defects of sheep and induced significant new bone formation in both, metaphyseal drill hole or segmental defects of the tibia, respectively [24]. In another study, IGF-I was encapsulated in a series of different PLGAs and PLA, resulting in a range of initial bursts (14–36% of total IGF-I content) followed by lag times from 2 to 34 days. IGF-I release kinetics from these microparticles were correlated to osteoinduction using a metaphyseal drill hole defect in sheep and resulted in a down-regulation of inflammatory marker genes in defects treated with IGF-I microspheres and over-expression of growth factor genes in those defects treated with formulations resulting in osteogenic responses [17]. Release of IGF-I from PLGA microparticles was also demonstrated in an *in vivo* study and following the evaluation of pharmacokinetic parameters. An initial burst and a subsequent controlled release over 14 – 18 days was reported after subcutaneous administration of the formulation into Sprague-Dawley rats [76]. Alternative

manufacturing methods deployed IGF-I microspheres from PLGA to modulate release when loaded into scaffolds [75]. Another favored excipient for the encapsulation of biologics is the protein and biopolymer silk-fibroin [19, 21, 22,77-79]. IGF-I was directly incorporated into SF 3D scaffolds intended for use as implants [22]. The IGF-I release profile was controlled by the overall crystallinity of SF, yielding IGF-I release profiles ranging from 9 – 11 days for low crystalline and more than 24 days for high crystalline SF scaffolds. Seeding these scaffolds with human mesenchymal stem cells resulted in chondrogenic differentiation of human mesenchymal stem cells with cartilage-like tissue deposition within three weeks. [20]. IGF-I was also incorporated in SF microparticles [21]. These microparticles were prepared with a laminar jet break technique resulting in spherical structures with encapsulation efficiencies approaching 100% and particle sizes of 400 to 450  $\mu\text{m}$ . *In vitro* IGF-I release was up to 7 weeks and the growth factor was still bioactive in spite of the long time in release medium. Other studies used cross-linked alginate scaffolds for IGF-I delivery [80]. A steady IGF-I release was observed from these scaffolds for three days *in vitro*, followed by a declining release for up to 14 days. Alginate gels were also used as injectable scaffolds loaded with IGF-I containing PLGA microparticles, calciumcarbonat, and tricalciumphosphat ( $\beta$ - TCP) granules. This system was developed for bone regeneration [23]. The release of bioactive IGF-I from the scaffolds was demonstrated for 28 days and the supplementation of the alginate gel with  $\beta$ -TCP resulted in faster gelation and improved properties regarding stiffness and swelling. Lastly, chitosan was used as a carrier for IGF-I loaded PLGA (faster release) or poly(3-hydroxybutyrate-co-3-hydroxyvalerate) (PHBV; slower release) nanocapsules, respectively, which were developed for the treatment of periodontal tissue defects. In conclusion, IGF-I can be delivered from pharmaceutically acceptable polymer carriers in bioactive form. Sustained delivery profiles have been demonstrated, ranging from days to weeks. Oxidation of methionine at position 59 (**Figure 1 D, F**) has to be minimized during formulation and storage. Basic pH conditions should be avoided at any time. Most studies profiled the growth factor for musculoskeletal use and orthotopic implantation into skeletal defects for fracture healing. IGF-I is stable in acidic environments (*vide supra*). Therefore, delivery form PLGA microspheres - with PLGA producing acidic by-products during degradation [81] - was tolerated in terms of stability during manufacture and storage. Successful delivery was also reported from the biopolymer silk-fibroin. Furthermore,

localized release into a healing fracture, which in early phases is ischemic and, therefore, acidic, would further suggest delivery into freshly injured bone defects for facilitated healing.

### ***Administration of IGF-I and IGFBP-3 complexes***

The combination of IGF-I with IGF-binding protein-3 (IGFBP-3) is an interesting therapeutic strategy extending the natural IGF-I protection mechanism to therapeutic intervention. The complex substantially increases IGF-I stability in the blood and thereby increases the half-life [82]. IGFBP-3 is one of the six IGF-binding proteins known to control IGF-I tissue distribution and modulating receptor binding. *In vivo*, circulating IGF-I forms a ternary complex with IGFBP-3 and another protein, the acid labile subunit (ALS). A complex of equimolar amounts of IGF-I and IGFBP-3 (Mecasermin rinfabate, IPLEX™) was approved for the U.S. market in 2005 for growth failure in children [83]. Today, the complex is marketed in Italy for amyotrophic lateral sclerosis / Lou-Gehrig-Syndrom and is applied once a day by subcutaneous injection [82, 84]. Maximum IGF-I levels following subcutaneous administration of 0.5 mg/kg were achieved in  $21 \pm 9$  hours for healthy adults and  $19 \pm 8$  hours in children with growth hormone insensitivity [82]. In spite of the strong pharmacokinetic impact, IGF-I pharmacology was unaffected when delivered from the IGFBP-3 complex [82, 83]. In conclusion, biomimetic delivery of IGF-I from the IGFBP-3 complex is an interesting approach allowing once daily dosing. Several clinical trials have been performed to evaluate the potential of this complex in diseases such as diabetes, osteoporosis, burns, growth hormone insensitivity syndrome or low birth weight children [82].

## **Biotechnological modification of IGF-I**

### ***PEGylation***

PEGylation is a well-established process to enhance pharmacokinetic and pharmacodynamic properties of biologics [85, 86]. Advantages of PEGylated protein modifications may include better stability by reduced metabolism rates, prolonged residence in the blood circulation due to reduced excretion as well as reduced immunogenic potential [85, 86]. Furthermore, the incorporation of the hydrophilic PEG increases the peptide's solubility. Hence, several PEGylated biopharmaceuticals have already been introduced into the market over the last twenty years (e.g. Pegaspargase – Oncaspar [87], Peginterferon alfa-2a – Pegasys [88], Certolizumab

pegol – Cimzia [89] and many others [90-101]. Site-specific PEGylation of IGF-I has also been reported to enhance IGF-I delivery. For example, IGF-I PEGylated (PEG-IGF-I) at position 68 (Figure 1 F) is as potent as non PEGylated IGF-I as assessed in a model of contraction-induced muscle injury in 3-week-old mdx dystrophic mice and PEG-IGF-I was discussed in terms of a potential advantage over IGF-I in terms of a better safety profile with respect to hypoglycaemia [102]. Another benefit is the markedly extended availability of PEG-IGF-I in the blood circulation compared to IGF-I. *In vitro* studies had detailed a reduced affinity of PEG-IGF-I to the IGF-I receptor, the Insulin receptor, and to IGFBPs. Furthermore, PEG-IGF-I increased the levels of IGFBP-2 and IGFBP-3 after subcutaneous injection. The efficacy of PEG-IGF-I for central nervous system disorders (e.g. mental retardation) was studied using a mouse model of brain amyloidosis [103]. Successful therapy required adequate central availability of IGF-I and PEGylation was instrumental in achieving higher steady-state levels in brain tissue and cerebrospinal fluid as compared to undecorated IGF-I following a single dose subcutaneously. Brain plasticity processes were modulated by PEG-IGF-I after two weeks and chronic treatment enhanced synaptic functions, Insulin/IGF-I signaling and cognitive performance. Similarly, PEG-IGF-I demonstrated significant enhancement in muscle force, motor coordination and animal survival in a mouse model with a mild type of familial amyotrophic lateral sclerosis (ALS) but more advanced phenotypes were not relieved [104]. Another study compared PEG-IGF-I to undecorated IGF-I for skeletal muscle regeneration after myotoxic injury in mice [105]. Intramuscular administration of PEG-IGF-I resulted in higher spatial residence time and concentration in the skeletal muscle as compared to IGF-I. A benefit was demonstrated for PEG-IGF-I administration at day 4 post injury by improved skeletal muscle regeneration as compared to saline or IGF-I, but no benefit was demonstrated for later time points. The optimal site for IGF-I decoration with PEG remains to be found. However, recent studies shed light on appropriate sites using three IGF-I variants, PEGylated at lysines K 27 (B domain; **Figure 1 B, F**), K 65 and K 68 (D domain; **Figure 1 E, F**). These were analyzed regarding binding properties, signal transduction and impact on cell viability and cell migration [106]. The PEGylation of lysine K 65 and K 68 resulted in a 2-fold decrease of receptor phosphorylation in 3T3 fibroblasts and MCF-7 breast cancer cells, respectively. This negative impact of bulky PEG residues at positions K 65 and K 68 on receptor binding can readily be assumed, as both amino acids positioned on the D domain have been suggested for receptor binding (**Figure 1 E**), although the

precise role of the IGF-I D domain (amino acid Pro 63 – Ala 70, **Figure 1 A, F**) in receptor binding is still under discussion [28, 107]. Previous studies also suggested this outcome, with the exchange of K 65 and K 68 to alanine (A) resulting in a 10-fold affinity loss of IGF-I to its receptor [28]. PEGylation of lysine K 27 (**Figure 1 B, F**) resulted in 10- and 3-fold lower receptor stimulation in 3T3 fibroblasts and MCF-7 breast cancer cells, respectively [106]. The authors linked this finding to K 27's close location to Tyr 31 and Tyr 24 – all of which being located within the binding sites of IGF-I to its receptor on the B domain (**Figure 1 B**) - which are important for receptor interaction [106, 108-111]. The affinity to IGFBP-1 - 5 was 10 fold reduced for all PEGylated IGF-I variants (K 27, K 65 and K 68), which may result from steric hindrance of the large PEG residue. All PEGylated IGF-I variants positively impacted cell viability, however, the ability to stimulate cell migration was lost after the introduction of a PEG chain into IGF-I. Also, signaling differences were detected. PEGylation resulted in reduced AKT signaling in MCF-7, whereas the MAPK pathway was not impacted by PEG variants compared to unmodified IGF-I. The authors suggested that these findings raised evidence that migration was preferably induced by the AKT pathway and more insight is required before fully understanding this observation. In conclusion, PEGylation of IGF-I at various sites resulted in a prolonged half-life and reduced affinity to its receptor and its IGFBPs. One may speculate that using longer IGF-I variants allows the attachment of a PEG more distant from the sites essential for IGF-I receptor binding or interaction with binding proteins. In fact, such longer peptides are naturally occurring and outlined below. An interesting alternative to PEGylation is the attachment of polypeptide chains containing Pro, Ala and Ser (PASylation) to proteins [112]. This decoration strategy address the same pharmacokinetic goal compared to the addition of PEG residues and consequently an increased plasma half-life of biologics. Further coupling strategies are known for other proteins than IGF-I including the conjugation to biodegradable hydroxyethyl starch (HES) [113] or to albumin [114].

### ***E-peptides***

E-peptides are synthesized by Nature through alternative splicing to modulate the pharmacokinetics of IGF-I. Thereby, C-terminal extensions ranging from lengths of 35 and 77 amino acids are introduced, referred to as E-peptides (IGF-Ea, IGF-Eb and IGF-Ec) [115]. IGF-Ea, IGF-Eb and IGF-Ec induced cell proliferation and cell differentiation in different cells and

were mitogenic, angiogenic and induced cell migration [115]. Furthermore, these E-peptides had an increased stability in human serum [116]. These naturally occurring IGF-I variants are interesting molecules for systemic administration when a longer half-life is targeted. Previously, we successfully manufactured IGF-I extended with an Ea-peptide in *E. coli* (**Figure 1 F**). Furthermore, we aimed at expanding the possibilities of IGF-I decoration, since many studies such as pegylation, were confined by their chemical strategies, limiting sites of decoration to lysines (K). For that, we currently follow an alternative strategy for targeted decoration by engineering an IGF-I variant with propargyl-protected lysine derivatives with an alkyne function (Plk) using *BL21(DE3) E. coli* (**Figure 1 F**). We replaced position 3 (E → Plk) and included a 33 amino acid extension (Ea-peptide), into which another Plk was introduced at position 29' (K → Plk, **Figure 1 F**). In order to introduce these unnatural amino acids into the peptide sequence, the deoxyribonucleic acid (DNA) is modified at the intended site of modification by an amber codon [117, 118]. The amber codon is a stop codon (TAG) and, therefore, requires further adaptation of *E. coli* in order to proceed with the synthesis of the Plk modified peptide. This adaptation is realized by co-expression of two further genes from another bacterium, *Methanosarcina barkeri*, which by nature can utilize the TAG triplets for tRNA binding with the attached amino acids. These genes are naturally not present in *E. coli* or mammals. These genes from *Methanosarcina barkeri* are pyrrolysyl-transfer-RNA-synthetase (pylRS) and its cognate t-RNA (tRNA<sup>Pyl</sup>) and co-transformed into *E. coli*. Therefore, *E. coli* co-expressed pylRS for binding of the unnatural amino acid Plk (chemically synthesized and supplemented to the culture medium) to the tRNA<sup>Pyl</sup> and the IGF-I gene with the TAG triplet at the two positions of the IGF-I – E-peptide clone. Thereby, we engineered an IGF-I – E-peptide with alkyne functions (**Figure 1 F**). In return, these alkyne functions can be decorated with molecules with an azido group under Cu(I) catalysis (Huisgen azide–alkyne cycloaddition) in a strictly site specific fashion [117, 119]. By means of this strategy, conjugates may be produced avoiding the current product heterogeneity through coupling of lysines. The dual functionality is instrumental to simultaneously modify the biologic at both positions, but analogues with one replacement are accessible by the same strategy.



## ***Targeted IGF-I delivery***

Targeted IGF-I delivery is another approach to localize IGF-I in certain parts of the body and simultaneously modulate systemic side effects. For this purpose, different modifications in the structure of IGF-I were established. A rat IGF-I sequence was fused on its N terminus (**Figure 1 F**) with a heparin-binding domain of HB-EGF (heparin-binding EGF-like growth factor) to achieve accumulation of heparin-binding IGF-I (HB-IGF-I) in cartilage tissue [120]. It was demonstrated that HB-IGF-I bound selectively to heparin and several cell surfaces. The bioactivity of HB-IGF-I was not impacted by the heparin-binding domain. Furthermore, HB-IGF-I retention was shown in explanted cartilage tissue. The decorated growth factor induced sustained proteoglycan synthesis of chondrocytes *in vitro*. Subsequent studies detail the mechanism of HB-IGF-I retention in cartilage [121]. It was found that binding through chondroitin sulfate was responsible for the retention of HB-IGF-I in the explanted cartilage tissue, whereas heparin sulfate was not involved. Binding assays showed that HB-IGF-I had higher affinity for heparin sulfate compared to chondroitin sulfate and that rising concentration of glycosaminoglycans increased the binding affinities [121]. Accordingly, the decoration of IGF-I with heparin-binding domains was instrumental to localize the growth factor in tissues with high amounts of chondroitin sulfate such as cartilage and not in tendon or muscle tissue, even one day after intraarticular injection in rats. Sustained IGF-I delivery to cartilage was also confirmed in explants from human knee cartilage. The development of another HB-IGF-I, consisting of a human full-length mature IGF-I sequence and on its N terminus (**Figure 1 F**) a human heparin-binding domain featuring a mutation of Cys<sup>17</sup> residue resulted in HB-IGF-I presence up to 8 days in cartilage upon intraarticular injection in adult Lewis rats [122]. The lasting presence of HB-IGF-I resulted in profound impact on local proteoglycan synthesis and cell proliferation for at least 4 days, while native IGF-I failed to impact biological responses 2 days after application [122]. HB-IGF-I also proved efficient in a rat model of osteoarthritis. Another study targeted the known impact of IGF-I on regeneration upon myocardial infarction. For that, IGF-I was tagged to a fluorescent dye (Hoechst) by streptavidin-biotin linkage. Hoechst binds to double-stranded DNA [123]. Upon i.v. dosing into rats, the complex of IGF-I and Hoechst targeted extracellular DNA released from necrotic cells in the myocardial infarction zone. Further analyses indicated that i.v. delivered Hoechst-IGF-I prevented cardiac fibrosis and decreased dysfunction after myocardial infarction. This therapeutic strategy enabled targeting of

necrotic heart tissue, and retention of the complex at this site following systemic administration. In conclusion, several studies showed that IGF-I decoration is instrumental to allow IGF-I targeting to various tissues as well as controlling local persistence and bioactivity.

## CONCLUSION

IGF-I is a powerful anabolic therapeutic for many diseases. The intended indication drives the formulation and basically falls into one of two buckets: Localized treatment or systemic treatment. Localized treatment typically aims at reducing frequent administrations and, therefore, depot systems are an attractive option to meet this goal. The release from these systems is the rate limiting step, such that controlled IGF-I delivery is achieved. Successful systems have been described, but long term stability challenges particularly when working with polymers yielding acidic byproducts must be conducted before the feasibility of this approach can be postulated. Repair of musculoskeletal defects and cartilage is one of the more often chosen indications. IGF-I is naturally stored in bone and released during remodeling, i.e. in environments with decreased pH as compared to physiologically normal pH. It is for its biological role and its ability to withstand lower pH that IGF-I retains its integrity under these conditions. These insights also drive the handling of IGF-I during manufacture, within which exposure to basic pH should be avoided resulting in rapid aggregation. A variety of these depots have been presented, allowing delivery of IGF-I from days to months following administration. An alternative to local implantation for localized delivery is by means of targeting. Successful targeting modalities upon IGF-I decoration with polysaccharides have been presented in relevant animal model systems and provide promising alternatives to complex pharmaceutical platforms such as microparticles. Current studies aim at identifying optimal decoration sites for IGF-I and focus should also extend from IGF-I to modification of IGF-I E-peptides, accordingly. Incorporation of unnatural amino acids providing novel functional groups is instrumental to yield highest possible control of the decoration sites. Previous approaches delivering IGF-I in a complex with a binding protein have been successful. *In vivo*, the binding to different binding proteins impacted the distribution of IGF-I and future studies must detail if this can be deployed for targeting purposes in a biomimetic fashion. Parenteral delivery has been demonstrated for various routes, with some studies following the hypothesis that what has been demonstrated for Insulin might be extrapolated to IGF-I and by virtue of the proteins' sequence homology. However, each novel

site of administration requires a new safety assessment, particularly when used chronically. Buccal, oral, and pulmonary delivery have been demonstrated or postulated along with typical administration routes such as i.v. or subcutaneous. Some of these are served with liquid formulations. In these cases, oxidation particularly of methionine 59 must be closely followed. Although Met(o)59 is not substantially impacting IGF-I potency, oxidation must be controlled from general quality considerations. Supplementation of formulations with methionine or other reducing excipients can prevent Met(o)59 formation. Adequate buffers have to be used to prevent pH deviation to alkaline conditions. In conclusion, the suite of promising pharmaceutical dosage forms ranges from liquid systems with demonstrated pharmaceutical quality to allow human use to decorated IGF-Is profiled in various animal model systems (**Figure 2**). Solid IGF-I systems have been demonstrated for immediate release (pulmonary) and as implants for sustained drug delivery.

## **ACKNOWLEDGMENTS**

This work has been supported by the German Federal Ministry of Education and Research (BMBF; grant number 13N13454) and by the German Academic Exchange Service/DAAD (grant number 57058983).

### REFERENCES

- [1] R.M. Cooke, T.S. Harvey, I.D. Campbell, Solution Structure Of Human Insulin-Like Growth Factor-I - A Nuclear-Magnetic-Resonance And Restrained Molecular-Dynamics Study, *Biochemistry*, 30 (1991) 5484-5491.
- [2] W.D. Salmon, W.H. Daughaday, A Hormonally Controlled Serum Factor Which Stimulates Sulfate Incorporation By Cartilage Invitro, *Journal of Laboratory and Clinical Medicine*, 49 (1957) 825-836.
- [3] W.H. Daughaday, W.D. Salmon, J.I. Vandenbr, J.J. Vanwyk, M.S. Raben, K. Hall, Somatomedin - Proposed Designation For Sulfation Factor, *Nature*, 235 (1972) 107-&.
- [4] E. Rinderknecht, R.E. Humbel, The Amino Acid Sequence Of Human Insulin-Like Growth Factor I And Its Structural Homology With Proinsulin, *The Journal of biological chemistry*, 253 (1978) 2769-2776.
- [5] D.R. Clemmons, *Insulin-Like Growth Factors: Their Binding Proteins And Growth Regulation*, Lippincott Williams and Wilkins, 530 Walnut Street, Philadelphia, PA, 19106-3261, USA 2-6 Boundary Row, London, SE1 8HN, UK, 2000.
- [6] J.I. Jones, D.R. Clemmons, *Insulin-Like Growth-Factors And Their Binding-Proteins - Biological Actions*, *Endocrine Reviews*, 16 (1995) 3-34.
- [7] G. Steeleperkins, J. Turner, J.C. Edman, J. Hari, S.B. Pierce, C. Stover, W.J. Rutter, R.A. Roth, Expression And Characterization Of A Functional Human Insulin-Like Growth Factor-I Receptor, *Journal of Biological Chemistry*, 263 (1988) 11486-11492.
- [8] L. Gauguin, B. Klapproth, W. Sajid, A.S. Andersen, K.A. McNeil, B.E. Forbes, P. De Meyts, Structural Basis For The Lower Affinity Of The Insulin-Like Growth Factors For The Insulin Receptor, *Journal of Biological Chemistry*, 283 (2008) 2604-2613.

- 
- [9] Y. Zick, N. Sasaki, R.W. Reesjones, G. Grunberger, S.P. Nissley, M.M. Rechler, Insulin-Like Growth Factor-I (Igf-I) Stimulates Tyrosine Kinase-Activity In Purified Receptors From A Rat-Liver Cell-Line, *Biochemical and Biophysical Research Communications*, 119 (1984) 6-13.
- [10] N. Sasaki, R.W. Reesjones, Y. Zick, S.P. Nissley, M.M. Rechler, Characterization Of Insulin-Like Growth Factor-I-Stimulated Tyrosine Kinase-Activity Associated With The Beta-Subunit Of Type-I Insulin-Like Growth-Factor Receptors Of Rat-Liver Cells, *Journal of Biological Chemistry*, 260 (1985) 9793-9804.
- [11] D. Leroith, H. Werner, D. Beitnerjohnson, C.T. Roberts, Molecular And Cellular Aspects Of The Insulin-Like Growth-Factor-I Receptor, *Endocrine Reviews*, 16 (1995) 143-163.
- [12] W.L. Lowe, Biological Actions Of The Insulin-Like Growth Factors, in: D. LeRoith (Ed.) *Insulin-Like Growth Factors: Molecular And Cellular Aspects*, CRC Press, Boca Raton, 1991, pp. 49-85.
- [13] R. Eshet, H. Werner, B. Klinger, A. Silbergeld, Z. Laron, D. Leroith, C.T. Roberts, Up-Regulation Of Insulin-Like Growth Factor-I (Igf-I) Receptor Gene-Expression In Patients With Reduced Serum Igf-I Levels, *Journal of Molecular Endocrinology*, 10 (1993) 115-120.
- [14] S. Perrini, L. Laviola, M.C. Carreira, A. Cignarelli, A. Natalicchio, F. Giorgino, The GH/IGF1 Axis And Signaling Pathways In The Muscle And Bone: Mechanisms Underlying Age-Related Skeletal Muscle Wasting And Osteoporosis, *Journal of Endocrinology*, 205 (2010) 201-210.
- [15] D.R. Clemmons, W.H. Busby, T. Arai, T.J. Nam, J.B. Clarke, J.I. Jones, D.K. Ankrapp, Role Of Insulin-Like Growth Factor Binding Proteins In The Control Of IGF Actions, *Progress in Growth Factor Research*, 6 (1996) 357-366.

[16] V.R. Sara, K. Hall, Insulin-Like Growth-Factors And Their Binding-Proteins, *Physiological Reviews*, 70 (1990) 591-614.

[17] V. Luginbuehl, E. Zoidis, L. Meinel, B. von Rechenberg, B. Gander, H.P. Merkle, Impact Of IGF-I Release Kinetics On Bone Healing: A Preliminary Study In Sheep, *European journal of pharmaceutics and biopharmaceutics : official journal of Arbeitsgemeinschaft fur Pharmazeutische Verfahrenstechnik e.V.*, 85 (2013) 99-106.

[18] O. Germershaus, I. Schultz, T. Luhmann, M. Beck-Broichsitter, P. Hogger, L. Meinel, Insulin-Like Growth Factor-I Aerosol Formulations For Pulmonary Delivery, *European journal of pharmaceutics and biopharmaceutics : official journal of Arbeitsgemeinschaft fur Pharmazeutische Verfahrenstechnik e.V.*, 85 (2013) 61-68.

[19] E. Wenk, A.J. Meinel, S. Wildy, H.P. Merkle, L. Meinel, Microporous Silk Fibroin Scaffolds Embedding PLGA Microparticles For Controlled Growth Factor Delivery In Tissue Engineering, *Biomaterials*, 30 (2009) 2571-2581.

[20] X. Wang, E. Wenk, X. Zhang, L. Meinel, G. Vunjak-Novakovic, D.L. Kaplan, Growth Factor Gradients Via Microsphere Delivery In Biopolymer Scaffolds For Osteochondral Tissue Engineering, *Journal of controlled release : official journal of the Controlled Release Society*, 134 (2009) 81-90.

[21] E. Wenk, A.J. Wandrey, H.P. Merkle, L. Meinel, Silk Fibroin Spheres As A Platform For Controlled Drug Delivery, *Journal of controlled release : official journal of the Controlled Release Society*, 132 (2008) 26-34.

[22] L. Uebersax, H.P. Merkle, L. Meinel, Insulin-Like Growth Factor I Releasing Silk Fibroin Scaffolds Induce Chondrogenic Differentiation Of Human Mesenchymal Stem Cells, *Journal of controlled release : official journal of the Controlled Release Society*, 127 (2008) 12-21.

- 
- [23] V. Luginbuehl, E. Wenk, A. Koch, B. Gander, H.P. Merkle, L. Meinel, Insulin-Like Growth Factor I-Releasing Alginate-Tricalciumphosphate Composites For Bone Regeneration, *Pharmaceutical research*, 22 (2005) 940-950.
- [24] L. Meinel, E. Zoidis, J. Zapf, P. Hassa, M.O. Hottiger, J.A. Auer, R. Schneider, B. Gander, V. Luginbuehl, R. Bettschart-Wolfisberger, O.E. Illi, H.P. Merkle, B.v. Rechenberg, Localized Insulin-Like Growth Factor I Delivery To Enhance New Bone Formation, *Bone*, 33 (2003) 660-672.
- [25] L. Meinel, O.E. Illi, J. Zapf, M. Malfanti, H.P. Merkle, B. Gander, Stabilizing Insulin-Like Growth Factor-I In Poly(D,L-Lactide-Co-Glycolide) Microspheres, *Journal of Controlled Release*, 70 (2001) 193-202.
- [26] M.E. Davis, P.C.H. Hsieh, T. Takahashi, Q. Song, S.G. Zhang, R.D. Kamm, A.J. Grodzinsky, P. Anversa, R.T. Lee, Local Myocardial Insulin-Like Growth Factor 1 (IGF-1) Delivery With Biotinylated Peptide Nanofibers Improves Cell Therapy For Myocardial Infarction, *Proceedings of the National Academy of Sciences of the United States of America*, 103 (2006) 8155-8160.
- [27] M.M. Rechler, Insulin-Like Growth-Factor Binding-Proteins, *Vitamins and Hormones*, Vol 47, 47 (1993) 1-114.
- [28] A. Denley, L.J. Cosgrove, G.W. Booker, J.C. Wallace, B.E. Forbes, Molecular Interactions Of The IGF System, *Cytokine & growth factor reviews*, 16 (2005) 421-439.
- [29] J. Frystyk, Free Insulin-Like Growth Factors - Measurements And Relationships To Growth Hormone Secretion And Glucose Homeostasis, *Growth Hormone & IGF Research*, 14 (2004) 337-375.

## CHAPTER I

---

- [30] H.P. Guler, J. Zapf, C. Schmid, E.R. Froesch, Insulin-Like Growth Factor-I And Factor-II In Healthy Man - Estimations Of Half-Lives And Production-Rates, *Acta Endocrinologica*, 121 (1989) 753-758.
- [31] Y.R. Boisclair, R.P. Rhoads, I. Ueki, J. Wang, G.T. Ooi, The acid-labile subunit (ALS) of the 150 kDa IGF-binding protein complex: an important but forgotten component of the circulating IGF system, *Journal of Endocrinology*, 170 (2001) 63-70.
- [32] F.E. Carrick, M.G. Hinds, K.A. McNeil, J.C. Wallace, B.E. Forbes, R.S. Norton, Interaction of insulin-like growth factor (IGF)-I and -II with IGF binding protein-2: mapping the binding surfaces by nuclear magnetic resonance, *Journal of Molecular Endocrinology*, 34 (2005) 685-698.
- [33] C.M. Duan, Q.J. Xu, Roles Of Insulin-Like Growth Factor (IGF) Binding Proteins In Regulating IGF Actions, *Gen. Comp. Endocrinol.*, 142 (2005) 44-52.
- [34] X.L. Yan, B.E. Forbes, K.A. McNeil, R.C. Baxter, S.M. Firth, Role of N- and C-terminal residues of insulin-like growth factor (IGF)-binding protein-3 in regulating IGF complex formation and receptor activation, *Journal of Biological Chemistry*, 279 (2004) 53232-53240.
- [35] [http://www.ema.europa.eu/docs/en\\_GB/document\\_library/EPAR\\_-\\_Product\\_Information/human/000704/WC500032225.pdf](http://www.ema.europa.eu/docs/en_GB/document_library/EPAR_-_Product_Information/human/000704/WC500032225.pdf).
- [36] R.G. Clark, Recombinant Human Insulin-Like Growth Factor I (IGF-1): Risks And Benefits Of Normalizing Blood IGF-I Concentrations, *Hormone Research*, 62 (2004) 93-100.
- [37] S.E. Fineberg, T. Kawabata, D. Finco-Kent, C. Liu, A. Krasner, Antibody Response To Inhaled Insulin In Patients With Type 1 Or Type 2 Diabetes. An Analysis Of Initial Phase II And III Inhaled Insulin (Exubera) Trials And A Two-Year Extension Trial, *Journal of Clinical Endocrinology & Metabolism*, 90 (2005) 3287-3294.



- 
- [38] C.L. Olsen, E. Chan, D.S. Turner, M. Iravani, M. Nagy, J.L. Selam, N.D. Wong, K. Waxman, M.A. Charles, Insulin Antibody-Responses After Long-Term Intraperitoneal Insulin Administration Via Implantable Programmable Insulin Delivery Systems, *Diabetes Care*, 17 (1994) 169-176.
- [39] D.A. Brooks, Immune Response To Enzyme Replacement Therapy In Lysosomal Storage Disorder Patients And Animal Models, *Mol. Genet. Metab.*, 68 (1999) 268-275.
- [40] N. Dybdal, M. Elwell, B. Christian, R. Clark, P. Fielder, D. Kennedy, D. Shopp, A. Thakur, J. Clarke, Lifetime (104 Week) Daily Subcutaneous rhIGF-I Treatment In The Rat (Abstract), 85th Annual Meeting of the Endocrine Society, Philadelphia, 3-318.
- [41] G. Guercio, M.A. Rivarola, E. Chaler, M. Maceiras, A. Belgorosky, Relationship Between The GH/IGF-I Axis, Insulin Sensitivity, And Adrenal Androgens In Normal Prepubertal And Pubertal Boys, *Journal of Clinical Endocrinology & Metabolism*, 87 (2002) 1162-1169.
- [42] M. Morishita, N.A. Peppas, Is The Oral Route Possible For Peptide And Protein Drug Delivery, *Drug Discov. Today*, 11 (2006) 905-910.
- [43] E. Mathiowitz, J.S. Jacob, Y.S. Jong, G.P. Carino, D.E. Chickering, P. Chaturvedi, C.A. Santos, K. Vijayaraghavan, S. Montgomery, M. Bassett, C. Morrell, Biologically Erodable Microsphere As Potential Oral Drug Delivery System, *Nature*, 386 (1997) 410-414.
- [44] A.M. Lowman, M. Morishita, M. Kajita, T. Nagai, N.A. Peppas, Oral Delivery Of Insulin Using Ph-Responsive Complexation Gels, *Journal of pharmaceutical sciences*, 88 (1999) 933-937.
- [45] M. Saffran, G.S. Kumar, C. Savariar, J.C. Burnham, F. Williams, D.C. Neckers, A New Approach To The Oral-Administration Of Insulin And Other Peptide Drugs, *Science*, 233 (1986) 1081-1084.

## CHAPTER I

---

- [46] P. Fonte, F. Araujo, S. Reis, B. Sarmento, Oral Insulin Delivery: How Far Are We?, *Journal of diabetes science and technology*, 7 (2013) 520-531.
- [47] L. Heinemann, Y. Jacques, Oral Insulin And Buccal Insulin: A Critical Reappraisal, *Journal of diabetes science and technology*, 3 (2009) 568-584.
- [48] C. Damge, C.P. Reis, P. Maincent, Nanoparticle Strategies For The Oral Delivery Of Insulin, *Expert Opin. Drug Deliv.*, 5 (2008) 45-68.
- [49] L. Illum, Nasal Drug Delivery - Possibilities, Problems And Solutions, *Journal of Controlled Release*, 87 (2003) 187-198.
- [50] W.A. Ritschel, G.B. Ritschel, B.E.C. Ritschel, P.W. Lucker, Rectal Delivery System For Insulin, *Methods Find. Exp. Clin. Pharmacol.*, 10 (1988) 645-656.
- [51] L.H. du Plessis, A.F. Kotze, H.E. Junginger, Nasal And Rectal Delivery Of Insulin With Chitosan And N-Trimethyl Chitosan Chloride, *Drug Deliv.*, 17 (2010) 399-407.
- [52] <http://www.fda.gov/downloads/advisorycommittees/committeesmeetingmaterials/drugs/endocrinologicandmetabolicdrugsadvisorycommittee/ucm390865.pdf>.
- [53] [http://www.ema.europa.eu/docs/en\\_GB/document\\_library/EPAR\\_-\\_Product\\_Information/human/000588/WC500054704.pdf](http://www.ema.europa.eu/docs/en_GB/document_library/EPAR_-_Product_Information/human/000588/WC500054704.pdf).
- [54] J. Fransson, A. Hagman, Oxidation Of Human Insulin-Like Growth Factor I In Formulation Studies .2. Effects Of Oxygen, Visible Light, And Phosphate On Methionine Oxidation In Aqueous Solution And Evaluation Of Possible Mechanisms, *Pharmaceutical research*, 13 (1996) 1476-1481.
- [55] J.R. Fransson, Oxidation Of Human Insulin-Like Growth Factor I In Formulation Studies .3. Factorial Experiments Of The Effects Of Ferric Ions, EDTA, And Visible Light On Methionine

---

Oxidation And Covalent Aggregation In Aqueous Solution, *Journal of pharmaceutical sciences*, 86 (1997) 1046-1050.

[56] I. Schultz, F. Vollmers, T. Lühmann, J.-C. Rybak, R. Wittmann, K. Stank, H. Steckel, B. Kardziej, M. Schmidt, P. Högger, L. Meinel, Pulmonary Insulin-Like Growth Factor I Delivery From Trehalose And Silk-Fibroin Microparticles, *ACS Biomaterials Science & Engineering*, (2015) 150129161644009.

[57] R.I. Henkin, Inhaled Insulin-Intrapulmonary, Intranasal, And Other Routes Of Administration: Mechanisms Of Action, *Nutrition*, 26 (2010) 33-39.

[58] S. Turker, E. Onur, Y. Ozer, Nasal Route And Drug Delivery Systems, *Pharm. World Sci.*, 26 (2004) 137-142.

[59] R.G. Thorne, S. Lagalwar, Y.E. Rahman, W.H. Frey, II, Intranasal Administration Of Insulin-Like Growth Factor-I (IGF-I): A Non-Invasive CNS Drug Delivery Strategy For Bypassing The Blood-Brain Barrier, *Growth Hormone and IGF Research*, 9 (1999) 387.

[60] X.F. Liu, J.R. Fawcett, R.G. Thorne, T.A. DeFor, W.H. Frey, Intranasal Administration Of Insulin-Like Growth Factor-I Bypasses The Blood-Brain Barrier And Protects Against Focal Cerebral Ischemic Damage, *Journal of the Neurological Sciences*, 187 (2001) 91-97.

[61] R.G. Thorne, G.J. Pronk, V. Padmanabhan, W.H. Frey, Delivery Of Insulin-Like Growth Factor-I To The Rat Brain And Spinal Cord Along Olfactory And Trigeminal Pathways Following Intranasal Administration, *Neuroscience*, 127 (2004) 481-496.

[62] S. Lin, L.-W. Fan, P.G. Rhodes, Z. Cai, Intranasal Administration Of IGF-1 Attenuates Hypoxic-Ischemic Brain Injury In Neonatal Rats, *Experimental Neurology*, 217 (2009) 361-370.

## CHAPTER I

---

[63] S. Lin, P.G. Rhodes, Z. Cai, Whole Body Hypothermia Broadens The Therapeutic Window Of Intranasally Administered IGF-1 In A Neonatal Rat Model Of Cerebral Hypoxia-Ischemia, *Brain Research*, 1385 (2011) 246-256.

[64] Z. Cai, L.W. Fan, S. Lin, Y. Pang, P.G. Rhodes, Intranasal Administration Of Insulin-Like Growth Factor-1 Protects Against Lipopolysaccharide-Induced Injury In The Developing Rat Brain, *Neuroscience*, 194 (2011) 195-207.

[65] C. Lopes, M. Ribeiro, A.I. Duarte, S. Humbert, F. Saudou, L.P. de Almeida, M. Hayden, A.C. Rego, IGF-1 Intranasal Administration Rescues Huntington's Disease Phenotypes In Yac128 Mice, *Mol. Neurobiol.*, 49 (2014) 1126-1142.

[66] G. Paslakis, W.F. Blum, M. Deuschle, Intranasal Insulin-Like Growth Factor I (IGF-I) As A Plausible Future Treatment Of Depression, *Med. Hypotheses*, 79 (2012) 222-225.

[67] P.J.S. Vig, S.H. Subramony, D.R. D'Souza, J. Wei, M.E. Lopez, Intranasal Administration Of IGF-I Improves Behavior And Purkinje Cell Pathology In SCA1 Mice, *Brain Research Bulletin*, 69 (2006) 573-579.

[68] M.I.U. Remigius Uchenna Agu, Michoel Armand, Renaat Kinget, N. Verbeke, The Lung As A Route For Systemic Delivery Of Therapeutic Proteins And Peptides, (2001).

[69] J.S. Patton, J. Bukar, S. Nagarajan, Inhaled Insulin, *Adv. Drug Deliv. Rev.*, 35 (1999) 235-247.

[70] J. Kling, Sanofi To Propel Inhalable Insulin Afrezza Into Market, *Nat. Biotechnol.*, 32 (2014) 851-852.

[71] K. Rave, E. Potocka, L. Heinemann, T. Heise, A.H. Boss, M. Marino, D. Costello, R. Chen, Pharmacokinetics And Linear Exposure Of AFRESA Compared With The Subcutaneous Injection Of Regular Human Insulin, *Diabetes, obesity & metabolism*, 11 (2009) 715-720.

- 
- [72] J. Rosenstock, D.L. Lorber, L. Gnudi, C.P. Howard, D.W. Bilheimer, P.C. Chang, R.E. Petrucci, A.H. Boss, P.C. Richardson, Prandial Inhaled Insulin Plus Basal Insulin Glargine Versus Twice Daily Biaspart Insulin For Type 2 Diabetes: A Multicentre Randomised Trial, *The Lancet*, 375 (2010) 2244-2253.
- [73] E.M. Pritchard, P.B. Dennis, F. Omenetto, R.R. Naik, D.L. Kaplan, Review Physical And Chemical Aspects Of Stabilization Of Compounds In Silk, *Biopolymers*, 97 (2012) 479-498.
- [74] N.V. Katre, J. Asherman, H. Schaefer, M. Hora, Multivesicular Liposome (Depofoam) Technology For The Sustained Delivery Of Insulin-Like Growth Factor-I (IGF-I), *Journal of pharmaceutical sciences*, 87 (1998) 1341-1346.
- [75] A. Clark, T.A. Milbrandt, J.Z. Hilt, D.A. Puleo, Retention Of Insulin-Like Growth Factor I Bioactivity During The Fabrication Of Sintered Polymeric Scaffolds, *Biomedical Materials*, 9 (2014).
- [76] M. Singh, B. Shirley, K. Bajwa, E. Samara, M. Hora, D. O'Hagan, Controlled Release Of Recombinant Insulin-Like Growth Factor From A Novel Formulation Of Polylactide-Co-Glycolide Microparticles, *Journal of Controlled Release*, 70 (2001) 21-28.
- [77] L. Meinel, D.L. Kaplan, Silk Constructs For Delivery Of Musculoskeletal Therapeutics, *Adv. Drug Deliv. Rev.*, 64 (2012) 1111-1122.
- [78] E. Wenk, H.P. Merkle, L. Meinel, Silk Fibroin As A Vehicle For Drug Delivery Applications, *Journal of controlled release : official journal of the Controlled Release Society*, 150 (2011) 128-141.
- [79] S. Hofmann, C.T. Foo, F. Rossetti, M. Textor, G. Vunjak-Novakovic, D.L. Kaplan, H.P. Merkle, L. Meinel, Silk Fibroin As An Organic Polymer For Controlled Drug Delivery, *Journal of controlled release : official journal of the Controlled Release Society*, 111 (2006) 219-227.

## CHAPTER I

---

- [80] L. Wang, J. Shansky, C. Borselli, D. Mooney, H. Vandeburgh, Design And Fabrication Of A Biodegradable, Covalently Crosslinked Shape-Memory Alginate Scaffold For Cell And Growth Factor Delivery, *Tissue engineering. Part A*, 18 (2012) 2000-2007.
- [81] K. Fu, D.W. Pack, A.M. Klibanov, R. Langer, Visual Evidence Of Acidic Environment Within Degrading Poly(Lactic-Co-Glycolic Acid) (PLGA) Microspheres, *Pharmaceutical research*, 17 (2000) 100-106.
- [82] R.M. Williams, A. McDonald, M. O'Savage, D.B. Dunger, Mecasermin Rinfabate: RhIGF-1/RhIGFbp-3 Complex: Iplex (TM), *Expert Opinion on Drug Metabolism & Toxicology*, 4 (2008) 311-324.
- [83] S.F. Kemp, K.M. Thrailkill, Investigational Agents For The Treatment Of Growth Hormone-Insensitivity Syndrome, *Expert Opin. Investig. Drugs*, 15 (2006) 409-415.
- [84] <http://www.fda.gov/Drugs/ResourcesForYou/HealthProfessionals/ucm118117.htm>.
- [85] J.M. Harris, R.B. Chess, Effect Of Pegylation On Pharmaceuticals, *Nat. Rev. Drug Discov.*, 2 (2003) 214-221.
- [86] F.M. Veronese, G. Pasut, Pegylation, Successful Approach To Drug Delivery, *Drug Discov. Today*, 10 (2005) 1451-1458.
- [87] [http://www.oncaspar.de/pdf/20120730\\_PB\\_Oncaspar\\_DE.pdf](http://www.oncaspar.de/pdf/20120730_PB_Oncaspar_DE.pdf).
- [88] [http://www.ema.europa.eu/docs/en\\_GB/document\\_library/EPAR\\_-\\_Product\\_Information/human/000395/WC500039195.pdf](http://www.ema.europa.eu/docs/en_GB/document_library/EPAR_-_Product_Information/human/000395/WC500039195.pdf).
- [89] [http://www.ema.europa.eu/docs/en\\_GB/document\\_library/EPAR\\_-\\_Summary\\_for\\_the\\_public/human/001037/WC500069733.pdf](http://www.ema.europa.eu/docs/en_GB/document_library/EPAR_-_Summary_for_the_public/human/001037/WC500069733.pdf).
- [90] [http://www.ema.europa.eu/docs/en\\_GB/document\\_library/EPAR\\_-\\_Summary\\_for\\_the\\_public/human/002810/WC500179078.pdf](http://www.ema.europa.eu/docs/en_GB/document_library/EPAR_-_Summary_for_the_public/human/002810/WC500179078.pdf).

[91] J. Tack, M. Corsetti, Naloxegol For The Treatment Of Opioid-Induced Constipation, Expert review of gastroenterology & hepatology, 8 (2014) 855-861.

[92] [http://www.ema.europa.eu/docs/en\\_GB/document\\_library/Medicine\\_QA/2013/06/WC500144933.pdf](http://www.ema.europa.eu/docs/en_GB/document_library/Medicine_QA/2013/06/WC500144933.pdf).

[93] [http://www.ema.europa.eu/docs/en\\_GB/document\\_library/EPAR\\_-\\_Product\\_Information/human/002208/WC500138318.pdf](http://www.ema.europa.eu/docs/en_GB/document_library/EPAR_-_Product_Information/human/002208/WC500138318.pdf).

[94] [http://www.ema.europa.eu/docs/en\\_GB/document\\_library/EPAR\\_-\\_Summary\\_for\\_the\\_public/human/000739/WC500033667.pdf](http://www.ema.europa.eu/docs/en_GB/document_library/EPAR_-_Summary_for_the_public/human/000739/WC500033667.pdf).

[95] [http://www.ema.europa.eu/docs/en\\_GB/document\\_library/EPAR\\_-\\_Summary\\_for\\_the\\_public/human/000620/WC500026216.pdf](http://www.ema.europa.eu/docs/en_GB/document_library/EPAR_-_Summary_for_the_public/human/000620/WC500026216.pdf).

[96] [http://www.ema.europa.eu/docs/en\\_GB/document\\_library/EPAR\\_-\\_Product\\_Information/human/000420/WC500025945.pdf](http://www.ema.europa.eu/docs/en_GB/document_library/EPAR_-_Product_Information/human/000420/WC500025945.pdf).

[97] [http://www.ema.europa.eu/docs/en\\_GB/document\\_library/EPAR\\_-\\_Product\\_Information/human/000409/WC500054629.pdf](http://www.ema.europa.eu/docs/en_GB/document_library/EPAR_-_Product_Information/human/000409/WC500054629.pdf).

[98] A. Gabizon, H. Shmeeda, Y. Barenholz, Pharmacokinetics Of Pegylated Liposomal Doxorubicin - Review Of Animal And Human Studies, Clin. Pharmacokinet., 42 (2003) 419-436.

[99] [http://www.ema.europa.eu/docs/en\\_GB/document\\_library/EPAR\\_-\\_Product\\_Information/human/000089/WC500020180.pdf](http://www.ema.europa.eu/docs/en_GB/document_library/EPAR_-_Product_Information/human/000089/WC500020180.pdf).

[100] [http://www.ema.europa.eu/docs/en\\_GB/document\\_library/EPAR\\_-\\_Product\\_Information/human/000280/WC500039388.pdf](http://www.ema.europa.eu/docs/en_GB/document_library/EPAR_-_Product_Information/human/000280/WC500039388.pdf).

[101] [http://www.accessdata.fda.gov/drugsatfda\\_docs/label/2008/019818s042lbl.pdf](http://www.accessdata.fda.gov/drugsatfda_docs/label/2008/019818s042lbl.pdf).

## CHAPTER I

---

[102] F. Metzger, W. Sajid, S. Saenger, C. Staudenmaier, C. van der Poel, B. Sobottka, A. Schuler, M. Sawitzky, R. Poirier, D. Tuerck, E. Schick, A. Schaubmar, F. Hesse, K. Amrein, H. Loetscher, G.S. Lynch, A. Hoeflich, P. De Meyts, H.J. Schoenfeld, Separation Of Fast From Slow Anabolism By Site-Specific Pegylation Of Insulin-Like Growth Factor I (IGF-I), *Journal of Biological Chemistry*, 286 (2011) 19501-19510.

[103] S. Saenger, C. Goeldner, J.R. Frey, L. Ozmen, S. Ostrowitzki, W. Spooren, T.M. Ballard, E. Prinssen, E. Borroni, F. Metzger, PEGylation Enhances The Therapeutic Potential For Insulin-Like Growth Factor I In Central Nervous System Disorders, *Growth hormone & IGF research : official journal of the Growth Hormone Research Society and the International IGF Research Society*, 21 (2011) 292-303.

[104] S. Saenger, B. Holtmann, M.R. Nilges, S. Schroeder, A. Hoeflich, H. Kletzl, W. Spooren, S. Ostrowitzki, T. Hanania, M. Sendtner, F. Metzger, Functional Improvement In Mouse Models Of Familial Amyotrophic Lateral Sclerosis By PEGylated Insulin-Like Growth Factor I Treatment Depends On Disease Severity, *Amyotroph. Lateral. Scler.*, 13 (2012) 418-429.

[105] K.J. Martins, S.M. Gehrig, T. Naim, S. Saenger, D. Baum, F. Metzger, G.S. Lynch, Intramuscular Administration Of PEGylated IGF-I Improves Skeletal Muscle Regeneration After Myotoxic Injury, *Growth hormone & IGF research : official journal of the Growth Hormone Research Society and the International IGF Research Society*, 23 (2013) 128-133.

[106] M. Sivaramakrishnan, A.S. Kashyap, B. Arnrein, S. Saenger, S. Meier, C. Staudenmaier, Z. Upton, F. Metzger, PEGylation Of Lysine Residues Reduces The Pro-Migratory Activity Of IGF-I, *Biochimica Et Biophysica Acta-General Subjects*, 1830 (2013) 4734-4742.



- 
- [107] W.G. Zhang, T.A. Gustafson, W.J. Rutter, J.D. Johnson, Positively Charged Side-Chains In The Insulin-Like Growth-Factor-I C-Regions And D-Regions Determine Receptor-Binding Specificity, *Journal of Biological Chemistry*, 269 (1994) 10609-10613.
- [108] M.L. Bayne, J. Applebaum, G.G. Chicchi, R.E. Miller, M.A. Cascieri, The Roles Of Tyrosine-24, Tyrosine-31, And Tyrosine-60 In The High-Affinity Binding Of Insulin-Like Growth Factor-I To The Type-1 Insulin-Like Growth-Factor Receptor, *Journal of Biological Chemistry*, 265 (1990) 15648-15652.
- [109] M.A. Cascieri, G.G. Chicchi, J. Applebaum, N.S. Hayes, B.G. Green, M.L. Bayne, Mutants Of Human Insulin-Like Growth Factor-I With Reduced Affinity For The Type-1 Insulin-Like Growth-Factor Receptor, *Biochemistry*, 27 (1988) 3229-3233.
- [110] A.P. Kolychev, Structural Organization Of Binding Determinants In The Molecule Of Insulin-Like Growth Factor-I (IGF-I), *J. Evol. Biochem. Physiol.*, 46 (2010) 87-112.
- [111] D.R. Hodgson, F.E.B. May, B.R. Westley, Mutations At Position-11 And Position-60 Of Insulin-Like-Growth-Factor-1 Reveal Differences Between Its Interactions With The Type-I Insulin-Like-Growth-Factor Receptor And The Insulin-Receptor, *Eur. J. Biochem.*, 233 (1995) 299-309.
- [112] M. Schlapschy, U. Binder, C. Borger, I. Theobald, K. Wachinger, S. Kisling, D. Haller, A. Skerra, PASylation: A Biological Alternative To Pegylation For Extending The Plasma Half-Life Of Pharmaceutically Active Proteins, *Protein Eng. Des. Sel.*, 26 (2013) 489-501.
- [113] R. Liebner, R. Mathaes, M. Meyer, T. Hey, G. Winter, A. Besheer, Protein HESylation For Half-Life Extension: Synthesis, Characterization And Pharmacokinetics Of HESylated Anakinra, *Eur. J. Pharm. Biopharm.*, 87 (2014) 378-385.

## CHAPTER I

---

- [114] D. Sleep, J. Cameron, L.R. Evans, Albumin As A Versatile Platform For Drug Half-Life Extension, *Biochimica Et Biophysica Acta-General Subjects*, 1830 (2013) 5526-5534.
- [115] A. Philippou, M. Maridaki, S. Pneumaticos, M. Koutsilieris, The Complexity Of The IGF1 Gene Splicing, Posttranslational Modification And Bioactivity, *Molecular Medicine*, 20 (2014) 202-214.
- [116] D.J. Glass, M. Fornaro, Stabilized Insulin-like Growth Factor Polypeptides, in: *Patent Application Publication US 2010/0234290 A1*, NOVARTIS AG, United States, 2010.
- [117] S. Eger, M. Scheffner, A. Marx, M. Rubini, Formation Of Ubiquitin Dimers Via Azide-Alkyne Click Reaction, *Methods in molecular biology*, 832 (2012) 589-596.
- [118] W. Wan, J.M. Tharp, W.R. Liu, Pyrrolysyl-tRNA Synthetase: An Ordinary Enzyme But An Outstanding Genetic Code Expansion Tool, *Biochimica et biophysica acta*, 1844 (2014) 1059-1070.
- [119] J.E. Moses, A.D. Moorhouse, The Growing Applications Of Click Chemistry, *Chem. Soc. Rev.*, 36 (2007) 1249-1262.
- [120] T. Tokunou, R. Miller, P. Patwari, M.E. Davis, V.F. Segers, A.J. Grodzinsky, R.T. Lee, Engineering Insulin-Like Growth Factor-1 For Local Delivery, *FASEB journal : official publication of the Federation of American Societies for Experimental Biology*, 22 (2008) 1886-1893.
- [121] R.E. Miller, A.J. Grodzinsky, K. Cummings, A.H. Plaas, A.A. Cole, R.T. Lee, P. Patwari, Intraarticular Injection Of Heparin-Binding Insulin-Like Growth Factor 1 Sustains Delivery Of Insulin-Like Growth Factor 1 To Cartilage Through Binding To Chondroitin Sulfate, *Arthritis and rheumatism*, 62 (2010) 3686-3694.

[122] F.S. Loffredo, J.R. Pancoast, L. Cai, T. Vannelli, J.Z. Dong, R.T. Lee, P. Patwari, Targeted Delivery To Cartilage Is Critical For In Vivo Efficacy Of Insulin-Like Growth Factor 1 In A Rat Model Of Osteoarthritis, *Arthritis & Rheumatology*, 66 (2014) 1247-1255.

[123] R.S. Khan, M.D. Martinez, J.C. Sy, K.D. Pendergrass, P.-I. Che, M.E. Brown, E.B. Cabigas, M. Dasari, N. Murthy, M.E. Davis, Targeting Extracellular DNA To Deliver IGF-1 To The Injured Heart, *Scientific Reports*, 4 (2014).

### ***Copyright***

This chapter is reprinted with permission from Schultz, I., Wurzel, J., Meinel, L. (2015). Drug Delivery of Insulin-like Growth Factor I. *European Journal of Pharmaceutics and Biopharmaceutics*, 2015, in press, doi:10.1016/j.ejpb.2015.04.026. License Date: May 26, 2015, License Number: 3636480399286.



# CHAPTER II

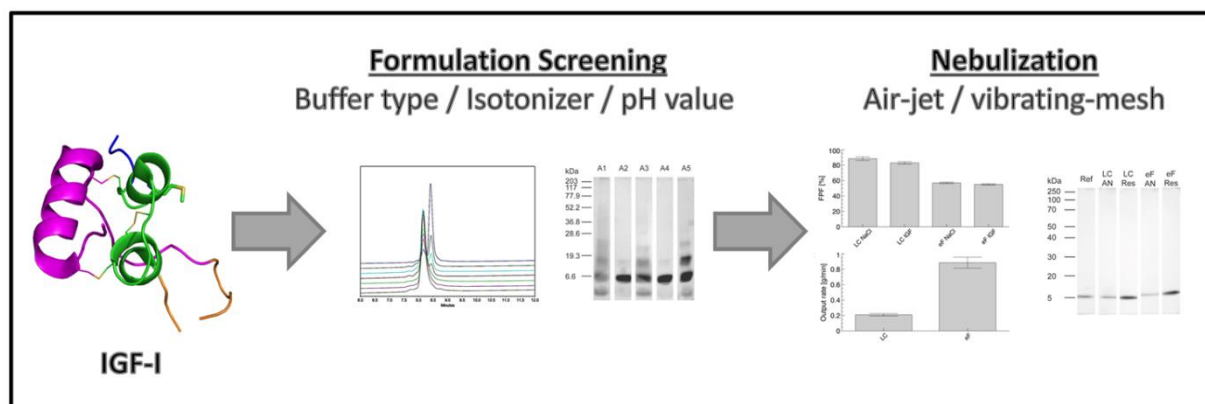
## INSULIN-LIKE GROWTH FACTOR-I AEROSOL FORMULATIONS FOR PULMONARY DELIVERY

Oliver Germershaus <sup>1,†</sup>, Isabel Schultz <sup>1,†</sup>, Tessa Lühmann <sup>1</sup>, Moritz Beck-Broichsitter <sup>2</sup>, Petra Högger <sup>1</sup>, Lorenz Meinel <sup>1,\*</sup>

<sup>1</sup>Institute for Pharmacy and Food Chemistry, University of Wuerzburg, Am Hubland, DE-97074 Wuerzburg, Germany

<sup>2</sup>Medical Clinic II, Department of Internal Medicine, University of Giessen, Klinikstrasse 33, DE-35392 Giessen, Germany

<sup>†</sup>the authors contributed equally to this work



*European Journal of Pharmaceutics and Biopharmaceutics* 2013 Sep;85(1):61-8.

doi: 10.1016/j.ejpb.2013.03.011.

### ABSTRACT

Injectable insulin-like growth factor-I (IGF-I) is therapeutically deployed for severe IGF-I deficiency and clinically explored for various other indications such as muscle wasting disease. In the present study, liquid IGF-I formulations for pulmonary application were screened with regard to buffer type (acetate, citrate, histidine and succinate), sodium chloride concentration (50 - 150 mM), and pH value (4.5 - 6.5). Methionine 59 oxidation (Met(o)) was observed in acetate buffer along with reducible dimer and trimer formation at low pH. Oxidation correlated with formation of covalent, reducible aggregates, and complete loss of potency was observed for severely aggregated samples. Bioactivity was partly retained in cases where complete oxidation but limited aggregation was found. In contrast, IGF-I integrity was preserved in histidine buffer during accelerated stability. After delivery from air-jet or vibrating-mesh nebulizers, limited Met(o) formation and no aggregation was observed. Nebulization performance regarding aerosol output rate, mass median aerodynamic diameter and fine particle fraction for liquid IGF-I formulation was comparable to 0.9% sodium chloride reference, confirming the suitability for pulmonary application. In conclusion, different IGF-I liquid formulations were studied and compositions were identified maintaining bioactivity and chemical stability throughout storage at accelerated conditions for up to 4 months as well as compatibility with air-jet and vibrating-mesh nebulizers.

---

## INTRODUCTION

Human insulin-like growth factor I (IGF-I, **Figure 1**) is a 7.6 kDa anabolic hormone playing a pivotal role in human growth and tissue regeneration [1, 2] at least in part due to the polypeptide's impact on glucose homeostasis [1, 3]. IGF-I in extracellular liquids is largely bound to a family of binding proteins (IGFBPs) impacting IGF-I metabolism and distribution. The plasma half-life of free IGF-I was estimated as short as 15 min, but is substantially prolonged up to several hours when bound to IGFBPs in binary and ternary complexes [1]. Recombinant human IGF-I (Mecasermin) has a reported half-life of 5.8 hours at doses of 0.12 mg/kg after subcutaneous injection, likely resulting from IGFBP binding upon administration [4]. The relatively short half-life and the paracrine IGF-I activity have sparked interest in the development of parenteral IGF-I depot systems providing sustained localized delivery, e.g. from poly(D,L-lactide-*co*-glycolide)acid (PLGA) microspheres [5-7]. However, PLGA microspheres may suffer from significant burst release, protein acylation, and protein degradation due to acid catalyzed hydrolysis of the PLGA core [8-11]. Hence, easy to use, stable and convenient formulations are the focus of this contribution reducing discomfort during administration and increasing patient compliance.

Successful pulmonary administration of insulin was reported as early as 1924 [12, 13]. With the development and marketing approval of Exubera<sup>®</sup> (Nektar Therapeutics and Pfizer), it was shown that peptides of the insulin family can be safely and efficiently delivered by the pulmonary route and that this approach is technically and clinically feasible [14-16]. Given the structural similarity of IGF-I and insulin proteins we hypothesized that IGF-I is a viable candidate for pulmonary delivery [17, 18]. Exubera<sup>®</sup> was unsuccessfully commercialized, however, has clearly demonstrated the excellent feasibility for the pulmonary route and from a pharmaceutical development perspective. IGF-I has a couple of advantages over insulin when it comes to pulmonary administration, perhaps most importantly that the pharmacodynamic impact in response to pharmacokinetic fluctuations is by far less critical or the intermittent versus chronic treatment approach and among other reasons [19] – overall shifting the risk-benefit ratio of IGF-I versus insulin in a positive direction.

Despite the fact that IGF-I is commercially available, limited data has been published to date with respect to IGF-I formulation stability. Fransson et al. in a series of publications studied

factors impacting IGF-I oxidation in liquid and solid state [20-22] as well as its solubility and physical stability in different solvents [23].

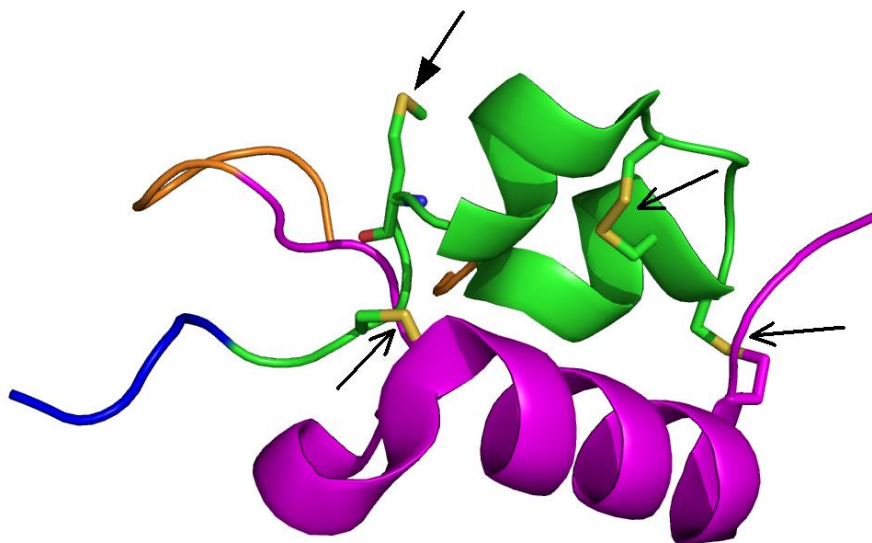


**Figure 1.** Structure of IGF-I with methionine 59 (filled arrow) and intramolecular disulfid bridges (open arrows). The structure was taken from 1GZR.pdb.

However, none of these studies identified a liquid IGF-I formulation suitable for long-term storage. Such information can only be retrieved from commercial products such as Increlex<sup>®</sup> (Ipsen Pharmaceuticals), which is composed of 10 g/L Mecasermin, 9 g/L benzyl alcohol, 100 mM sodium chloride, 2 g/L polysorbate 20, and 50 mM acetate at a pH value of approximately 5.4 [4]. Furthermore, to date no studies investigating IGF-I stability during nebulization were published to our knowledge.

This study identified formulation compositions suitable for long-term storage of a liquid IGF-I suitable for nebulization. Such products are typically stored at 2-8 °C; we therefore decided to investigate product stability under accelerated conditions at 25 °C [24]. Furthermore, the product was analyzed nebulization performance with regard to nebulizer output rate, mass median aerodynamic diameter (MMAD) and fine particle fraction (FPF) as well as IGF-I stability during nebulization.



---

## MATERIALS AND METHODS

### Materials

Recombinant human IGF-I was a kind gift from Novartis Pharma AG (Basel, Switzerland). IGF-I stock solution was provided at 7.6 g/L and was stored at -80 °C until use. Eagle's minimum essential medium, bovine serum albumin (BSA), glutamine, non-essential amino acids (NEA), penicillin-streptomycin and 3-[4,5-dimethylthiazol-2-yl]-2,5 diphenyltetrazolium bromide (MTT) were purchased from Sigma Aldrich (Schnelldorf/Taufkirchen, Germany). Fetal bovine serum (FBS) was from Gibco (Darmstadt, Germany). Acetonitrile and trifluoroacetic acid were of HPLC grade (VWR, Ismaning, Germany). All other chemicals used were at least of ReagentPlus grade and were obtained from Sigma-Aldrich (unless noted otherwise).

### Methods

#### *Sample preparation and stability study*

A formulation screen was performed using a set of buffers (acetate, citrate, histidine and succinate) at a concentration of 50 mM and pH of 4.5, 5.5 or 6.5. In addition, 50, 100 or 150 mM NaCl was added to the formulations. IGF-I concentration in all formulations was 0.2 g/L. All samples were sterile filtered using 0.22 µm syringe filters (Techno Plastic Products AG, Switzerland) into amber glass HPLC vials. Vials were closed with screw caps with polytetrafluoroethylene (PTFE)/silicone septum (PTFE side facing the product). All samples were stored in a closed card box at controlled room temperature (20-25 °C) for up to 4 months representing accelerated conditions under the assumption that long-term storage of the product would be at 2-8 °C [24]. At predetermined time points of 1, 2, 3, 4, 8, 12, and 16 weeks samples were withdrawn from storage and analyzed by RP-HPLC. Bioactivity and formation of covalent aggregates was analyzed at the end of the storage period.

#### *Determination of IGF-I content and purity*

IGF-I content and degradation products were assessed by RP-HPLC using a VWR Hitachi LaChromUltra HPLC system equipped with a diode array detector as previously described with modification [5]. Separation was performed using a Zorbax 300SB-CN reversed-phase

chromatography column (4.6mm \* 150mm, 5µm) at 40 °C. The flow rate was set to 0.8 mL/min, the sample volume injected per run was 20 µl. Two eluents were used, eluent A consisted of 5% acetonitrile and 0.2% trifluoroacetic acid in water and eluent B was 80% acetonitrile and 0.2% trifluoroacetic acid in water. Separation started with 74% (v/v) eluent A and was changed over 30 min to 100% eluent B. Then, initial conditions were set to wash the column. IGF-I was detected at 214 nm. The IGF-I peak area as well as total IGF-I related area were used for the evaluation.

### ***MALDI-TOF***

20 µl of each sample were desalted using Zip Tip® pipette tips (C<sub>18</sub> resin, Millipore, Billerica, MA) according to the manufacturer's instructions. 5 µl of the eluate were embedded in a matrix consisting of equal parts of napinic acid and acetonitrile (can)/0.1% trifluoroacetic acid (TFA) in water (1:4). Matrix-assisted laser desorption ionization (MALDI)-MS spectra were acquired in the linear positive mode by using an Autoflex II LRF instrument from Bruker Daltonics Inc. (Billerica, USA) fitted with a 337 nm wavelength nitrogen laser. Mass spectra were calibrated externally with protein standard I also from Bruker Daltonics Inc. (Billerica, USA), containing insulin, ubiquitin, myoglobin and cytochrom C.

### ***Reducing and Non-reducing SDS-PAGE***

SDS-PAGE was applied to identify aggregates in stored liquid IGF-I formulations. Samples were mixed with 0.35 M Tris-HCl (pH 6.8), 30% glycerol, 10% SDS, 9.3% dithiothreitol and 0.012% bromphenol blue and heated at 95 °C for 5 minutes. Afterwards the samples were transferred into the stacking gel consisting of 3.9% acrylamide (prepared from a stock solution of 30% (m/m) of acrylamide and 0.8% (m/m) of bisacrylamide), 0.125 M Tris-HCl buffer (pH 6.8), 0.1% SDS and 61.24% water. 0.05% ammonium persulfate and 0.1% N,N,N',N'-tetramethylethylenediamin (TEMED) were used for the gel polymerization. The separating gel was 12% acrylamide, 0.37 M Tris-HCl (pH 8.8), 0.1% SDS, 34.9% water, 0.03% ammonium persulfate and 0.07% TEMED. For molecular weight estimation of single bands, a SDS-PAGE standard (Bio-Rad Laboratories GmbH, München, Germany) was loaded onto the gel and the electrophoresis was carried out at 80 V. Protein was detected by silver staining (Pierce Silver Stain Kit, Thermo Fisher, Rockford,

IL, USA) following the manufacturer's instructions and gels were documented using a FluorChem FC2 imaging system (Protein Simple, Santa Clara, CA).

### ***IGF-I bioassay to assess bioactivity***

Human osteosarcoma cell proliferation is IGF-I responsive and has been used as a potency assay [25]. Briefly, MG-63 cells (ATCC-Number CRL-1427, ATCC, Manassas, VA) cultured in growth medium (MEM containing 8.8% FBS, 1.77 mM L-glutamine, 88 U/mL penicillin G and 88 µg/µL streptomycin, 0.88% non-essential amino acids (NEA)), were trypsinized and then resuspended in assay medium (MEM containing 0.452% BSA, 1.82 mM L-Glutamine, 91 U/mL penicillin G and 91 µg/µL streptomycin, 0.91% NEA) to a concentration of  $2 \times 10^5$  cells/mL. 100 µL of the suspension ( $2 \times 10^4$  cells) were transferred to each well of a 96-well tissue culture plate and incubated for 24 h at 37 °C and 5% CO<sub>2</sub>. A dilution series of IGF-I stock solution from 100 ng/mL to 0.05 ng/mL was prepared. Samples diluted to 6.25 ng/ml were applied on the same plate with the reference dilution series and incubated for 48 h at 37 °C and 5% CO<sub>2</sub>. After incubation the cells were treated with 3-(4,5-dimethylthiazol-2-yl)-2,5-diphenyltetrazolium bromide (MTT) at 5.0 g/L in PBS for 4.5 h at 37 °C. Subsequently, the medium was removed and the formed purple formazan crystals were solubilized in 2-propanol, 3% SDS and 0.04 N HCl. The absorbance of the wells was read at 570 nm using a Spectramax 250 microplate reader (Molecular Devices, Sunnyvale, CA). Relative bioactivity was calculated by fitting absorbance of reference dilution series on each 96-well plate using simple two variable exponential functions.

### ***Nebulization experiments***

All nebulization experiments were performed with formulation containing 0.2 g/L IGF-I in 50 mM histidine and 150 mM NaCl at pH 6.5. Aerosols were generated using two different nebulizers. An air-jet nebulizer Pari LC Sprint was used in conjunction with the red nozzle insert and a PariBoy SX compressor (Pari GmbH, Starnberg, Germany). In addition, a vibrating-mesh nebulizer (eFlow rapid, Pari GmbH, Starnberg, Germany) was used for nebulization. All nebulizers were loaded with 6 mL formulation at room temperature and operated continuously until 5 mL of solution were nebulized, unless stated otherwise. After passing the nebulizers,

samples were collected using a gas washing bottle holding a volume of 4 mL of 50 mM histidine buffer, 150 mM NaCl, pH 6.5. While this sampling setup did not allow for quantitative collection of the aerosol, it enabled the assessment of IGF integrity after nebulization and avoided destabilizing conditions after nebulization, such as solvent evaporation resulting in increase of protein concentration or protein degradation at the air/liquid interface. After nebulization, a sample was drawn from the nebulizer reservoir and subjected to analysis. The aerosol output was calculated by difference in weight before and after 2 minutes of nebulization and reported as nebulizer output rate in g/mL min. Aerosol particle size was determined by laser light diffraction (Helos, Sympatec, Clausthal-Zellerfeld, Germany) as described earlier [26]. The MMAD was calculated according to the following equation:

$$MMAD = VMD(\rho_p / (\rho_w \chi))^{1/2}$$

where VMD is the volume median diameter,  $\rho_p$  is the particle density ( $\text{g/cm}^3$ ),  $\rho_w$  is the density of water ( $\text{g/cm}^3$ ), and  $\chi$  is the dynamic particle shape factor (for spherical particles  $\chi = 1$ ). Particle distributions were also characterized according to geometric standard deviation (GSD) and FPF (percentage of particles  $\leq 5.25 \mu\text{m}$ ). As a reference, 154 mM NaCl solution was used to specify aerosol characteristics [27].

### *Statistical analysis*

MODDE 9.0 (Umetrics, Umea, Sweden) was used to establish and analyze the experimental design. We used a full factorial screening design with one center point. Two quantitative factors (pH value and NaCl concentration) and one qualitative categorical factor (buffer type) were included into the design. This design resulted in 17 individual experiments/conditions. As response variable, (i) the rate of the decrease of the IGF-I peak, (ii) the rate of decrease of the total peak area and (iii) the bioactivity were used. Analysis was performed using multiple linear regression from which scaled and centered regression coefficients were obtained for each term. The statistical significance of each term was evaluated with a level of  $p \leq 0.05$  to denote significance. The model for each response variable was optimized by backward elimination of insignificant terms ( $p > 0.05$ ) from the model. Model validity was evaluated by goodness of fit ( $R^2$ ), and goodness of prediction ( $Q^2$ ). Statistical data analysis was performed by one-way analysis of variance (ANOVA) and Tukey's or Sidak's procedure for *post hoc* comparison. Values with  $p \leq 0.05$  were considered statistically significant.

---

## RESULTS

### *Stability of IGF-I in liquid formulations*

The focus of this study was to establish suitable formulations for a potential pulmonary application of IGF-I by nebulization. Therefore, minimal formulations consisting of a buffer and isotonic component were investigated. We selected acetate, citrate, histidine and succinate buffer at 50 mM strength at pH values between 4.5 and 6.5 and chose to use sodium chloride as isotonic agent at concentrations between 50 and 150 mM. A screening approach using statistical design of experiments was chosen to obtain maximum, statistically sound information with a practicable number of experiments (**Table 1**).

The chemical stability of IGF-I was assessed by RP-HPLC, enabling separation of native IGF-I and its degradation products [5, 20, 28]. Oxidation of methionine 59 (Met(o)) was reported to be the most prominent degradation pathway for IGF-I (**Figure 1**) [20-22]. We observed a reduction of the main peak area (**Figure 2**) and an increase of the degradation peak at retention time of 8.1 minutes. The degradation peak was found to represent IGF-I species with an increased molecular weight of +16 g/mol (MALDI-TOF data not shown) presumably representing Met(o)-IGF-I as has been described before [20, 28]. Apart from chemical degradation of IGF-I, a decrease of total area of main and degradation product peaks was observed, indicating an overall loss of soluble protein (**Figure 3 A**). The impact of formulation factors on the reduction of total area and main peak area over time, respectively, was assessed by fitting the data to pseudo zero order degradation kinetics and calculation of reaction rate constants. Multiple linear regression models with the input parameters pH, buffer type and NaCl concentration were calculated for the responses (i) degradation rate coefficient for the total area and (ii) for IGF-I peak area, respectively. The response variable degradation rate of the main peak was best fitted with a reduced linear model ( $R^2=0.747$ ) with the factor buffer type being the only significant input parameter (**Figure 4 A**). Acetate buffer, independent of pH and NaCl concentration under the chosen experimental conditions resulted in rapid IGF-I oxidation and full conversion to Met(o) within 2-3 weeks at room temperature (**Figure 2**).

**Table 1.** Composition of formulations tested in the formulation screen.

<b>Formulation identifier</b>	<b>Buffer type</b>	<b>pH</b>	<b>NaCl [mM]</b>
<b>A1</b>	Acetate	4.5	150
<b>A2</b>	Acetate	6.5	150
<b>A3</b>	Acetate	4.5	50
<b>A4</b>	Acetate	6.5	50
<b>A5</b>	Acetate	5.5	100
<b>C1</b>	Citrate	4.5	150
<b>C2</b>	Citrate	6.5	150
<b>C3</b>	Citrate	4.5	50
<b>C4</b>	Citrate	6.5	50
<b>H1</b>	Histidine	4.5	50
<b>H2</b>	Histidine	6.5	50
<b>H3</b>	Histidine	4.5	150
<b>H4</b>	Histidine	6.5	150
<b>S1</b>	Succinate	4.5	50
<b>S2</b>	Succinate	6.5	50
<b>S3</b>	Succinate	4.5	150
<b>S4</b>	Succinate	6.5	150

Oxidation was less pronounced in citrate buffer and only minor oxidation was observed in succinate or histidine buffer, respectively. The loss of soluble protein was best fitted using a reduced two-factor interaction model ( $R^2=0.853$ ; **Figure 4 B**). Buffer type and pH as well as the interaction of these input parameters significantly impacted the loss of soluble protein. For example, acetate buffer at low pH values as well as succinate buffer at low pH value and low NaCl concentration resulted in significant protein loss. In contrast, the formulation of IGF-I in

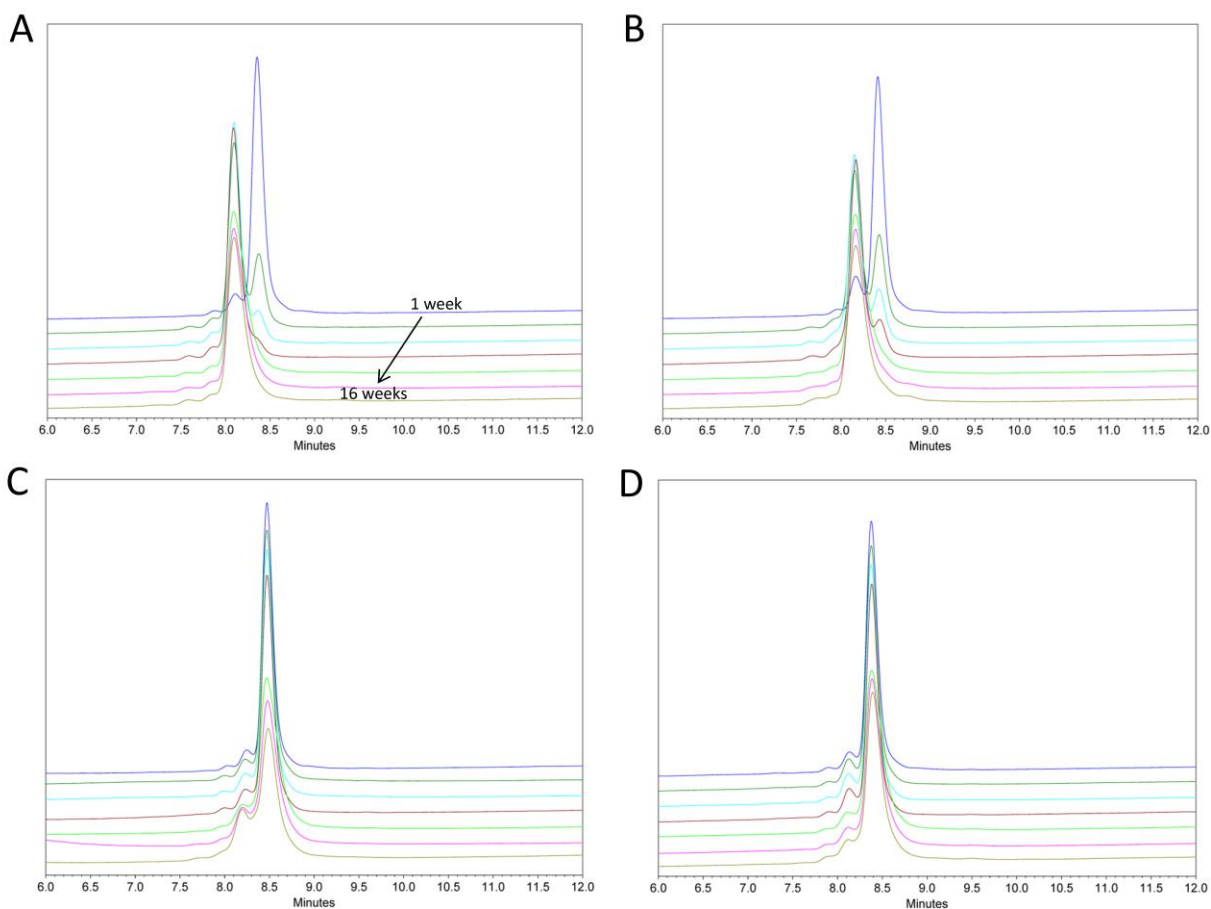


**Figure 2.** Representative RP-HPLC chromatograms of formulations in (A) acetate, (B) citrate, (C) histidine, and (D) succinate buffer at pH 6.5 and 150 mM NaCl, respectively. Chromatograms for each timepoint during accelerated stability are shown in overlay as detailed in (A) and detector response in all overlays was scaled equally.

acetate and succinate buffer at higher pH reduced protein loss as did the switch to the histidine or citrate buffer system at any of the pH values tested.

To further assess physical stability, samples were analyzed by reducing (data not shown) and non-reducing SDS-PAGE at the end of the storage period (**Figure 5**). Acetate formulations characterized by a significant loss of soluble protein observed in RP-HPLC (i.e. A1, A3 and A5) revealed formation of dimers and trimers in non-reducing SDS-PAGE. Analysis of the formulation samples under reducing conditions showed no high molecular weight species, i.e. the observed aggregates were reducible (data not shown). In contrast to formation of dimers and trimers in the case of low pH acetate buffer, non-reducing SDS-PAGE of IGF-I in S1 formulation revealed formation of high molecular weight aggregates which were also not

detectable under reducible conditions. Furthermore, a band of lower apparent molecular weight was observed in non-reducing SDS-PAGE in cases where significant Met(o) formation was observed in RP-HPLC.

Relative biological activity was determined using a MG-63 proliferation assay on samples collected at the end of the storage period (**Figure 3 B**). Bioactivity results were best fitted by a reduced linear model ( $R^2=0.861$ ) with buffer type being the only significant factor impacting bioactivity (**Figure 4 C**). It was observed that overall IGF-I bioactivity was negatively affected after storage of formulations containing acetate buffer, followed by succinate buffer. Storage of IGF-I in citrate buffer did not significantly affect bioactivity compared to the overall mean. However, formulations containing histidine buffer significantly improved retention of bioactivity compared to the overall mean. Statistical evaluation of effects within individual buffer types revealed that a pH of 4.5 significantly reduced IGF-I potency as compared to formulations at pH 6.5 in the acetate buffer system (A1, 3, 5 versus A2, A4; **Figure 3 B**). However, the amount of NaCl in the formulation did not impact IGF-I stability (A1 versus A3 or A2 versus A4; **Figure 3 B**). In contrast, within the citrate buffer formulation group, a pH of 4.5 better protected the potency as compared to pH 6.5 and the amount of NaCl significantly impacted IGF-I potency during storage (C2 versus C4; **Figure 3 B**). Overall, the citrate buffer system performed better as compared to the acetate system. A succinate buffer at pH of 4.5 formulated with 50 mM NaCl was found less efficient in protecting IGF-I potency, an effect which was leveraged by either addition of 150 mM NaCl or an increase in pH (S1 versus S3 or S2, respectively; **Figure 3 B**). Within the histidine buffer group, the amount of NaCl had a significant effect on IGF-I potency during storage with 150 mM performing better as compared to 50 mM (H1 versus H3; **Figure 3 B**).



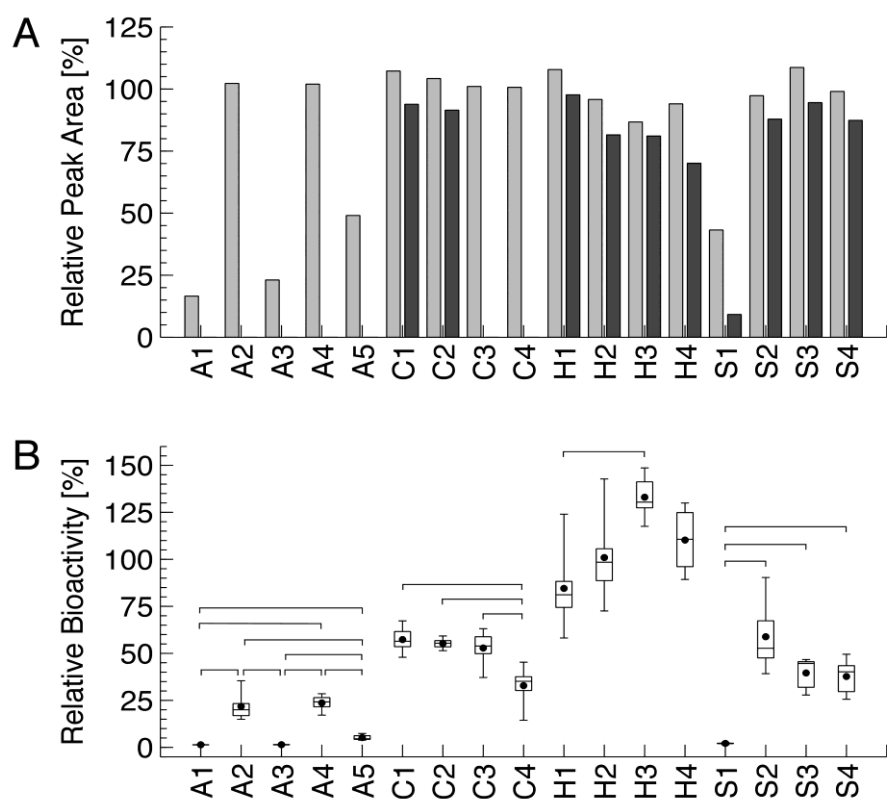


**Figure 3.** Results of RP-HPLC analysis after 4 months storage at room temperature with (A) total area and IGF-I peak area given by light gray and dark gray bars, respectively. (B) Relative IGF-I bioactivity with median, interquartile range (boxes), and overall data range (whiskers). Statistical significant differences among groups are highlighted by the horizontal bars ( $p < 0.05$ ).

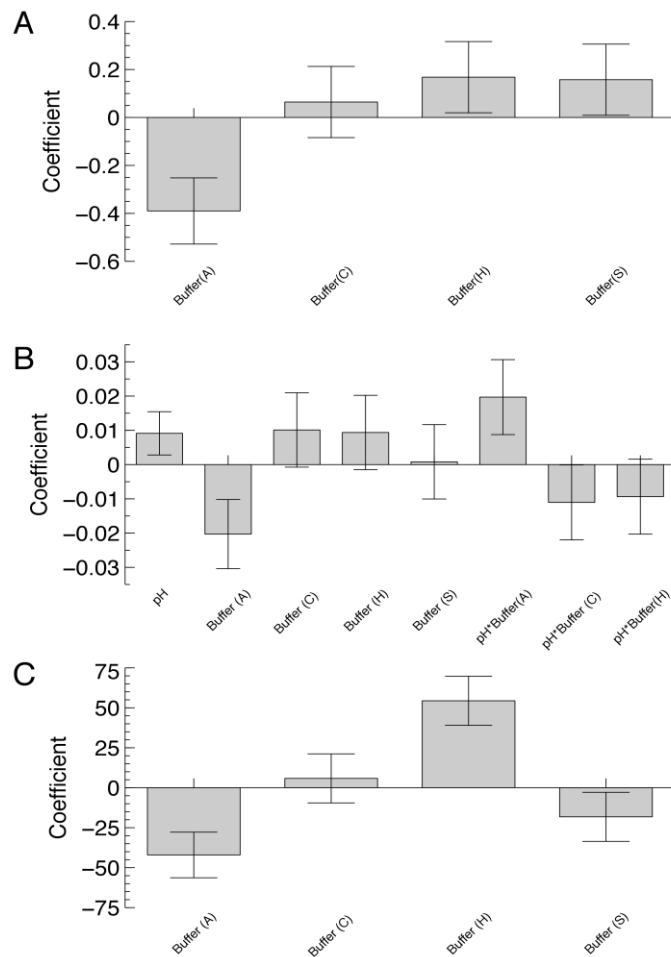


**Figure 4.** Effects of factors and factor combinations on the reaction rate coefficients (A) for IGF-I peak area, (B) total peak area, and (C) relative bioactivity. Effects are shown as coefficients  $\pm$  confidence intervals (0.95 level). Buffer type is coded as follows: A acetate, C citrate, H histidine, S succinate.

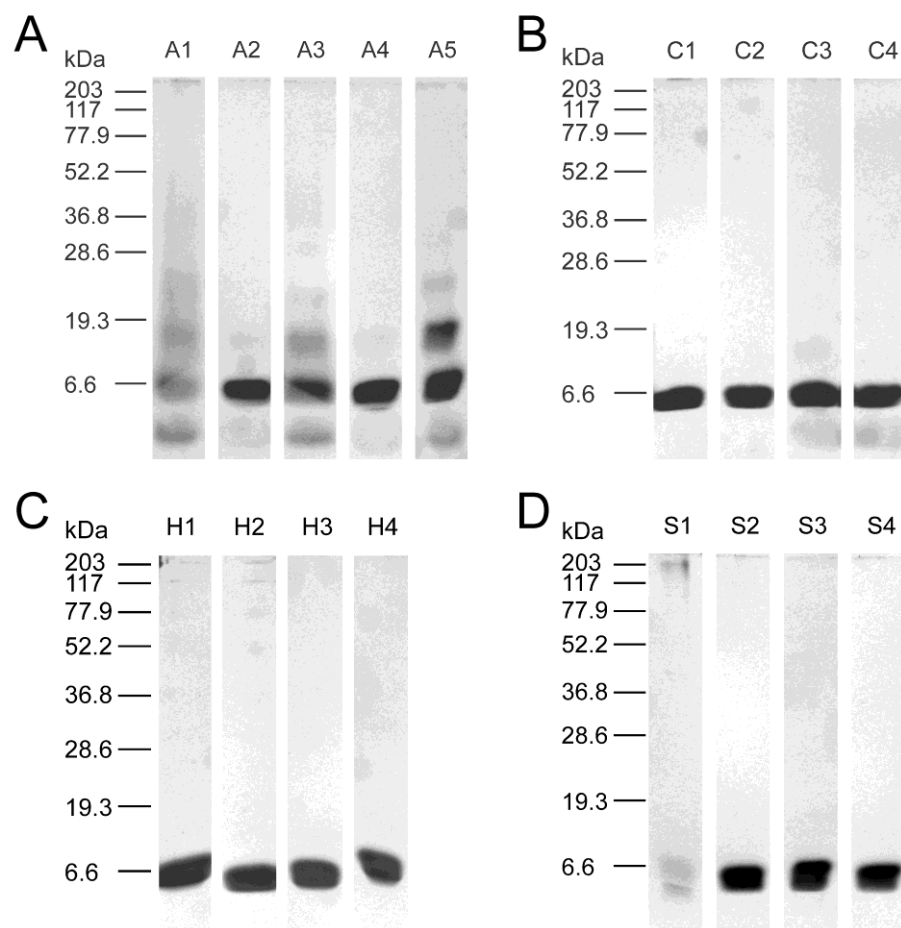


**Figure 5.** SDS-PAGE analysis of samples after 4 months storage. Formulations in acetate (A), citrate (B), histidine (C), and succinate (D) buffer were separated under non-reducing conditions.

### *IGF-I stability during nebulization and aerosol properties*

The impact of nebulization on protein integrity was studied using a standard air-jet and a new generation vibrating-mesh nebulizer. All experiments were performed with a formulation consisting of 50 mM histidine buffer at pH 6.5 and 150 mM NaCl (H4 in **Table 1**), whose stability was regarded as optimal and which was expected to be well tolerated (**Figure 3**). Formation of covalent aggregates was not observed in non-reducing SDS-PAGE following air-jet as well as vibrating-mesh nebulization (**Figure 6**).

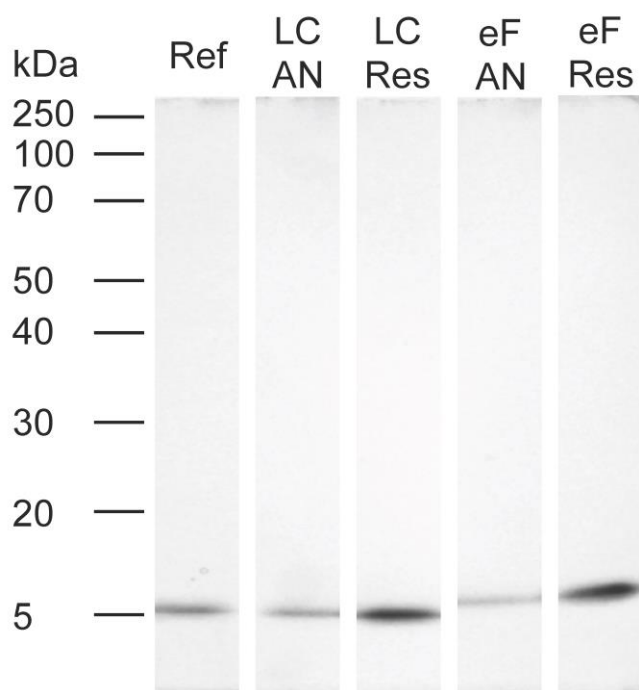


**Figure 6.** Analysis of formation of covalent aggregates during nebulization by nonreducing SDS-PAGE. IGF-I integrity prior to nebulization (Ref) is compared to integrity after nebulization (AN) from air-jet (denoted LC) and vibrating-mesh nebulizer (denoted eF), respectively. Solutions recovered from the nebulizer reservoir from each of the nebulizers after nebulization are shown denoted as “Res”.

Solutions recovered from the nebulizer reservoir showed slightly increased concentrations compared to starting conditions but also no aggregate formation was observed. This concentration effect appeared to be more pronounced for the air-jet nebulizer as described earlier [26]. Solutions after nebulization by either device had increased levels of Met(o)-IGF-I and 7% points decrease of the IGF-I peak area. Similarly, a 1 – 3% point reduction in the IGF-I peak area was observed in the solutions recovered from nebulizer reservoirs (**Figure 7**).

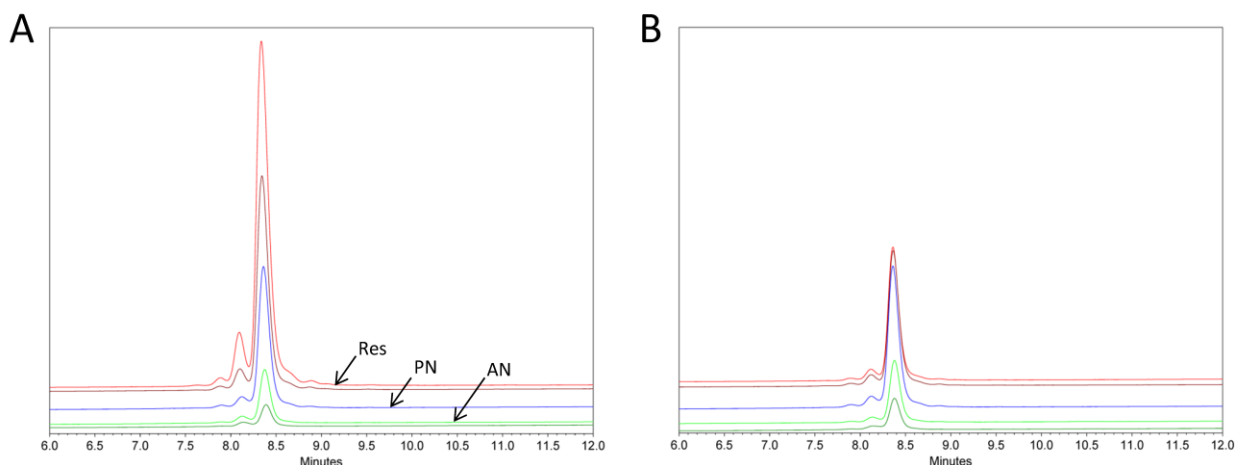


**Figure 7.** Evaluation of chemical degradation during nebulization by RP-HPLC. Solutions prior to nebulization (PN), after passing the nebulizer (AN) and recovered from the reservoir (Res) using air-jet (A) and vibrating-mesh nebulizer (B), respectively, were analyzed. Results from two experiments with each nebulizer are shown. Chromatograms are shown with detector response scaled equally.

Aerodynamic properties were determined using laser diffraction analysis with 0.9% NaCl solution as reference (**Figure 8**). The two nebulizers, according to their respective specifications, produced aerosols with differing MMAD and FPF (**Figure 8 A, B**). However, differences between actual formulations and reference solution were negligible. MMAD determined for formulation H4 was similar to the reference with values of  $2.7 \pm 0.1 \mu\text{m}$  for H4 and  $3.1 \pm 0.1 \mu\text{m}$  for reference, and  $4.9 \pm 0.1 \mu\text{m}$  for H4 and  $4.9 \pm 0.1 \mu\text{m}$  for reference for the air-jet and vibrating-mesh nebulizer, respectively. Similarly, FPF for formulation H4 was significantly reduced from  $88.5 \pm 2.3\%$  to  $82.9 \pm 1.6\%$  and from  $57.0 \pm 1.1\%$  to  $55.0 \pm 1.0\%$  compared to the reference solution for air-jet and vibrating-mesh nebulizer, respectively. The air-jet nebulizer generated finer aerosols (MMAD of  $3.1 \pm 0.1 \mu\text{m}$  with formulation H4) with a higher FPF ( $82.9 \pm 1.6\%$ ), but with a significantly lower output rate ( $0.21 \pm 0.02 \text{ g/min}$ ; **Figure 8 C**). In contrast, the vibrating-mesh nebulizer generated larger aerosol droplets (MMAD of  $4.9 \pm 0.1 \mu\text{m}$ ) and a lower FPF ( $55.0 \pm 1.0\%$ ), but with significantly improved and approximately four fold higher output rate ( $0.89 \pm 0.07 \text{ g/min}$ ; **Figure 8 C**), as compared to the air-jet device.

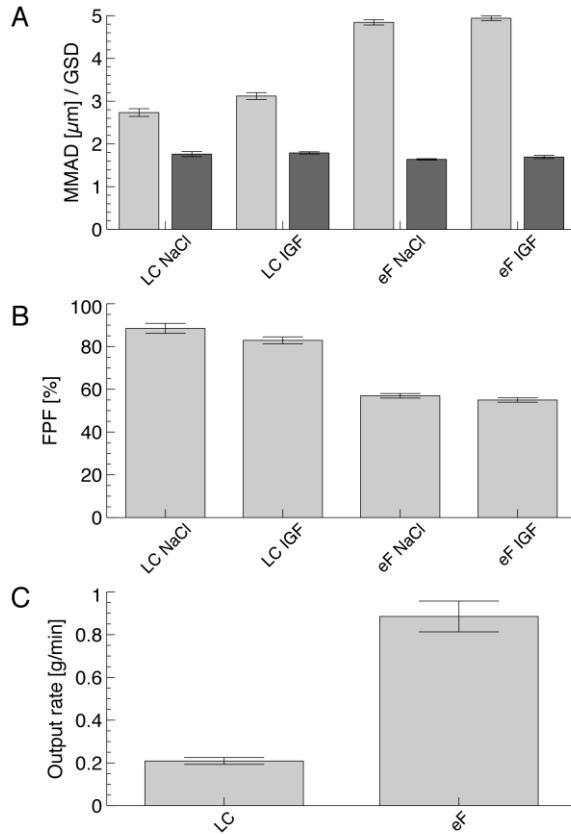


**Figure 8.** Results of aerodynamic characterization of aerosols generated by an air-jet (denoted LC) and a vibrating-mesh nebulizer (denoted eF) using an IGF-I formulation in histidine buffer at pH 6.5 and 150 mM NaCl against reference (154 mM NaCl). Results are given for (A) the mass median aerodynamic diameter (MMAD, light gray bars) and geometric standard deviation (GSD, dark gray bars), (B) fine particle fraction (FPF), and (C) nebulizer output rate.

---

## DISCUSSION

We studied the stability of different IGF-I formulations potentially suitable for inhalation at accelerated storage conditions. Salts and buffer ions can have complex effects on protein stability via direct interaction or indirect effects [29-31], driving the need to carefully select the buffer type, formulation pH and ionic strength. We observed significant oxidation, loss of soluble protein, dimer and trimer formation and loss of bioactivity in acetate buffer. Formation of reducible IGF-I dimers after exposure to multiple oxidative species has been reported earlier [20]. The formation of dimers was attributed to reduction of disulfides to sulfide radicals and reoxidation to new intra- or intermolecular disulfides. Furthermore, in studies on metal catalyzed oxidation of model peptides, an inverse relationship between pH value and methionine oxidation was shown, corroborating our results for oxidation of IGF-I at low pH values in acetate buffer [32]. We concluded that formulations containing acetate buffer under the chosen conditions (composition of formulations, IGF-I concentration and pH range) do not provide adequate IGF-I stabilization for long-term storage. To explain the contrast between the choice of acetate buffer for the commercial formulation of Mecasermin and our results, several points must be taken into consideration: The commercial product is formulated at approximately 50 fold higher IGF-I concentration. This factor alone may substantially affect degradation within protein formulations. For example, free methionine is an efficient antioxidant for methionine-oxidation sensitive proteins acting as a free radical scavenger [33]. Therefore, Met(o) formation might be a concern for low protein concentration formulations, while no detrimental effects might be observed at higher protein concentrations. Comparable results were reported by Lam et al., who studied methionine oxidation in a liquid monoclonal antibody (mAb) formulation [34]. In this study it was observed that methionine oxidation was more pronounced at mAb concentration of 5 mg/mL than at 20 mg/mL. However, the composition of low mAb concentration formulation differed significantly from high mAb concentration formulations, therefore it is difficult to assess the absolute effect of protein concentration versus other factors in this study. Despite the fact that Met(o) IGF-I was found bioactive [35, 36], severe oxidation is a concern from a pharmaceutical quality standpoint and might be particularly problematic if a link between oxidation and covalent aggregation can be established. Mecasermin commercial formulation contains 2 g/L of polysorbate 20, a non-ionic surfactant, which is known to efficiently protect the protein from aggregation [37] if used in properly purified form [32, 34]. On the other hand, polysorbates can

be a source of peroxides and therefore can also have detrimental effects on stability of oxidation sensitive proteins [32, 34] and affect nebulizer performance and aerosol droplet size as a result of changing the surface free energy of the system. Consequently, the addition of polysorbate was avoided in our study, following previous recommendation [38].

Different degradation and aggregation pattern was observed in other buffer systems than acetate. The succinate buffer formulation S1 (**Table 1**) demonstrated Met(o) formation but instead of formation of di-/trimers, aggregation into higher order aggregates was observed. Interestingly, this phenomenon depended on buffer type, pH value and NaCl concentration. The potential reasons for the observed differences between formulations are manifold. Excipient impurity is a serious challenge to pharmaceutical quality and, in case of trace metals a known cause driving oxidation and more specifically in the case reported here, might negatively impact IGF-I stability [32, 39, 40]. In addition, histidine and citrate are known for metal ion complexation, potentially resulting in antioxidant effects [41, 42]. Fransson et al. reported that IGF-I tertiary structure is impacted by different solutes [23]. Based on these findings, slight changes in the tertiary structure due to different solutes may impact solvent accessibility of methionine residues and hence IGF-I stability. However, future studies on IGF-I stability in different formulations are needed to address these hypotheses.

Histidine buffered formulations performed best as demonstrated by general stability (**Figures 3 A, 4**), absence of aggregation as determined by SDS-PAGE (**Figure 5**) and retained bioactivity (**Figure 3 B**) under the accelerated stability conditions tested here. Therefore, a formulation composed of 0.2 g/L IGF-I, 50 mM histidine, 150 mM NaCl at pH 6.5 was selected for further development.

The presented analysis mainly focused on biological activity and chemical IGF-I stability. Besides chemical degradation and dimer/trimer formation larger aggregates or particles may occur. However, the formation of particles has been reported to be related to protein concentration under quiescent storage [43] and particle or larger aggregate formation cannot be assessed by loss of HPLC main peak area for highly concentrated protein solutions with particles representing only a minute fraction of total protein mass [44]. Clearly, in such cases of high protein concentration, particles analysis is important to properly characterize the product. However, at low protein concentration as used herein, formation of particles would result in a drop of main peak area. The decrease of IGF-I peak area as observed for certain formulations can



therefore be due to chemical degradation or formation of dimers, trimers, higher multimers or even particles. Conversely, in formulations showing no decrease of IGF-I peak area, formation of significant amounts of larger aggregates or particles seems unlikely.

Protein instability during nebulization frequently challenges the use of this convenient administration mode. During nebulization formation of air-water interface, temperature changes and solvent loss in the nebulizer reservoir might result in significant protein aggregation or degradation [45]. For example, air-jet nebulization of granulocyte colony stimulating factor (G-CSF) resulted in the formation of approximately 40% non-covalent aggregates as well as similar levels of degradation products [46]. Similarly, a 50% activity loss was reported during nebulization for Aviscumin, a recombinant mistletoe lectin. In this study ultrasonic nebulization resulted in greater loss of bioactivity than air-jet nebulization [47]. IGF-I, when formulated in histidine buffer, 150 mM NaCl, pH 6.5 (H4 in **Table 1**) was readily nebulized and nebulizer performance was only marginally affected with regards to output rate and aerosol droplet size compared to a reference solution (**Figure 8**). Furthermore, nebulization – in spite of the procedure’s excessive stress on the IGF-I – resulted in limited Met(o) IGF-I formation and no formation of covalent aggregates was observed (**Figure 6 and 7**). Formulation H4 can therefore be regarded as suitable for nebulization and future studies may expand from this demonstrated success for IGF-I aerosol formulations as demonstrated on studies of chemical degradation and the formation of covalent dimers and trimers as well as non-covalent aggregates or particles.

We conclude that (i) the buffer type significantly impacted IGF-I stability and that the (ii) Met (o) IGF-I formation was correlated to formation of reducible dimers and trimers, a mechanism which was more pronounced at low formulation pH. A different aggregation pathway was observed in the succinate buffer system, characterized by Met(o) IGF-I formation and formation of larger reducible aggregates. The histidine buffer system significantly performed better than all other buffers tested and protected IGF-I over the entire pH range. This formulation can be nebulized with conventional air-jet or vibrating-mesh nebulizers while efficiently protecting protein stability thereby opening a reliable pulmonary approach for future *in vivo* pre-studies with this potent therapeutic.

## **ACKNOWLEDGMENTS**

We thank Gabriel Jones, Institute of Pharmacy and Food Chemistry, University of Wuerzburg, for kind assistance with SDS-PAGE experiments.

---

## REFERENCES

- [1] A. Juul, Serum levels of insulin-like growth factor I and its binding proteins in health and disease, *Growth Horm IGF Res*, 13 (2003) 113-170.
- [2] M. Pollak, Insulin-like growth factor physiology and cancer risk, *Eur J Cancer*, 36 (2000) 1224-1228.
- [3] J. Zapf, E.R. Froesch, Insulin-like growth factors/somatomedins: structure, secretion, biological actions and physiological role, *Horm Res*, 24 (1986) 121-130.
- [4] Scientific Discussion, in: *Increlex EPAR*, European Medicines Agency, London, 2007.
- [5] L. Meinel, O.E. Illi, J. Zapf, M. Malfanti, H.P. Merkle, B. Gander, Stabilizing insulin-like growth factor-I in poly(D,L-lactide-co-glycolide) microspheres, *J Control Release*, 70 (2001) 193-202.
- [6] M. Singh, B. Shirley, K. Bajwa, E. Samara, M. Hora, D. O'Hagan, Controlled release of recombinant insulin-like growth factor from a novel formulation of polylactide-co-glycolide microparticles, *J Control Release*, 70 (2001) 21-28.
- [7] X.M. Lam, E.T. Duenas, A.L. Daugherty, N. Levin, J.L. Cleland, Sustained release of recombinant human insulin-like growth factor-I for treatment of diabetes, *J Control Release*, 67 (2000) 281-292.
- [8] S.R. Mao, J. Xu, C.F. Cai, O. Germershaus, A. Schaper, T. Kissel, Effect of WOW process parameters on morphology and burst release of FITC-dextran loaded PLGA microspheres, *Int J Pharm*, 334 (2007) 137-148.
- [9] M.L. Houchin, E.M. Topp, Chemical degradation of peptides and proteins in PLGA: a review of reactions and mechanisms, *J Pharm Sci*, 97 (2008) 2395-2404.
- [10] Y. Zhang, S.P. Schwendeman, Minimizing acylation of peptides in PLGA microspheres, *J Control Release*, 162 (2012) 119-126.
- [11] T. Estey, J. Kang, S.P. Schwendeman, J.F. Carpenter, BSA degradation under acidic conditions: a model for protein instability during release from PLGA delivery systems, *J Pharm Sci*, 95 (2006) 1626-1639.
- [12] M. Gansslen, *Über die Inhalation von Insulin*, *Klin. Wochenschrift*, 4 (1925) 71.
- [13] W. Heubner, S.E. De Jongh, E. Laquer, *Über die Inhalation von Insulin*, *Klin. Wochenschrift*, 3 (1924) 2342.

## CHAPTER II

---

- [14] S. White, D.B. Bennett, S. Cheu, P.W. Conley, D.B. Guzek, S. Gray, J. Howard, R. Malcolmson, J.M. Parker, P. Roberts, N. Sadrzadeh, J.D. Schumacher, S. Seshadri, G.W. Sluggett, C.L. Stevenson, N.J. Harper, EXUBERA: pharmaceutical development of a novel product for pulmonary delivery of insulin, *Diabetes Technol Ther*, 7 (2005) 896-906.
- [15] T. Quattrin, A. Belanger, N.J. Bohannon, S.L. Schwartz, Efficacy and safety of inhaled insulin (Exubera) compared with subcutaneous insulin therapy in patients with type 1 diabetes: results of a 6-month, randomized, comparative trial, *Diabetes Care*, 27 (2004) 2622-2627.
- [16] P.A. Hollander, L. Blonde, R. Rowe, A.E. Mehta, J.L. Milburn, K.S. Hershon, J.L. Chiasson, S.R. Levin, Efficacy and safety of inhaled insulin (exubera) compared with subcutaneous insulin therapy in patients with type 2 diabetes: results of a 6-month, randomized, comparative trial, *Diabetes Care*, 27 (2004) 2356-2362.
- [17] D.R. Clemmons, Insulin like growth factors - their binding proteins and growth regulation. , in: E. Canalis (Ed.) *Skeletal Growth Factors*, Lippincott Williams & Wilkins, Philadelphia, 2000, pp. 79-99.
- [18] E. Rinderknecht, R.E. Humbel, The amino acid sequence of human insulin-like growth factor I and its structural homology with proinsulin, *J Biol Chem*, 253 (1978) 2769-2776.
- [19] P. Royle, N. Waugh, L. McAuley, L. McIntyre, S. Thomas, Inhaled insulin in diabetes mellitus, *Cochrane Database Syst Rev*, (2004) CD003890.
- [20] J.R. Fransson, Oxidation of human insulin-like growth factor I in formulation studies .3. Factorial experiments of the effects of ferric ions, EDTA, and visible light on methionine oxidation and covalent aggregation in aqueous solution, *J Pharm Sci*, 86 (1997) 1046-1050.
- [21] J. Fransson, E. Florin-Robertsson, K. Axelsson, C. Nyhlen, Oxidation of human insulin-like growth factor I in formulation studies: Kinetics of methionine oxidation in aqueous solution and in solid state, *Pharmaceut Res*, 13 (1996) 1252-1257.
- [22] J. Fransson, A. Hagman, Oxidation of human Insulin-like Growth Factor I in formulation studies .2. Effects of oxygen, visible light, and phosphate on methionine oxidation in aqueous solution and evaluation of possible mechanisms, *Pharmaceut Res*, 13 (1996) 1476-1481.
- [23] J. Fransson, D. Hallen, E. Florin-Robertsson, Solvent effects on the solubility and physical stability of human Insulin-like Growth Factor I, *Pharmaceut Res*, 14 (1997) 606-612.
- [24] Guideline Q1A: Stability testing of new drug substances and products, in: I.C.o. Harmonization (Ed.) Q1A(R2), 2003.

- [25] E. Wenk, A.J. Meinel, S. Wildy, H.P. Merkle, L. Meinel, Microporous silk fibroin scaffolds embedding PLGA microparticles for controlled growth factor delivery in tissue engineering, *Biomaterials*, 30 (2009) 2571-2581.
- [26] M. Beck-Broichsitter, P. Kleimann, T. Schmehl, T. Betz, U. Bakowsky, T. Kissel, W. Seeger, Impact of lyoprotectants for the stabilization of biodegradable nanoparticles on the performance of air-jet, ultrasonic, and vibrating-mesh nebulizers, *Eur J Pharm Biopharm*, 82 (2012) 272-280.
- [27] H. Steckel, F. Eskandar, K. Witthohn, Effect of excipients on the stability and aerosol performance of nebulized aviscumine, *Journal of aerosol medicine : the official journal of the International Society for Aerosols in Medicine*, 16 (2003) 417-432.
- [28] N.V. Katre, J. Asherman, H. Schaefer, M. Hora, Multivesicular liposome (DepoFoam) technology for the sustained delivery of insulin-like growth factor-I (IGF-I), *J Pharm Sci*, 87 (1998) 1341-1346.
- [29] M.C. Manning, D.K. Chou, B.M. Murphy, R.W. Payne, D.S. Katayama, Stability of protein pharmaceuticals: an update, *Pharmaceut Res*, 27 (2010) 544-575.
- [30] E.Y. Chi, S. Krishnan, T.W. Randolph, J.F. Carpenter, Physical stability of proteins in aqueous solution: mechanism and driving forces in nonnative protein aggregation, *Pharmaceut Res*, 20 (2003) 1325-1336.
- [31] B.S. Kendrick, T. Li, B.S. Chang, Physical stabilization of proteins in aqueous solution, in: J.F. Carpenter, M.C. Manning (Eds.) *Rationale Design of stable protein formulations - theory and practice*, Kluwer Academics/Plenum publishers, New York, 2002, pp. 61-84.
- [32] T.H. Nguyen, Oxidation degradation of protein pharmaceuticals, in: J.L. Cleland, R. Langer (Eds.) *Formulation and Delivery of Proteins and Peptides*, ACS Symposium Series, Washington DC, 1994.
- [33] J. Yin, J.W. Chu, M.S. Ricci, D.N. Brems, D.I. Wang, B.L. Trout, Effects of antioxidants on the hydrogen peroxide-mediated oxidation of methionine residues in granulocyte colony-stimulating factor and human parathyroid hormone fragment 13-34, *Pharmaceut Res*, 21 (2004) 2377-2383.
- [34] X.M. Lam, J.Y. Yang, J.L. Cleland, Antioxidants for prevention of methionine oxidation in recombinant monoclonal antibody HER2, *J Pharm Sci*, 86 (1997) 1250-1255.

- [35] E. Canova-Davis, M. Eng, V. Mukku, D.H. Reifsnyder, C.V. Olson, V.T. Ling, Chemical heterogeneity as a result of hydroxylamine cleavage of a fusion protein of human insulin-like growth factor I, *Biochem J*, 285 ( Pt 1) (1992) 207-213.
- [36] G. Forsberg, G. Palm, A. Ekebacke, S. Josephson, M. Hartmanis, Separation and characterization of modified variants of recombinant human insulin-like growth factor I derived from a fusion protein secreted from *Escherichia coli*, *Biochem J*, 271 (1990) 357-363.
- [37] H.J. Lee, A. McAuley, K.F. Schilke, J. McGuire, Molecular origins of surfactant-mediated stabilization of protein drugs, *Adv Drug Deliver Rev*, 63 (2011) 1160-1171.
- [38] H. Steckel, F. Eskandar, Factors affecting aerosol performance during nebulization with jet and ultrasonic nebulizers, *Eur J Pharm Sci*, 19 (2003) 443-455.
- [39] Y. Wu, J. Levons, A.S. Narang, K. Raghavan, V.M. Rao, Reactive impurities in excipients: profiling, identification and mitigation of drug-excipient incompatibility, *AAPS PharmSciTech*, 12 (2011) 1248-1263.
- [40] S. Li, C. Schoneich, R.T. Borchardt, Chemical instability of protein pharmaceuticals: Mechanisms of oxidation and strategies for stabilization, *Biotechnol Bioeng*, 48 (1995) 490-500.
- [41] L.C. Konigsberger, E. Konigsberger, P.M. May, G.T. Hefter, Complexation of iron(III) and iron(II) by citrate. Implications for iron speciation in blood plasma, *J Inorg Biochem*, 78 (2000) 175-184.
- [42] A.M. Wade, H.N. Tucker, Antioxidant characteristics of L-histidine, *J Nutr Biochem*, 9 (1998) 308-315.
- [43] H.C. Mahler, W. Friess, U. Grauschopf, S. Kiese, Protein aggregation: pathways, induction factors and analysis, *J Pharm Sci*, 98 (2009) 2909-2934.
- [44] S. Majumdar, B.M. Ford, K.D. Mar, V.J. Sullivan, R.G. Ulrich, J. D'Souza A, Evaluation of the effect of syringe surfaces on protein formulations, *J Pharm Sci*, 100 (2011) 2563-2573.
- [45] S.A. Shoyele, A. Slowey, Prospects of formulating proteins/peptides as aerosols for pulmonary drug delivery, *Int J Pharm*, 314 (2006) 1-8.
- [46] R.W. Niven, S.J. Prestrelski, M.J. Treuheit, A.Y. Ip, T. Arakawa, Protein nebulization .2. Stabilization of G-CSF to air-jet nebulization and the role of protectants, *Int J Pharm*, 127 (1996) 191-201.
- [47] H. Steckel, F. Eskandar, K. Witthohn, The effect of formulation variables on the stability of nebulized aviscumine, *Int J Pharm*, 257 (2003) 181-194.

***Copyright***

This chapter is reprinted with permission from Germershaus, O., Schultz, I., Luehmann, T., Beck-Broichsitter, M., Högger, P., Meinel, L. (2013). Insulin-Like Growth Factor-I Aerosol Formulations For Pulmonary Delivery. *European Journal of Pharmaceutics and Biopharmaceutics*, 2013, 85 (1), pp 61-68. doi:10.1016/j.ejpb.2013.03.011. License Date: May 24, 2015, License Number: 3635310689027.





## CHAPTER III

PULMONARY INSULIN-LIKE GROWTH FACTOR I  
DELIVERY FROM TREHALOSE AND SILK-FIBROIN  
MICROPARTICLES

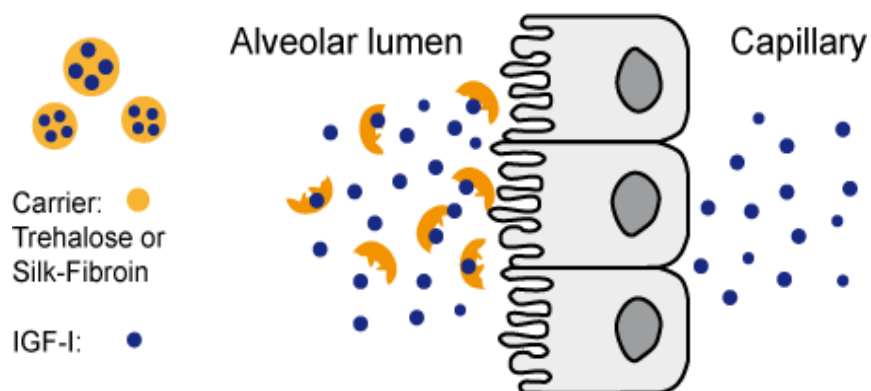
*Isabel Schultz, Frederic Vollmers, Tessa Lühmann, Jens-Christoph Rybak, Ronja Wittmann<sup>1</sup>,  
Katharina Stank<sup>1</sup>, Hartwig Steckel<sup>1</sup>, Boris Kardziej<sup>2</sup>, Michael Schmidt<sup>3</sup>,  
Petra Högger, Lorenz Meinel\**

Institute for Pharmacy and Food Chemistry, University of Wuerzburg, Am Hubland, DE-97074  
Wuerzburg, Germany

<sup>1</sup>Institute for Pharmacy, University of Kiel, Grasweg 9a, DE-24118 Kiel, Germany

<sup>2</sup>Thoraxzentrum Bezirk Unterfranken, DE-97702 Muennerstadt, Germany

<sup>3</sup>Medical Clinic and Polyclinic I, University of Wuerzburg, DE-97080 Wuerzburg, Germany



*ACS Biomaterials Science & Engineering, 2015, 1(2), pp 119-129.*

*doi: 10.1021/ab500101c.*

### ABSTRACT

Insulin-like growth factor I (IGF-I) is a strong anabolic peptide with promising therapeutic value in muscle wasting diseases such as sarcopenia. We report a pulmonary IGF-I delivery system deploying silk-fibroin (SF) as carrier and in comparison to trehalose. Both IGF-I delivery systems were characterized regarding IGF-I integrity, IGF-I release profiles and aerodynamic properties. Transepithelial *in vitro* transport of IGF-I using the pulmonary Calu-3 model cell system followed comparable kinetics and mechanism of uptake as earlier demonstrated for insulin (INS), for which effective pulmonary delivery is known. Microparticles were spray-dried using either trehalose or SF and resulting in geometries allowing alveolar deposition. The effective IGF-I shuttling through the epithelial barrier of the lung was demonstrated in an *ex vivo* human lung lobe model, and expanded the exciting possibility of this administration route to this effective and anabolic peptide.

---

## INTRODUCTION

Loss of muscle mass with age, referred to as sarcopenia, poses a major threat to physical integrity in the elderly [1]. Obvious outcomes are their tendency to bone fractures, a reduced ability to recover from severe illness [2], and reduced overall muscle function and ability for muscle (re-) generation, driving a loss in power capacity, relaxation, and contraction force as well as metabolic dysfunction such as insulin (INS) insensitivity [3, 4]. This decline in muscular function is also typical for other diseases, including amyotrophic lateral sclerosis, muscular dystrophies, or cancer. Insulin-like growth factor I (IGF-I) is an anabolic biologic, boosting satellite cell proliferation and differentiation and transgenic mice overexpressing IGF-I have a muscle mass increase as compared to wild type littermates [5-8]. The half-life of free IGF-I is between 10 and 12 minutes [9]. However, at least 99% of the total IGF-I concentration is bound to IGF binding proteins (IGFBP) in the circulation [10] and the plasma IGFBPs are responsible for an increase of the IGF-I half-life [11]. Indispensable prerequisites of a systemic therapy with IGF-I are efficacy and reproducible exposure profiles. Several human clinical trials give proof of the pulmonary absorption of peptides and proteins following a systemic effect but not for IGF-I to date [12]. Particularly INS, a 5808 g/mol peptide, is well studied and benefits toward other applications as for example the subcutaneous injection regarding pharmacokinetics and reproducible exposure profiles were described [13, 14]. In spite of the *Exubera* (pulmonary INS) disappointment, the *Afrezza* (pulmonary INS) approval in the US and a recent deal with a global pharmaceutical company demonstrated the continuing interest in pulmonary delivery of peptides in general and INS in particular. As INS and IGF-I share a high sequence homology, we hypothesize that many of the pulmonary INS achievements can be translated to IGF-I [15]. Major safety issues in INS therapy comprise hypoglycemia as reaction of an INS overdose. Appropriate dosaging of INS for pulmonary delivery is therefore critical. Although IGF-I can cause hypoglycemic effects, its hypoglycemic potential is about 10% compared to INS, indicating that the risk of acute hypoglycemia of pulmonary delivered IGF-I is strongly minimized compared to INS for pulmonary administration, rendering IGF-I an interesting candidate for pulmonary delivery [16].

Other reported acute side effects of IGF-I include suppression of growth hormone release (GH), headache, lipohypertrophy, and pain at the injection side after subcutaneous injection. INS and IGF-I are related proteins with high sequence homology. INS is effectively shuttled through

epithelial barriers [17, 18]. We hypothesize that this effective transepithelial transport INS can be extrapolated to IGF-I. Furthermore, we developed pulmonary IGF-I delivery systems as a powder for inhalation while tuning microparticle geometries for optimal alveolar landing. The absorption of IGF-I through the lung into the systemic circulation after the aerosolization of these formulations was analyzed in a human *ex vivo* lung model. Another goal was to evaluate SF as a novel carrier for pulmonary peptide delivery in comparison to trehalose, a frequently used excipient for pulmonary drug delivery systems. IGF-I has also been successfully encapsulated in PLGA microspheres and scaffolds and release profiles over several days have been reported [19-23]. However, PLGA microspheres are typically not selected in cases in which immediate bioavailability of an encapsulated biologic is desirable and reported stability challenges have been correlated to the formation of acidic degradation products of the polymer during microsphere degradation [22, 23]. In contrast, SF has been demonstrated to be particularly useful in the formulation of sensitive biologics. It might be advantageous if this benefit can be extended to pulmonary drug delivery of biologics, and in an effort to expand the paucity of excipients, be allowed for pulmonary use in the future [24, 25].

## EXPERIMENTAL DETAILS

### Materials

Recombinant human IGF-I was from Novartis (Basel, Switzerland) and *Bombyx mori* cocoons from Trudel Silk (Zürich, Switzerland). D-(+)-trehalose dihydrate, L-methionine, Eagle's minimum essential medium with Earle's salts (MEM), bovine serum albumin (BSA), 3-[4.5-dimethylthiazol-2-yl]-2.5 diphenyltetrazolium bromide (MTT), 1.1.1.3.3.3-hexafluoro-2-propanol (HFIP), fluorescein-sodium (fluorescein), rabbit zona occludens protein 1 (ZO-1) antibody (Prestige Antibodies), CF 555-labeled anti rabbit IgG, 4.6-diamidino-2-phenylindole dihydrochloride (DAPI), 4-morpholineethanesulfonic acid (MES) and glucose solution 45% were from Sigma Aldrich (Schnelldorf, Germany). Formaldehyde solution 4% (V/V), acetonitrile (HPLC grade) and trifluoroacetic acid (HPLC grade) were from VWR (Ismaning, Germany), 75 cm<sup>2</sup> tissue culture polystyrene (TCPS) cell culture flasks were from Nunc (Schwerte, Germany) and 12 well plates and high binding 96 well plates from Greiner

(Frickenhausen, Germany). Brij<sup>®</sup> 35, Triton X-100 and Mowiol 4-88 were from Carl Roth (Karlsruhe, Germany). Fetal bovine serum (FBS), penicillin G, streptomycin, non-essential amino acids (NEA), phosphate buffered saline (PBS) and Hank`s balanced salt solution (HBSS) were from Biochrom (Berlin, Germany). Polysorbate 20 was from Croda (Nettetal, Germany). Heparin-Na 5000 was from Ratiopharm (Ulm, Germany). Water (Milli-Q) was from a demineralization system (Millipore, Billerica, MA). All other chemicals used were of at least pharmaceutical grade and from Sigma-Aldrich unless otherwise noted.

### ***Silk-fibroin processing***

Aqueous SF solution was prepared as described before [26]. Briefly, *Bombyx mori* cocoons were cut and boiled two times in an aqueous calcium carbonate solution (0.02 M) for 1 hour. After washing in Milli-Q water and air-drying overnight, the SF was dissolved in 9.3 M lithiumbromide at 60 °C yielding a 20% (m/m) solution. SF solution was dialyzed (SpectraPor, MWCO 6000-8000 g/mol, Spectrum, Rancho Dominguez, CA) against borate buffer (300 mM borate, 150 mM NaCl, pH 9.0) for 24 hours and subsequently dialyzed against Milli-Q water for 48 hours. The concentration of the final SF solution was 25 mg/mL, determined by drying and weighing of a defined amount of SF solution. SF solution was stored in a refrigerator at 2-8 °C.

### ***IGF-I purification***

Supplied IGF-I solution was purified by cation exchange chromatography (CEX). Briefly, an Äkta purifier<sup>™</sup> system (GE, Munich, Germany) and a Hi Trap SP XL column (GE) were used. A 50 mM succinate buffer (pH 4.5) was used as binding buffer and the elution buffer consisted of 50 mM succinate and of 1 M sodium chloride (pH 4.5) and run with a linear gradient. Samples were dialyzed (SpectraPor, MWCO 2000 g/mol, Spectrum Laboratories, Rancho Dominguez, CA) against Milli-Q water and freeze dried. The concentration of IGF-I was determined as described before [27].

### ***IGF-I microparticle preparation and physical characterization***

A 1% (m/V) solution of trehalose/IGF-I (1:4; m/m) was mixed with polysorbate 20 (0.05%; m/V) and 1 mM L-methionine in a 5 mM histidine buffer at pH = 6.5. Spray drying (Nano Spray

Dryer B-90; Büchi, Switzerland) was at an inlet temperature of 70 °C, spray cap 4 µm mesh, and a flow rate of 115 L/min. In another set of experiments SF replaced trehalose (no L-methionine added) under otherwise identical conditions with spraying at an inlet temperature of 70 °C, spray cap of 5.5 µm mesh size and a flow rate at 130 L/min. IGF-I samples were taken (i) before spray drying, (ii) after pumping the solution through the spray drier's loop for 15 min and (iii) IGF-I released from the resulting spray-dried microparticles. SF microparticles were exposed to water vapor over a saturated sodium sulfate solution for 24 h (relative humidity of 98% (V/V) determined with a Hygro-Thermometer (VWR, Ismaning, Germany)). Another batch was prepared by placing the spray-dried microparticles into methanol for 30 min. Water vapor exposure or methanol treatment is instrumental in increasing SF crystallinity.<sup>25, 28, 29</sup> Finally, one batch of microparticles was used untreated. All microparticles were either used immediately or stored in a desiccator under vacuum at 2 – 8 °C. Fourier-Transform-Infrared Spectroscopy (FTIR) spectra (Jasco FT/IR 6100, Frankfurt, Germany) used 16 scans per measurement at a resolution of 4 cm<sup>-1</sup>, with a wavenumber range from 650 to 4000 cm<sup>-1</sup>. Wide-angle X-ray scattering (WAXS) patterns were obtained on a Bruker D8 (Bruker, Karlsruhe, Germany) using a Cu K $\alpha$  radiation source at 40 kV, 40 mA. Measurements were in reflection geometry (Goebel mirror with slit at 1.2 mm opening on the primary and an anti-scatter slit with 7.5 mm opening on the secondary beam path) along with axial soller slits (2.5° opening) on both sides. Detection was with a 1D-LynxEye detector (Bruker) in coupled  $\theta/2\theta$  mode from 5 – 50°, step size 0.025°, measurement time of 2.5 seconds per step. Dynamic water vapor sorption (DVS) was on a DVS-HT (Surface Measurement, London, UK) at 25 °C and nitrogen flow of 0.4 L/min. Two cycles of sorption/desorption isotherms were performed with steps of 10%. Each value was read at either < 0.0005% weight change or after a maximum of 3.5 hours.

### ***Aerodynamic properties of spray-dried microparticles***

A Next Generation Impactor (MSP, Shoreview, MN) was used. Approximately 5 mg microparticles were weighed into hydroxypropylmethylcellulose (HPMC) capsules, and the Cyclohaler (PB, Meerbusch, Germany) was used to deliver the powder. The flow was adjusted to 100 L/min. corresponding to a 4 kPa pressure drop (Flow Meter DFM2, Copley Scientific, Nottingham, UK). All stages were coated with a solution consisting of 15% (m/m) Brij 35, 85% (m/m) of a mixture of ethanol and glycerol (6+4; m/m) to avoid particle bouncing and to get an

effective impaction. The deposited microparticles from each part of the Next Generation Impactor (NGI) were collected by rinsing the throat and preseparator with 10 mL and the applicator and the eight stages with 5 mL Milli-Q water, respectively. The capsule was dissolved in 5 mL Milli-Q water. IGF-I content of the collected solutions were determined by ELISA (DuoSet Human, R&D Systems, Minneapolis, MN). The mass median aerodynamic diameter (MMAD), the geometric standard deviation (GSD) and the fine particle fraction (FPF; cumulative proportion of particles with an aerodynamic diameter of  $\leq 5 \mu\text{m}$ ) of delivered dose (regardless of application system) were calculated using the Copley Inhaler testing data analysis software (Version 3.00, Nottingham, UK). All samples were analyzed in triplicate.

### ***IGF-I microparticle visualization***

Scanning electron microscopy (SEM) images were recorded on a Zeiss Ultra plus field emission scanning electron microscope with a Gemini e-Beam column (Oberkochen, Germany). 300 microparticles were sized using the software Image J (National Institute of Health, Bethesda, MD) for the geometric mean diameter. Atomic force microscopy (AFM) was on a MultiMode AFM (Bruker AXS, Karlsruhe, Germany) in tapping mode. Silicon-cantilevers (Olympus, Tokyo, Japan) were used with a resonance frequency of 300 kHz and a spring rate of  $40 \text{ Nm}^{-1}$ .

### ***Determination of IGF-I content and purity***

IGF-I/trehalose microparticles were dissolved in 1 mL Milli-Q water and IGF-I/SF microparticles were solubilized in HFIP overnight at room temperature [30]. Subsequently, HFIP was evaporated by flushing with nitrogen gas and IGF-I was reconstituted in 1 mL histidine buffer (5 mM, pH 6.5). IGF-I was quantified by reverse phase high performance liquid chromatography (RP-HPLC)<sup>23</sup>. Briefly, a VWR Hitachi Elite La Chrom HPLC (Radnor, PA) system equipped with a diode array detector (VWR Hitachi L-2400) was used with a Zorbax 300SB-CN reversed-phase chromatography column (Agilent, Böblingen, Germany) at  $40^\circ\text{C}$ , flow rate of 0.8 mL/min. using a linear gradient of eluent A (5% (V/V) acetonitrile with 0.2% (V/V) trifluoroacetic acid (TFA) in Milli-Q water) and eluent B (80% (V/V) acetonitrile and 0.2% (V/V) TFA in Milli-Q water) and detection at  $\lambda = 214 \text{ nm}$ . IGF-I chromatograms were identical as recorded from IGF-I solutions obtained from dissolved IGF-I trehalose microparticles, from HFIP solubilized and

histidine buffer reconstituted SF microparticles or from spiking experiments of IGF-I solutions with SF or HFIP. IGF-I release from approximately 5 mg SF microparticles was studied in 1mL release medium (50 mM histidine (pH = 6.5), 100 mM sodium chloride, 0.02% (m/V) sodium azide) at 37 °C [20, 22, 23, 31]. Aliquots of supernatant (100 µL) were collected and volume was replaced by fresh medium. Samples were analyzed by RP-HPLC. Additionally, IGF-I/trehalose microparticles were analyzed by high performance gel filtration [32]. Briefly, a Superdex 75 10/300 GL column (GE Healthcare, Munich, Germany) with a flow buffer (50 mM sodium phosphate, 100 mM sodium sulfate and 1.0% (V/V) isopropanol, pH = 7.3) was used with a flow rate of 0.5 mL/min and detection at  $\lambda = 280$  nm. IGF-I/trehalose microparticles were analyzed by SDS-(sodium dodecyl sulfate) and native PAGE (polyacrylamide gel electrophoresis) as described before [33, 34]. For non-reduced SDS-PAGE, samples were mixed with sample buffer (0.35 M Tris-HCl at pH 6.8, 30% (V/V) glycerol, 10% (m/V) SDS, 0.012% (m/V) bromphenolblue) and for reduced conditions 9.3% (m/V) dithiothreitol was added. For native PAGE analysis, a continuous non-denaturing electrophoresis system (histidine/MES buffer, pH 6.1) was used. Proteins were detected by silver staining (Pierce, Rockford, IL) and documentation was on a FluorChem FC2 (Santa Clara, CA).

### ***IGF-I bioassay and transepithelial transport***

IGF-I bioactivity was evaluated (MG-63 cells; ATCC: CRL-1427, Manassas, VA) [31, 35]. Cells were cultured in growth medium (MEM, 8.8% (V/V) FBS, 1.77 mM L-glutamine, 88 U/mL penicillin, 88 µg/mL streptomycin, 0.88% NEA). Cells were resuspended in assay medium (MEM, 0.452% BSA (m/V), 1.82 mM L-glutamine, 91 U/mL penicillin, 91 µg/mL streptomycin and 0.91% NEA) and 100 µL ( $2 \times 10^4$  cells/mL) were seeded in each well of a 96 well plate (BD, Bedford, MA) and incubated at 37°C, 5% CO<sub>2</sub> for 24 hours. 100 ng/mL of released IGF-I and of IGF-I reference were deployed to perform a dilution series in assay medium. After incubation at 37 °C and 5% CO<sub>2</sub> for 30 minutes, 100 µL of the samples of the dilution series were transferred to the cells of the assay plate and left for 48 hours before incubation with 50 µL of MTT solution (5.0 g/L) for 4.5 hours. Subsequently, 200 µL of 2-propanol, 3% (m/V) SDS and 0.04 M HCl were added and read at  $\lambda = 570$  nm. Transepithelial transport was tested with Calu-3 cells, cultured in 10 mL of MEM (10% (V/V) FBS, 100 U/mL penicillin, 100 µg/mL streptomycin, 1% NEA, 1 mM sodium pyruvate, 2.88 g/L glucose (growth medium) in 75 cm<sup>2</sup> cell culture flasks at



37 °C and 5% CO<sub>2</sub>. For transport studies, 100000 cells/cm<sup>2</sup> were seeded on filter devices (1.13 cm<sup>2</sup> growth surface, 0.4 µm pores; Thinfert<sup>TM</sup>, Greiner, Frickenhausen, Germany) and 10 – 14 days in culture. Transepithelial electric resistance (TEER) was measured (Evom 2/STX 3 electrode; World Precision Instruments, Sarasota, FL). The final TEER values were calculated as  $TEER[\Omega cm^2] = (TEER_{Monolayer} - TEER_{Blank}) * A[cm^2]$  and TEER had to be >1000 Ωcm<sup>2</sup>. IGF-I (53-78 µg/mL) or INS (90 – 104 µg/mL) in growth medium were used as donor solution. Cells were incubated at 37 °C and 5% CO<sub>2</sub> and shaken at 100 rpm. Samples were collected from the acceptor chambers between 60 and 150 min and replaced with fresh medium and analyzed using the IGF-I Quantikine Elisa Kit (R&D) and Human Insulin Elisa Kit (Merck, Darmstadt, Germany). The apparent permeability coefficient (P<sub>app</sub>) of fluorescein sodium (20 µM; paracellular marker [36]) was determined on control monolayers in HBSS in parallel to IGF-I and INS experiments. Samples were collected over 60 min. (acceptor; replacement with HBSS) and P<sub>app</sub> values were calculated as described before [37]. The immunostaining on tight junctions was done on day 10 after washing with PBS and fixation in 4% (V/V) buffered formaldehyde at pH 6.9. Subsequently, monolayers were washed, permeabilized with 0.1% (V/V) Triton X-100 in PBS. After blocking 1 hour at room temperature (5% (m/V) BSA in PBS), an anti ZO-1 antibody (primary antibody), diluted 1:200 (V/V) in PBS was added for 2 h at room temperature. Monolayers were washed (PBS) and incubated with a secondary CF555 labeled goat anti-rabbit IgG, diluted 1:500 (V/V) in 5% (m/V) BSA/PBS, for 1 h at room temperature. The antibody solution was replaced by a DAPI solution, diluted 1:1000 (V/V) in PBS. After washing with PBS, filters were placed on a glass slide and embedded in a Mowiol 4-88 solution. For imaging, an epifluorescent Axio Observer.Z1 (Zeiss) was used. Following ethical approval, the impact of bronchoalveolar lavage (BALF) on IGF-I transepithelial transport was detailed [38]. The supernatant of centrifuged human BALF (a local Ethics Committee gave the permission for the study protocol) was concentrated using a Centriprep YM-50 (Merck), diluted in growth medium without FBS to a final concentration factor of 6.7x BALF. In this 6.7x BALF, IGF-I was diluted and used as donor solutions (16-58 µg/mL). Transport studies with inhibitors of transcytosis/endocytosis were performed. Stock solutions from the inhibitors (1000x in DMSO) were diluted 1:1000 (V/V) in growth medium to the following incubation media: 50 µM amiloride, 300 µM indometacine, 30 µM nocodazole, 5 µM phenylarsine oxide, 60 µM dynasore, control (growth medium with 0.1% (V/V) DMSO). Monolayers were preincubated at

37 °C for 30 min. with nocodazole and for 15 min with the other inhibitors. After removing the medium in both chambers, 0.5 mL of each IGF-I donor solution (51-75 µg/mL in incubation medium) was pipetted to the apical chambers and 1.5 mL incubation medium to the basolateral chambers. Samples were taken after 1 h basolaterally. Additionally inhibition studies with nocodazole and dynasore in 6.7 x BALF with IGF-I as donor solutions were performed.

### *Human lung perfusion model*

Patient characteristics have been described before (patients with bronchial carcinoma assigned to lobectomy, bilobectomy or pneumonectomy with lung resections at the Thoraxzentrum Bezirk Unterfranken, Münnerstadt, Germany) [39-41]. Each patient was informed about the experiment prior to surgery according to the Declaration of Helsinki and signed an informed consent and a local Ethics Committee gave the permission for the study protocol.

The perfusion buffer was Milli-Q water containing 5% (m/V) BSA, 2.5 mM calcium chloride dihydrate, 5.5 mM glucose monohydrate, 3.5 mM potassium chloride, 2.5 mM potassium dihydrogen phosphate, 1.18 mM magnesium sulphate heptahydrate, 85 mM sodium chloride, 20 mM sodium hydrogen carbonate, and 10000 U/10000 µg/L penicillin G/streptomycin, 2500 U/L heparin-Na [39-41]. Lung lobes were reperfused extracorporally in a half open circulation system as described before [39-41] under respiration (Evita 4, Draeger, Luebeck, Germany). The ventilation mode was biphasic positive airway pressure (BIPAP) to adjust volume for lung lobe size under pH control (Five-Go, Mettler Toledo, Gießen, Germany; adjusted with either carbon dioxide/0.5 M hydrochloric acid or 10% (m/V) hydrogen carbonate). Ventilation parameters were set to 20 – 25 mbar for maximal airway pressure ( $P_{\max}$ ), 1 mbar for positive and expiratory pressure (PEEP) and an inspiration rate of 15/min (Ventview, Draeger). Perfusion parameters were 97 mL/min at 37 °C and 28 mmHg perfusion pressure. IGF-I loaded trehalose (n = 3) and IGF-I-loaded SF microparticles (n = 3) were applied with an individual lung lobe per experiment. The system was equilibrated for about 5 min before drug application using a Dry Powder Insufflator (DP-4 M with Air Pump AP-1, Penn-Century, Wyndmoor, PA) in the inspiration phases. The retained IGF-I loaded trehalose and SF microparticles in the insufflator were dissolved in Milli-Q water (IGF-I<sub>retained</sub>) and after termination of the experiments all tubes and connectors between the bronchus of the lobes and the respirator were washed out with Milli-Q water (IGF-I<sub>adsorbed to plastic</sub>). IGF-I deposited in the lung lobes (IGF-I<sub>deposited</sub>) was calculated

using the following equation:  $IGF-I_{\text{deposited}} = IGF-I_{\text{loaded}} - IGF-I_{\text{retained}} - IGF-II_{\text{adsorbed to plastic}}$ . The  $IGF-I_{\text{deposited}}$  was used to set the 100% value for the IGF-I. Samples were collected from the venous output and were replaced by fresh perfusion buffer. The absorbed IGF-I (“systemically available” as evidenced by the *ex vivo* lung model) was recorded in [%] of the  $IGF-I_{\text{deposited}}$ . All samples were analyzed using the sandwich IGF-I Quantikine<sup>®</sup> Elisa Kit (R&D Systems, Minneapolis, MN).

### ***Statistical analysis***

Data were analyzed using an unpaired Student t-test or one way ANOVA followed by Tukey’s multiple comparison test. GraphPad Prism<sup>®</sup>6.04 (GraphPad Software, La Jolla, CA) or Minitab<sup>®</sup> 16 (Minitab, Coventry, UK) were used. Results were considered statistically significant at  $p \leq 0.05$  and results are displayed as mean with standard deviation (SD).

## **RESULTS**

### ***Transepithelial transport of IGF-I and insulin***

Specifications of Calu-3 monolayers included a (i) transepithelial electrical resistance value exceeding  $1000 \Omega \text{ cm}^2$  in analogy to previous reports [42], (ii) apparent permeability coefficients ( $P_{\text{app}}$ ) for fluorescein of approximately  $1.05 \pm 0.22 * 10^{-7} \text{ cm/sec}$ <sup>36</sup> and (iii) a qualitative assessment of tight junctions. The tight junctions of the Calu-3 cell monolayers were evenly distributed between cells, as indicated after ZO-1 labeling (**Figure 1 A**).

Therefore, and according to our specifications, monolayers were accepted for transport studies and deployed to analyze IGF-I and INS transport through the lung epithelial cell monolayer and to collect *in vitro* evidence for potential systemic availability following pulmonary delivery [43]. Transported IGF-I and INS followed a linear relationship over time ( $r^2 = 0.99$ ; **Figure 1 B**). Neither IGF-I nor INS concentrations in the donor chamber changed significantly before and after the experiment ( $n = 5$  for IGF-I,  $n = 4$  for INS; data not shown). IGF-I was distributed to the basolateral compartment with a  $P_{\text{app}}$  of  $1.49 \pm 0.35 * 10^{-8} \text{ cm/sec}$  ( $n = 13$ ) and INS with a  $P_{\text{app}}$  of  $2.11 \pm 0.57 * 10^{-8} \text{ cm/sec}$  ( $n = 10$ ) and both  $P_{\text{app}}$  values were statistically different from each other. The amounts [%] of transported INS were statistically higher as compared to IGF-I at each

time point. Addition of concentrated (6.7x) human BALF to the cell culture medium significantly increased the permeation of IGF-I through the Calu-3 monolayer (**Figure 1 C**). This increase in IGF-I transport was not due to BALF affecting the tight junctions since there was neither a significant difference in the TEER values nor regarding permeation of fluorescein between IGF-I with medium or IGF-I with BALF in medium after the experiments (data not shown). The permeation of IGF-I was significantly decreased by the microtubules disrupting endocytosis inhibitor nocodazole [44, 45] and the dynamin GTPase inhibitor dynasore [46-48], but not significantly impacted by the caveolae-mediated endocytosis inhibitor indometacine [46], the macropinocytosis inhibitor amiloride [46] or the clathrin-mediated endocytosis inhibitor phenylarsine oxide [46] (**Figure 2**). Incubation of Calu-3 cells with human BALF in combination with nocodazole revealed a significant inhibition of IGF-I permeation while dynasore showed no effect on IGF-I permeation.

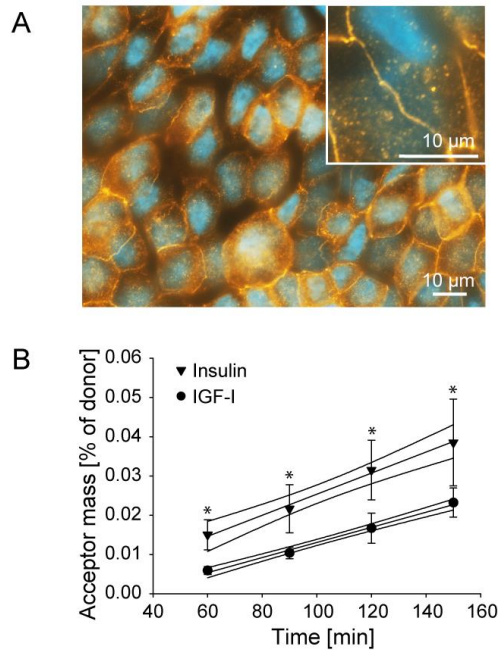


**Figure 1.** (A) Confluent Calu-3 monolayer recorded by epi-fluorescence microscopy. Tight junction protein (ZO-1) staining (orange) and DAPI cell nuclei staining (blue). (B) IGF-I and INS transport through Calu-3 [% of donor chamber] monolayer versus time [min]. (C) Apparent permeability of IGF-I in growth medium (control) and in bronchoalveolar Lavage (BALF) across Calu-3. The data are presented as mean  $\pm$  standard deviation. Apparent permeability coefficient abbreviated as Papp. Asterisks highlight significant difference ( $p < 0.05$ ).

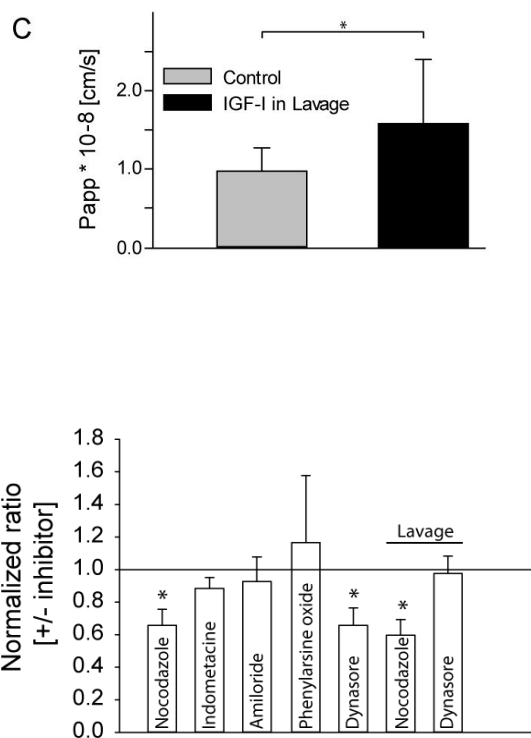


**Figure 2.** Transport studies of IGF-I in Calu-3 with inhibitors of transcytosis and endocytosis. The data represent the permeated amount of IGF-I (acceptor/donor) normalized to control. Asterisks highlight significant difference ( $p < 0.05$ ).

---

### *Morphology and physical characterization of spray-dried microparticles*

Microparticle morphology was assessed by SEM (**Figure 3**). IGF-I-loaded untreated SF microparticles had a spherical morphology with a mean diameter of  $1.23 \pm 0.55 \mu\text{m}$  (**Figure 3 A**) and a microparticle size range from  $0.25 \mu\text{m}$  to  $3.15 \mu\text{m}$ . IGF-I-loaded trehalose microparticles were in a comparable size range ( $0.40 \mu\text{m} - 3.15 \mu\text{m}$ ) and the mean diameter of  $1.18 \pm 0.45 \mu\text{m}$  was not significantly different as compared to IGF-I-loaded untreated SF microparticles (**Figure 3 B**). The diameter of untreated SF microparticles was corroborated by AFM measurements with a diameter of  $1.40 \pm 0.55 \mu\text{m}$  and a range from  $0.80$  to  $2.20 \mu\text{m}$ , respectively. The root mean square of the surface roughness of a representative microparticle was about  $1.60 \text{ nm}$  (**Figure 3 C**) with occasional microparticles having rougher surfaces up to  $16 \text{ nm}$  (**Figure S1 A**). Representative methanol-treated (**Figure S1 B**) and water vapor-exposed (**Figure S1 C**) SF microparticles had a root mean square of the microparticle surface roughness between  $4$  and  $8 \text{ nm}$  and  $3$  and  $7 \text{ nm}$ , respectively. The aerodynamic properties of spray-dried microparticles were characterized and IGF-I-loaded trehalose microparticles had a mass median aerodynamic diameter (MMAD) of  $3.1 \pm 0.05 \mu\text{m}$  ( $n = 3$ ) and IGF-I-loaded untreated SF microparticles had a comparable MMAD of  $3.4 \pm 0.3 \mu\text{m}$  ( $n = 3$ ; **Figure 3 D**). The fine particle fraction of IGF-I loaded-trehalose microparticles was significantly higher ( $64.1 \pm 1.9\%$ ) than the fine particle fraction of IGF-I-loaded untreated SF microspheres ( $41.3 \pm 0.6\%$ ; **Figure S2**).

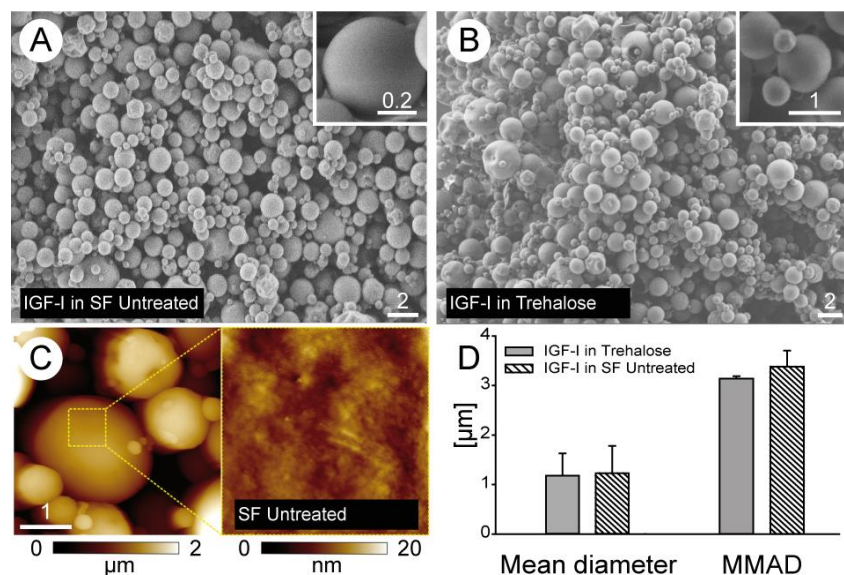


**Figure 3.** SEM images of IGF-I-loaded (A) untreated SF and (B) trehalose microparticles with magnification (inset). (C) AFM images of untreated SF microparticles with color bars indicating the surface roughness. (D) Mean diameter [ $\mu\text{m}$ ] and mass median aerodynamic diameter (MMAD;  $\mu\text{m}$ ) of IGF-I-loaded trehalose and untreated SF microparticles ( $n = 3$ ).

Wide-angle X-ray powder diffraction (WAXS) of untreated SF microparticles resulted in a broad peak between  $2\Theta \sim 10^\circ$  and  $30^\circ$  [49]. Silk I ( $\alpha$ -form; type II  $\beta$ -turn) [50] structure for SF has been reported with peaks at  $2\Theta \sim 12.2^\circ$ ,  $19.7^\circ$ ,  $24.7^\circ$ , and  $28.2^\circ$ , respectively, whereas silk II ( $\beta$ -form; anti-parallel  $\beta$ -pleated sheet) [50] structure was reported with peaks at  $2\Theta \sim 9.1^\circ$ ,  $18.9^\circ$ , and  $20.7^\circ$ , respectively [51, 52]. Notably, untreated SF microparticles analyzed after 20 months of storage *in vacuo* did not demonstrate conformational changes as analyzed by XRPD (data not shown). Methanol-treated microparticles had two diffraction signals at  $2\Theta \sim 19.9^\circ$  and  $\sim 24.1^\circ$ , suggesting a presence of the silk I structure. Water vapor-exposed microparticles resulted in sharper peaks as compared to methanol-treated microparticles, with three signals at  $2\Theta \sim 12.1^\circ$ ,  $19.9^\circ$ , and  $24.1^\circ$ , respectively, attributed to a silk I structure, as well as a small shoulder at  $20.7^\circ$ , indicating formation of a silk II structure. No evidence for a silk II structure was collected in untreated or methanol-treated microparticles (**Figure 4 A**). FTIR spectra of unloaded spray-dried SF microparticles were recorded after exposure to water vapor, methanol treatment, and

compared to untreated microparticles as control (**Figure 4 B**). The analysis of conformational changes of SF in response to treatment is typically focusing on the amide I (carbonyl stretching vibration of the amide group [53];  $1700 - 1600 \text{ cm}^{-1}$ ) and amide II (N-H bending and C-N stretching [53];  $1600 - 1500 \text{ cm}^{-1}$ ) absorption of the peptide backbone [54], with the absorption at  $1625 \text{ cm}^{-1}$  being assigned to (intermolecular [54]) antiparallel  $\beta$ -sheet, often found in crystallized proteins [55], and in the context of SF reflecting stacked antiparallel  $\beta$ -sheet structure [56] or silk II structure [49]. A band at  $1647 - 1655 \text{ cm}^{-1}$  is reflecting random coil structure [54]. Regions within  $1540 - 1520 \text{ cm}^{-1}$  and  $1270 - 1230 \text{ cm}^{-1}$  are assigned to amide II and amide III (C-N stretching coupled to the N-H in-plane bending vibration [53]) [57, 58]. The spectra from all microparticles had strong bands at  $1517 \text{ cm}^{-1}$  and  $1235 \text{ cm}^{-1}$ , reflecting no changes upon treatment with methanol or exposure to water vapor for the amide II and III, respectively. A shift from  $1645 \text{ cm}^{-1}$  to  $1622 \text{ cm}^{-1}$  was observed upon treatment and as compared to untreated microparticles, reflecting an increase in crystallinity and providing evidence that intermolecular/stacked antiparallel  $\beta$ -sheet structures have formed and that random coil structure was reduced upon treatment (**Figure 4 B**). Weakly observable shoulders at  $1270 \text{ cm}^{-1}$  as recorded for the methanol-treated and water vapor-exposed microparticles corroborated the  $\beta$ -sheet conformation and were absent for the untreated microparticles. The band observed for the untreated microparticles at about  $1645 \text{ cm}^{-1}$  suggested a random coil conformation and absence of  $\beta$ -sheet for amide I. The peak at  $1517 \text{ cm}^{-1}$  suggested  $\beta$ -sheet recorded in the amide II region in all groups [57]. All groups had strong bands at  $1235 \text{ cm}^{-1}$ , indicating a random coil structure. Therefore, the FTIR data reflected a shift from random coil conformation to an increase in  $\beta$ -sheet content following treatment of the microparticles with methanol or water vapor.

The absorption of water vapor to the microparticles was followed gravimetrically (**Figure 4 C**; **Figure S3**). Absorption characteristics of methanol-treated and water vapor-exposed microparticles were comparable, with virtually no difference in sorption and desorption isotherms (hysteresis) for each cycle of the experiment (**Figure 4 C**). In contrast, water absorption of untreated SF microparticles was different in the first cycle compared to the second cycle. Starting from a relative humidity of  $\sim 50\%$ , negative values were obtained in the first cycle and reflecting that the moisture content was lower during desorption as compared to sorption (hysteresis). However, the second cycle resulted in positive values and consequently in isotherms nearly coinciding with the microparticles previously exposed to water vapor and reflecting the



rapid conformational change of SF in response to water vapor (**Figure 4 C**). Total water sorption in terms of mass change [%] for untreated, methanol-treated, and water vapor-exposed microparticles at a relative humidity of 90% was as follows for 2 independent experiments and cycle 1 and 2, respectively, with [21.1; 20.8 and 18.7; 18.3], [17.9; 18.3 and 16.8; 17.3], [18.3; 18.6 and 17.5; 17.8] (**Figure S3**).

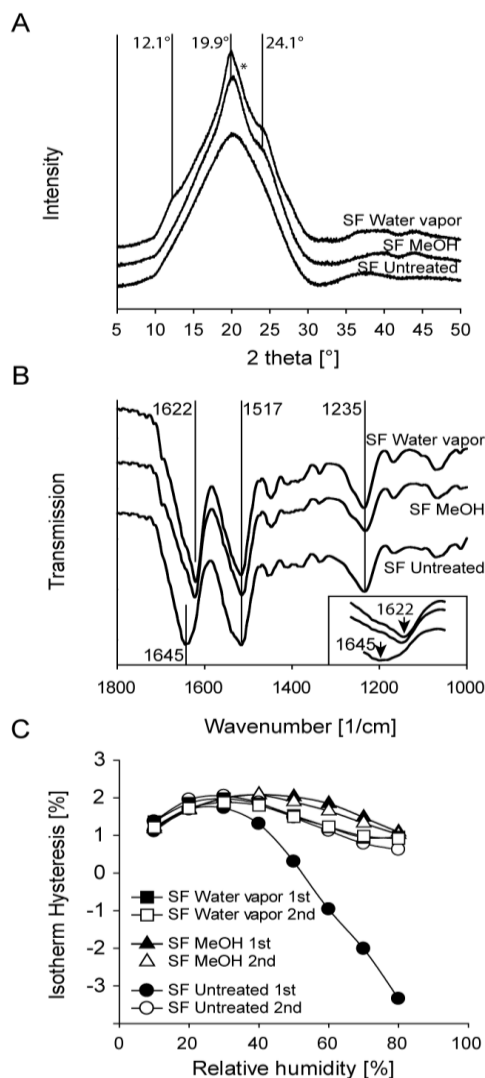


**Figure 4.** (A) X-ray diffraction pattern of water vapour-exposed, methanol-treated, and untreated SF microparticles. Asterisk indicates additional shoulder at approx. 20.7° for water vapor-exposed microparticles. (B) FTIR spectra of water vapor-exposed, methanol-treated, and untreated SF microparticles with magnification (inset). (C) Dynamic vapor sorption isotherm hysteresis plot of water vapor-exposed, methanol-treated, and untreated SF microparticles.

### *IGF-I stability and release*

During spray drying, the IGF-I in solution was exposed to pumping stress, heat, disintegration of the continuous fluid into droplets by means of a piezoelectric atomizer, and ultimately collection and recovery, the impact of which was detailed. IGF-I solution with trehalose was stable

throughout the process as assessed by reversed-phase HPLC (**Figure 5 A**). Furthermore, no small or large covalent aggregates were formed as analyzed by nonreduced SDS-PAGE (**Figure 5 B**), Native PAGE (**Figure 5 C**), or noncovalent aggregates by reduced SDS-PAGE (**Figure 5 D**), respectively. Size exclusion chromatography demonstrated that low-molecular-weight aggregates (mainly low aggregation numbers such as dimers and trimers) did not increase due to treatment (**Figure 5 E**).

The data indicated that IGF-I can be successfully processed by spray drying with no impact on IGF-I degradation or aggregation. Furthermore, IGF-I was stable in trehalose microparticles upon microparticle dissolution (**Figure 5 A**). Based on these results deploying trehalose, the experiments were extended to SF as carrier. The mean IGF-I peak from untreated SF microparticles decreased significantly by 5.7% as compared to before spray drying ( $p < 0.01$ ) (**Figure S4 A**). Furthermore, the peak from methionine 59 IGF-I [22, 23, 59]. (Met(o)-IGF-I) significantly increased (5.1%) as compared to before spray drying (please note, that IGF-I trehalose microparticles contained methionine as antioxidizing excipient, whereas IGF-I SF microparticles did not; **Figure S4 B**). This increase in the Met (59) peak was confirmed for microparticles stored for 18 months *in vacuo* (data not shown). After methanol and water vapor treatment and as compared to untreated microparticles, the IGF-I peak significantly decreased by 2.7% and 2.2% and the Met(o)-IGF-I peak significantly increased by 2.2% and 2.0%, respectively (**Figure S4 A, S4 B**) with no other degradation products being detected by chromatography (**Figure 5 F, G**).

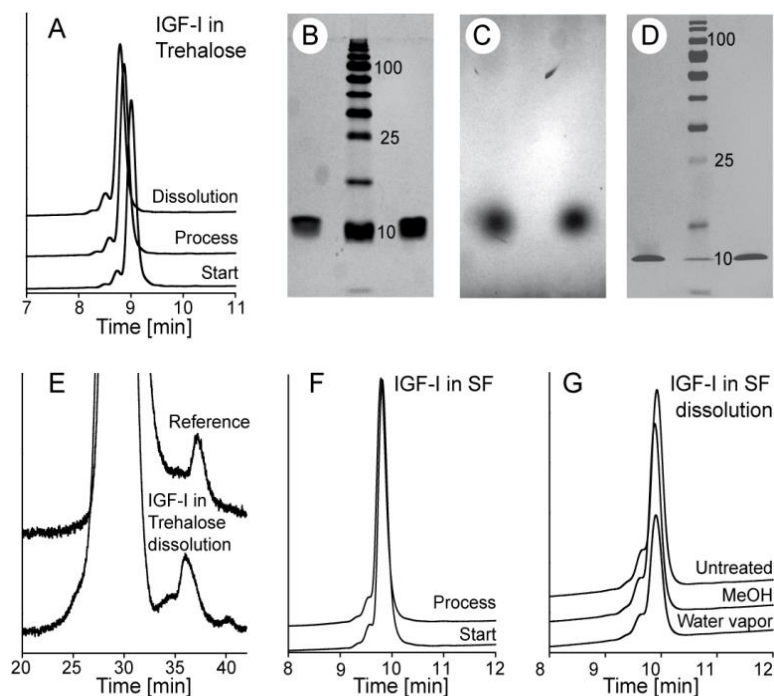


**Figure 5.** (A) HPLC chromatogram of IGF-I/trehalose solution samples taken before spray drying (start), during the spray drying process (process) and upon dissolution of the resulting microparticles (dissolution). (B) Nonreduced SDS-PAGE of trehalose microparticles (left) and IGF-I reference (right) with a molecular weight ladder in between [numbers in kDa]. (C) Native PAGE of IGF-I released from trehalose microparticles (left) and IGF-I reference (right) and (D) reduced SDS-PAGE of trehalose microparticles (left) and IGF-I reference (right) with a molecular weight ladder in between [numbers in kDa]. (E) SEC chromatogram of IGF-I reference solution (reference) and IGF-I from dissolved trehalose microparticles (trehalose dissolution). HPLC chromatogram of (F) IGF-I/SF solutions before spray drying (start), and during the spray drying process (process) and (G) of IGF-I from dissolved untreated, methanol-treated and water vapor-exposed microparticles, respectively.

IGF-I loading of trehalose microparticles (74.4%) was significantly higher as compared to untreated SF microparticles (50.4%), methanol-treated (48.0%), or water vapor-exposed microparticles (30.4%), respectively (**Figure 6 A**). No significant differences were observed for the loading of untreated and methanol-treated SF microparticles. However, loading of water vapor-exposed microparticles was 20% lower and significantly different from the loading of untreated microparticles. This is at least in part a result of the water vapor-exposed microparticles being weighed in wet stage, with an additional mass due to the adsorbed water of about 20%, nearly quantitatively matching the observed differences (**Figure S3 C**). *In vitro* IGF-I release from the trehalose microparticles into the release medium was instantaneous (data not shown). However, IGF-I release from SF microparticles was characterized by an exponential rise to maximum within three hours (**Figure 6 B**).

IGF-I potency was demonstrated for trehalose microparticles (**Figure 6 C**) and for untreated SF microparticles (**Figure 6 D**) and no potency assays were run on IGF-I released from methanol-treated or water vapor-exposed microparticles in light of previously reported data, indicating that exposure of IGF-I within SF scaffolds to these post-treatments did not impact the growth factor's potency [31, 35].

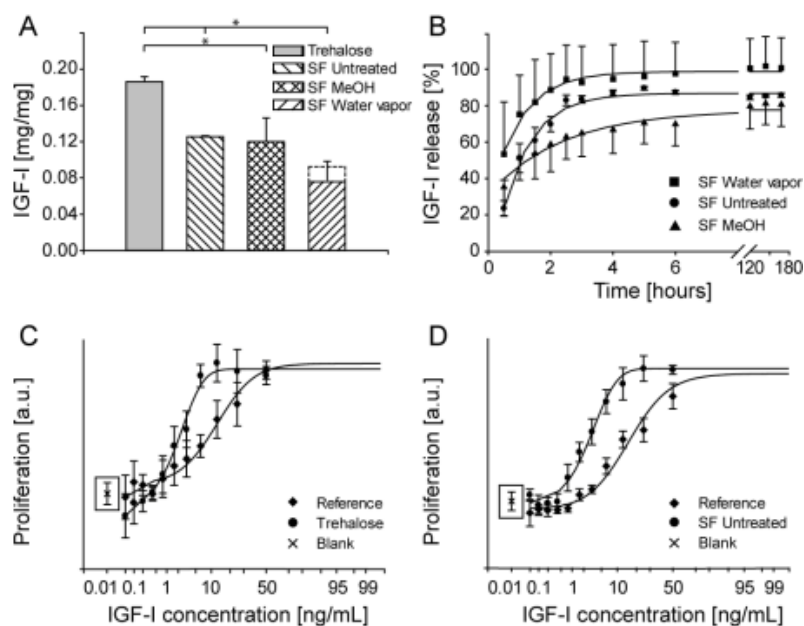


**Figure 6.** Loading of trehalose, untreated SF, methanol-treated SF and water vapor-exposed SF microparticles (mean  $\pm$  standard deviation;  $n=4$ ;  $n=3$  for trehalose). The loading on water vapor exposed microparticles was determined from wet microparticles, with the dotted bar indicating the results for an extrapolated dried state (water loss information was obtained from DVS experiments; see supplementary Figure 4). (B) IGF-I release [%] over time [hours] for water vapor-exposed, untreated, and methanol-treated SF microparticles, respectively (mean  $\pm$  standard error;  $n=3$ ). (C) MG-63 cell proliferation assay of IGF-I released from trehalose microparticles [arbitrary units] over IGF-I concentration [ng/mL] and (D) from untreated SF microparticles. Diluted IGF-I solutions were used for reference and the blank values are highlighted in the separated boxes (mean  $\pm$  standard deviation;  $n=3$ ; blank value  $n=12$ ). Asterisks highlight significant difference ( $p < 0.05$ ).

### *Lungperfusion with IGF-I trehalose microparticles and IGF-I SF microparticles*

The distribution of IGF-I to the perfusion buffer was studied in six human lung lobe perfusion experiments, three of which with IGF-I-loaded trehalose and three with IGF-I-loaded untreated SF microparticles. Transepithelial transport and “systemic” availability was measured in the

perfusion buffer of the *ex vivo* human lung lobe model and followed a linear pattern. Uptake kinetics from trehalose and SF microparticles were identical (**Figure 7**).

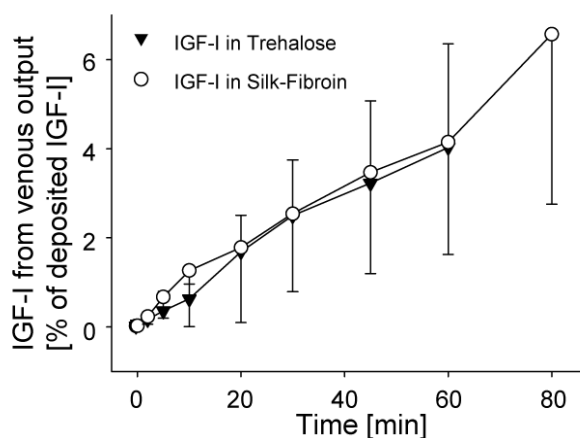


**Figure 7.** IGF-I recorded in the perfusion buffer using the *ex vivo* human lung lobe model. IGF-I-loaded microparticles from trehalose and untreated SF had identical “systemic” availability patterns ( $n = 3$  for each group, mean  $\pm$  mean deviation). Upwards facing error bars are for IGF-I trehalose microparticles, downwards facing error bars for untreated IGF-I SF microparticles.

## DISCUSSION

Transepithelial *in vitro* transport studies supported the assumption that IGF-I is systemically available upon pulmonary delivery and in analogy to inhaled INS (**Figure 1 B**). The higher permeation coefficient of INS was impacted by the lower molecular weight of INS (5.8 kDa) compared to IGF-I (7.6 kDa), with a relationship between the molecular mass and the permeation rate in Calu-3 monolayer having been described [60] and suggesting the contribution of a paracellular transport mechanism [45]. However, transcellular pathways also play a significant role for the uptake of proteins in alveolar epithelial cells. Previously, an enhanced INS transport has been observed in the presence of high molecular weight (>100 kDa) fractions of rat BALF [38]. In the present study we also found a significantly enhanced permeation of IGF-I under co-incubation with concentrated human BALF (**Figure 1 C**). The identity of the relevant transport-enhancing protein(s) yet needs to be clarified. A potential candidate might be  $\alpha_2$ -macroglobulin which is present in BALF and contributes to the regulation of transport processes [61, 62]. Interestingly, in the presence of  $\alpha_2$ -macroglobulin a more pronounced effect of IGF-I has been observed, which might be due to a higher uptake of IGF-I [63]. In the present study, further investigations revealed that the endocytotic transport of IGF-I across Calu-3 cells was clathrin, caveolae and macrocytosis independent, but dynamin dependent. Similar results have been

reported for INS [46, 64]. Within the constraints of this assessment evidence is provided that INS and IGF-I at least in part share common pathways across alveolar cells. These pathways include para- and transcellular routes and the precise mechanism appears to be dependent on factors such as cell type or the presence of transport-enhancing proteins [38, 64, 65].

Several physical-chemical properties of silk-fibroin (SF) impact drug delivery. Main parameters include crystallinity (analyzed by FTIR and XRPD), morphology (AFM and SEM), water vapor sorption (DVS), and characteristics for pulmonary delivery (aerodynamic diameter). For intrapulmonary administration, the aerodynamic properties critically impact successful particle landing in the alveoli and thereby systemic drug absorption. Typically, a mass median aerodynamic diameter (MMAD) of 1  $\mu\text{m}$  to 5  $\mu\text{m}$  is instrumental in targeting the deep regions of the lung, including the small airways and alveoli and 80% of particles with a diameter of  $< 3 \mu\text{m}$  are typically expected to reach the lower airways in healthy adult subjects [14]. Extrapolating from these studies, the MMAD of IGF-I-loaded trehalose microparticles ( $3.1 \pm 0.05 \mu\text{m}$ ) and of IGF-I-loaded untreated SF microparticles ( $3.4 \pm 0.3 \mu\text{m}$ ) would suggest alveolar landing as a prerequisite for systemic availability (**Figure 3 D**).

The comparable geometric diameters and aerodynamic parameters including MMAD (**Figure 3 D; Figure S2**) along with geometric standard deviations below 1.2, suggested a homogenous particle size distribution and similar geometrical and bulk properties, for both IGF-I-loaded trehalose and untreated IGF-I-loaded SF microparticles. Post-manufacture treatment (i.e. methanol treatment or exposure to water vapor) of the SF microparticles increased the  $\beta$ -sheet content/overall crystallinity [35], did not substantially impact IGF-I stability, and resulted in water insolubility. However, we did observe a shift from IGF-I to Met(o)-IGF-I for the SF but not the trehalose formulation and assigned it to the antioxidative potential of methionine which was co-formulated with the trehalose microparticles but not with SF (**Figure S4 B**). The sum of the IGF-I and the Met(o)-IGF-I peak areas as analyzed by RP-HPLC added up to comparable values between the control IGF-I solution and all microparticle formulations, suggesting that no further chemical instability other than oxidation of the methionine in position 59 of the IGF-I peptide occurred [59]. Nevertheless, the loading was significantly different for trehalose and SF microparticles, respectively (**Figure 6 A**). This finding opened two interpretations, either (i) IGF-I loss as a result of covalent or noncovalent aggregates or (ii) IGF-I complexation with SF in solution (i.e. upon IGF-I release from the microparticle) leading to invisible complexes in

solution of IGF-I (pI~7.8 [15]) with the SF biopolymer (pI~4.5 [66]) presumably through electrostatic and van-der-Waals interaction, respectively. Interpretation (ii) is building off recently detailed thermodynamic studies between protamine - a basic model protein - and SF, and should be only carefully conducted in light of the differences among protamine (pI~12) and IGF-I [67]. Nevertheless, the finding that potency of IGF-I was retained in untreated SF microparticles (**Figure 6 D**) and “systemic” exposure as approximated by *ex vivo* use of the human lung lobe model (**Figure 7**) provided evidence that complexation in solution is more likely than a loss as a result of aggregation based on the assumption that aggregation would lead to a loss in potency. However, these findings highlight the need to develop robust purification and analytical techniques for the characterization of SF drug delivery systems.

IGF-I release profiles from SF (untreated and methanol-treated/water vapor-exposed) did not differ significantly from each other (**Figure 6 B**). This finding was unexpected in light of the typically strong impact of methanol treatment/water vapor exposure on protein drug release profiles from SF scaffold materials [25], including IGF-I [31]. This is a result of the special spray drier setup used in this study, based on a piezo crystal for droplet generation in contrast to the spraying method used before [68]. It has been shown that ultrasound high frequency treatment of SF – as mediated by the piezo crystal - increased crystallinity [69]. We speculate that the increase of crystallinity as a result of the use of the piezo crystal for droplet generation was sufficient to increase the crystallinity to an extent, such that sustained release profiles were found for IGF-I. Further increase in crystallinity by water vapor exposure or methanol treatment did not further impact the profile as compared to untreated SF microparticles. Microparticles exposed to water vapor or treated with methanol had an increase in crystallinity as compared to untreated SF microparticles and a silk I conformation (**Figure 4 A**). Silk I is a preferable conformation as linked to rapid SF degradation kinetics [70] - a desired feature for pulmonary delivery addressing concerns of particle longevity and the risk of posing an inflammatory challenge in the lung as a result of chronic particle presence. Previous reports have already reported that silk-I conformation is maintained in spite of methanol treatment when formulated into microparticles under appropriate conditions [71]. Finally, systemic IGF-I availability was assessed in an *ex vivo* human lung lobe model. SF carriers were equivalent to trehalose in shuttling IGF-I across the pulmonary epithelial barrier. SF is well known for its general capacity for stabilizing complex molecules, including antibodies and peptides [24, 25, 29]. Furthermore, SF has been



demonstrated to have comparable biocompatibility to type I collagen and improved safety characteristics as compared to synthetic polymers such as poly(lactic-co-glycolic acid) using intramuscular implantation for safety assessment in rats [72] and when implanted into bone defects in sheep [28]. In spite of the benign character of SF evidenced before, the pulmonary route constitutes a new site of administration requiring additional toxicological profiling. From a technical perspective, the equivalence for trehalose and SF carriers for transepithelial transport in the lung lobe model places SF as an interesting candidate to expand the notoriously short list of excipient for the formulation of dry powders for inhalation and more strongly within the field of systemic peptide delivery through the lungs. Longer lasting kinetic studies are required to corroborate these findings from the *ex vivo* human lung lobe model for later time points. We used a human lung lobe model to successfully demonstrate pulmonary absorption from both IGF-I formulations, those in trehalose and those in SF carrier, respectively. This lung perfusion model has been previously used to compare different formulations of inhaled glucocorticoids and was found to excellently mirror clinical pharmacokinetics of the drug preparations [44]. The current study was the first time that an aerosolized protein was administered to the lung lobe model. Assuming that a total of 10 mg powder blend is used per capsule and that the bioavailability is 6% (latest value reported in *ex vivo* lung lobe model experiments), a minimum of 112 µg or 76 µg IGF-I can be made systemically available per inhalation for the trehalose and untreated SF microparticles, respectively.

## CONCLUSION

*In vitro* studies demonstrated for the first time the transepithelial IGF-I flux and in analogy to INS. IGF-I was successfully formulated into pulmonary drug delivery systems by deploying trehalose and SF as carriers, respectively. The use of both carriers, trehalose and SF, resulted in effective and comparable shuttling of IGF-I through an *ex vivo* human lung lobe model. Therefore, the general feasibility of pulmonary IGF-I delivery was demonstrated from trehalose and SF, opening pulmonary delivered and systemic IGF-I e.g. for a future therapy of muscle wasting diseases such as sarcopenia.

### ACKNOWLEDGMENTS

We thank Dr. Vladimir Stepanenko and Prof. Frank Würthner (Center for Nanosystems Chemistry, Würzburg) for the AFM and SEM measurements and their help with the data analyses. Recombinant human IGF-I was kindly provided by Novartis and Bombyx mori cocoons from Trudel Silk. This work was supported by DAAD grant „Kooperation in pharmazeutischen Wissenschaften und Lehre, # 57058983 and the Bayerische Forschungstiftung “Formosa”.

---

## REFERENCES

1. Roubenoff, R. (2003) Catabolism of aging: is it an inflammatory process?, *Curr Opin Clin Nutr Metab Care*6, 295-299.
2. Goldspink, G. (1999) Changes in muscle mass and phenotype and the expression of autocrine and systemic growth factors by muscle in response to stretch and overload, *J. Anat.*194, 323-334.
3. Dela, F., and Kjaer, M. (2006) Resistance training, insulin sensitivity and muscle function in the elderly, *Essays Biochem.*42, 75-88.
4. Perrini, S., Laviola, L., Carreira, M. C., Cignarelli, A., Natalicchio, A., and Giorgino, F. (2010) The GH/IGF1 axis and signaling pathways in the muscle and bone: mechanisms underlying age-related skeletal muscle wasting and osteoporosis, *J. Endocrinol.*205, 201-210.
5. Mourkioti, F., and Rosenthal, N. (2005) IGF-1, inflammation and stem cells: interactions during muscle regeneration, *Trends Immunol.*26, 535-542.
6. Rommel, C., Bodine, S. C., Clarke, B. A., Rossman, R., Nunez, L., Stitt, T. N., Yancopoulos, G. D., and Glass, D. J. (2001) Mediation of IGF-1-induced skeletal myotube hypertrophy by PI(3)K/Akt/mTOR and PI(3)K/Akt/GSK3 pathways, *Nat. Cell Biol.*3, 1009-1013.
7. Solomon, A. M., and Bouloux, P. M. G. (2006) Modifying muscle mass - the endocrine perspective, *J. Endocrinol.*191, 349-360.
8. Vinciguerra, M., Musaro, A., and Rosenthal, N. (2010) Regulation of muscle atrophy in aging and disease, *Adv. Exp. Med. Biol.*694, 211-233.

### CHAPTER III

---

9. Guler, H. P., Zapf, J., Schmid, C., and Froesch, E. R. (1989) Insulin-like growth factors I and II in healthy man. Estimations of half-lives and production rates, *Acta endocrinologica*121, 753-758.
10. Frystyk, J. (2004) Free insulin-like growth factors -- measurements and relationships to growth hormone secretion and glucose homeostasis, *Growth Horm IGF Res*14, 337-375.
11. Denley, A., Cosgrove, L. J., Booker, G. W., Wallace, J. C., and Forbes, B. E. (2005) Molecular interactions of the IGF system, *Cytokine Growth Factor Rev*16, 421-439.
12. Patton, J. S., and Byron, P. R. (2007) Inhaling medicines: delivering drugs to the body through the lungs, *Nat. Rev. Drug Discovery*6, 67-74.
13. Santos Cavaiola, T., and Edelman, S. (2014) Inhaled Insulin: A Breath of Fresh Air? A Review of Inhaled Insulin, *Clin. Ther.*36, 1275-1289.
14. Patton, J. S. (1996) Mechanisms of macromolecule absorption by the lungs, *Adv. Drug Delivery Rev.*19, 3-36.
15. Clemmons, D. R. (2000) Insulin-like growth factors - their binding proteins and growth regulation, In *Skeletal growth factors* (Canalis, E., Ed.), Lippincott Williams & Wilkins, Philadelphia.
16. Clark, R. G. (2005) Recombinant human insulin-like growth factor I (IGF-I): risks and benefits of normalizing blood IGF-I concentrations, *Horm. Res.*62, 93-100.
17. Agency, E. M. (2008) Exubera: EPAR - all authorized presentations, European Medicines Agency, London.
18. Agency, E. M. (2008) Exubera: EPAR - scientific discussion.

- 
19. Luginbuehl, V., Zoidis, E., Meinel, L., von, R. B., Gander, B., and Merkle, H. P. (2013) Impact of IGF-I release kinetics on bone healing: A preliminary study in sheep, *Eur. J. Pharm. Biopharm.*85, 99-106.
  20. Luginbuehl, V., Wenk, E., Koch, A., Gander, B., Merkle, H. P., and Meinel, L. (2005) Insulin-like Growth Factor I-Releasing Alginate-Tricalciumphosphate Composites for Bone Regeneration, *Pharm. Res.*22, 940-950.
  21. Luginbuehl, V., Meinel, L., Merkle, H. P., and Gander, B. (2004) Localized delivery of growth factors for bone repair, *Eur. J. Pharm. Biopharm.*58, 197-208.
  22. Meinel, L., Zoidis, E., Zapf, J., Hassa, P., Hottiger, M. O., Auer, J. A., Schneider, R., Gander, B., Luginbuehl, V., Bettschart-Wolfisberger, R., Illi, O. E., Merkle, H. P., and von, R. B. (2003) Localized insulin-like growth factor I delivery to enhance new bone formation, *Bone (San Diego, CA, U. S.)*33, 660-672.
  23. Meinel, L., Illi, O. E., Zapf, J., Malfanti, M., Peter, M. H., and Gander, B. (2001) Stabilizing insulin-like growth factor-I in poly(d,l-lactide-co-glycolide) microspheres, *J. Controlled Release*70, 193-202.
  24. Guziewicz, N. A., Massetti, A. J., Perez-Ramirez, B. J., and Kaplan, D. L. (2013) Mechanisms of monoclonal antibody stabilization and release from silk biomaterials, *Biomaterials*34, 7766-7775.
  25. Wenk, E., Merkle, H. P., and Meinel, L. (2011) Silk fibroin as a vehicle for drug delivery applications, *J. Controlled Release*150, 128-141.
  26. Meinel, L., Hofmann, S., Karageorgiou, V., Zichner, L., Langer, R., Kaplan, D., and Vunjak-Novakovic, G. (2004) Engineering cartilage-like tissue using human mesenchymal stem cells and silk protein scaffolds, *Biotechnol. Bioeng.*88, 379-391.

### CHAPTER III

---

27. Edelhoch, H. (1967) Spectroscopic determination of tryptophan and tyrosine in proteins, *Biochemistry*6, 1948-1954.
28. Uebersax, L., Apfel, T., Nuss, K. M. R., Vogt, R., Kim, H. Y., Meinel, L., Kaplan, D. L., Auer, J. A., Merkle, H. P., and von, R. B. (2013) Biocompatibility and osteoconduction of macroporous silk fibroin implants in cortical defects in sheep, *Eur. J. Pharm. Biopharm.*85, 107-118.
29. Meinel, L., and Kaplan, D. L. (2012) Silk constructs for delivery of musculoskeletal therapeutics, *Adv. Drug Delivery Rev.*64, 1111-1122.
30. Wang, X., Wenk, E., Zhang, X., Meinel, L., Vunjak, G., and Kaplan, D. L. (2010) Growth Factor Gradients via Microsphere Delivery in Biopolymer Scaffolds for Osteochondral Tissue Engineering, *134*, 0–4.
31. Uebersax, L., Merkle, H. P., and Meinel, L. (2008) Insulin-like growth factor I releasing silk fibroin scaffolds induce chondrogenic differentiation of human mesenchymal stem cells, *J. Controlled Release*127, 12-21.
32. Fransson, J. R. (1997) Oxidation of human insulin-like growth factor I in formulation studies. 3. Factorial experiments of the effects of ferric ions, EDTA, and visible light on methionine oxidation and covalent aggregation in aqueous solution, *Journal of pharmaceutical sciences*86, 1046–1050.
33. Laemmli, U. K. (1970) Cleavage of Structural Proteins during the Assembly of the Head of Bacteriophage T4, *Nature*227, 680–685.
34. McLellan, T. (1982) Electrophoresis buffers for polyacrylamide gels at various pH, *Analytical Biochemistry*126, 94–99.

- 
35. Wenk, E., Wandrey, A. J., Merkle, H. P., and Meinel, L. (2008) Silk fibroin spheres as a platform for controlled drug delivery, *J. Controlled Release*132, 26-34.
  36. Ehrhardt, C., Fiegel, J., Fuchs, S., Abu-Dahab, R., Schaefer, U. F., Hanes, J., and Lehr, C.-M. (2002) Drug absorption by the respiratory mucosa: cell culture models and particulate drug carriers, *Journal of aerosol medicine : the official journal of the International Society for Aerosols in Medicine*15, 131–139.
  37. Vllasaliu, D., Fowler, R., Garnett, M., Eaton, M., and Stolnik, S. (2011) Barrier characteristics of epithelial cultures modelling the airway and intestinal mucosa: a comparison, *Biochemical and biophysical research communications*415, 579-585.
  38. Bahhady, R., Kim, K.-J., Borok, Z., Crandall, E. D., and Shen, W.-C. (2008) Characterization of protein factor(s) in rat bronchoalveolar lavage fluid that enhance insulin transport via transcytosis across primary rat alveolar epithelial cell monolayers, *Eur. J. Pharm. Biopharm.*69, 808-816.
  39. Gnadt, M., Trammer, B., Kardziev, B., Bayliss, M. K., Edwards, C. D., Schmidt, M., and Hoegger, P. (2012) Comparison of the bronchodilating effects of inhaled  $\beta$ 2-agonists after methacholine challenge in a human lung reperfusion model, *Eur. J. Pharm. Biopharm.*81, 617-626.
  40. Gnadt, M., Trammer, B., Freiwald, M., Kardziev, B., Bayliss, M. K., Edwards, C. D., Schmidt, M., Friedel, G., and Hoegger, P. (2012) Methacholine delays pulmonary absorption of inhaled  $\beta$ 2-agonists due to competition for organic cation/carnitine transporters, *Pulm. Pharmacol. Ther.*25, 124-134.
  41. Freiwald, M., Valotis, A., Kirschbaum, A., McClellan, M., Murdter, T., Fritz, P., Friedel, G., Thomas, M., and Hogger, P. (2005) Monitoring the initial pulmonary absorption of

- two different beclomethasone dipropionate aerosols employing a human lung reperfusion model, *Respir Res*6, 21.
42. Mathias, N. R., Timoszyk, J., Stetsko, P. I., Megill, J. R., Smith, R. L., and Wall, D. A. (2002) Permeability characteristics of Calu-3 human bronchial epithelial cells: in vitro-in vivo correlation to predict lung absorption in rats, *J. Drug Targeting*10, 31-40.
43. Florea, B. I., Cassara, M. L., Junginger, H. E., and Borchard, G. (2003) Drug transport and metabolism characteristics of the human airway epithelial cell line Calu-3, *J. Controlled Release*87, 131-138.
44. Breitfeld, P. P., McKinnon, W. C., and Mostov, K. E. (1990) Effect of nocodazole on vesicular traffic to the apical and basolateral surfaces of polarized MDCK cells, *J. Cell Biol.*111, 2365-2373.
45. Hastings, R. H., Folkesson, H. G., and Matthav, M. A. (2004) Mechanisms of alveolar protein clearance in the intact lung, *Am. J. Physiol.*286, L679-L689.
46. Oda, K., Yumoto, R., Nagai, J., Katayama, H., and Takano, M. (2011) Mechanism underlying insulin uptake in alveolar epithelial cell line RLE-6TN, *Eur. J. Pharmacol.*672, 62-69.
47. Kirchhausen, T., Macia, E., and Pelish, H. E. (2008) Use of dynasore, the small molecule inhibitor of dynamin, in the regulation of endocytosis, *Methods Enzymol.*438, 77-91.
48. Macia, E., Ehrlich, M., Massol, R., Boucrot, E., Brunner, C., and Kirchhausen, T. (2006) Dynasore, a cell-permeable inhibitor of dynamin, *Dev. Cell*10, 839-850.
49. Lu, Q., Hu, X., Wang, X., Kluge, J. A., Lu, S., Cebe, P., and Kaplan, D. L. (2010) Water-insoluble silk films with silk I structure, *Acta Biomater.*6, 1380-1387.



- 
50. Sohn, S., Strey, H. H., and Gido, S. P. (2004) Phase Behavior and Hydration of Silk Fibroin, *Biomacromolecules*5, 751-757.
  51. Li, M., Ogiso, M., and Minoura, N. (2003) Enzymatic degradation behavior of porous silk fibroin sheets, *Biomaterials*24, 357-365.
  52. Marsh, R. E., Corey, R. B., and Pauling, L. (1955) An investigation of the structure of silk fibroin, *Biochim Biophys Acta*16, 1-34.
  53. Teramoto, H., and Miyazawa, M. (2005) Molecular Orientation Behavior of Silk Sericin Film as Revealed by ATR Infrared Spectroscopy, *Biomacromolecules*6, 2049-2057.
  54. Hu, X., Kaplan, D., and Cebe, P. (2006) Determining Beta-Sheet Crystallinity in Fibrous Proteins by Thermal Analysis and Infrared Spectroscopy, *Macromolecules*39, 6161-6170.
  55. Goormaghtigh, E., Cabiaux, V., and Ruyschaert, J. M. (1990) Secondary structure and dosage of soluble and membrane proteins by attenuated total reflection Fourier-transform infrared spectroscopy on hydrated films, *Eur J Biochem*193, 409-420.
  56. Chen, X., Knight, D. P., Shao, Z., and Vollrath, F. (2001) Regenerated Bombyx silk solutions studied with rheometry and FTIR, *Polymer*42, 09969-09974.
  57. Ha, S.-W., Tonelli, A. E., and Hudson, S. M. (2005) Structural Studies of Bombyx mori Silk Fibroin during Regeneration from Solutions and Wet Fiber Spinning, *Biomacromolecules*6, 1722-1731.
  58. Zhao, H., Heusler, E., Jones, G., Werner, V., Germershaus, O., Ritzer, J., Luehmann, T., Li, L., and Meinel, L. (2014) Decoration of silk fibroin by click chemistry for biomedical application, *J Struct Biol*.

59. Germershaus, O., Schultz, I., Luhmann, T., Beck-Broichsitter, M., Hogger, P., and Meinel, L. (2013) Insulin-like growth factor-I aerosol formulations for pulmonary delivery, *Eur. J. Pharm. Biopharm.*85, 61-68.
60. Grainger, C. I., Greenwell, L. L., Lockley, D. J., Martin, G. P., and Forbes, B. (2006) Culture of Calu-3 Cells at the Air Interface Provides a Representative Model of the Airway Epithelial Barrier, *Pharm. Res.*23, 1482-1490.
61. Lindahl, M., Stahlbom, B., Svartz, J., and Tagesson, C. (1998) Protein patterns of human nasal and bronchoalveolar lavage fluids analyzed with two-dimensional gel electrophoresis, *Electrophoresis*19, 3222-3229.
62. Rehman, A. A., Ahsan, H., and Khan, F. H. (2013) Alpha-2-macroglobulin: A physiological guardian, *J. Cell. Physiol.*228, 1665-1675.
63. Westwood, M., Aplin, J. D., Collinge, I. A., Gill, A., White, A., and Gibson, J. M. (2001)  $\alpha$ 2-Macroglobulin: a new component in the insulin-like growth factor/insulin-like growth factor binding protein-1 axis, *J. Biol. Chem.*276, 41668-41674.
64. Ikehata, M., Yumoto, R., Kato, Y., Nagai, J., and Takano, M. (2009) Mechanism of insulin uptake in rat alveolar type II and type I-like epithelial cells, *Biol. Pharm. Bull.*32, 1765-1769.
65. Pezron, I., Mitra, R., Pal, D., and Mitra, A. K. (2002) Insulin aggregation and asymmetric transport across human bronchial epithelial cell monolayers (Calu-3), *J. Pharm. Sci.*91, 1135-1146.
66. Cheng, Q., Peng, T.-Z., Hu, X.-B., and Yang, C. F. (2005) Charge-selective recognition at fibroin-modified electrodes for analytical application, *Anal. Bioanal. Chem.*382, 80-84.

- 
67. Germershaus, O., Werner, V., Kutscher, M., and Meinel, L. (2014) Deciphering the mechanism of protein interaction with silk fibroin for drug delivery systems, *Biomaterials*, Ahead of Print.
  68. Hino, T., Tanimoto, M., and Shimabayashi, S. (2003) Change in secondary structure of silk fibroin during preparation of its microspheres by spray-drying and exposure to humid atmosphere, *J. Colloid Interface Sci.*266, 68-73.
  69. Samal, S. K., Kaplan, D. L., and Chiellini, E. (2013) Ultrasound Sonication Effects on Silk Fibroin Protein, *Macromol. Mater. Eng.*298, 1201-1208.
  70. Bonner, J. C. (2007) Lung fibrotic responses to particle exposure, *Toxicol. Pathol.*35, 148-153.
  71. Lammel, A. S., Hu, X., Park, S.-H., Kaplan, D. L., and Scheibel, T. R. (2010) Controlling silk fibroin particle features for drug delivery, *Biomaterials*31, 4583-4591.
  72. Meinel, L., Hofmann, S., Karageorgiou, V., Kirker-Head, C., McCool, J., Gronowicz, G., Zichner, L., Langer, R., Vunjak-Novakovic, G., and Kaplan, D. L. (2005) The inflammatory responses to silk films in vitro and in vivo, *Biomaterials*26, 147-155.

## SUPPORTING INFORMATION.

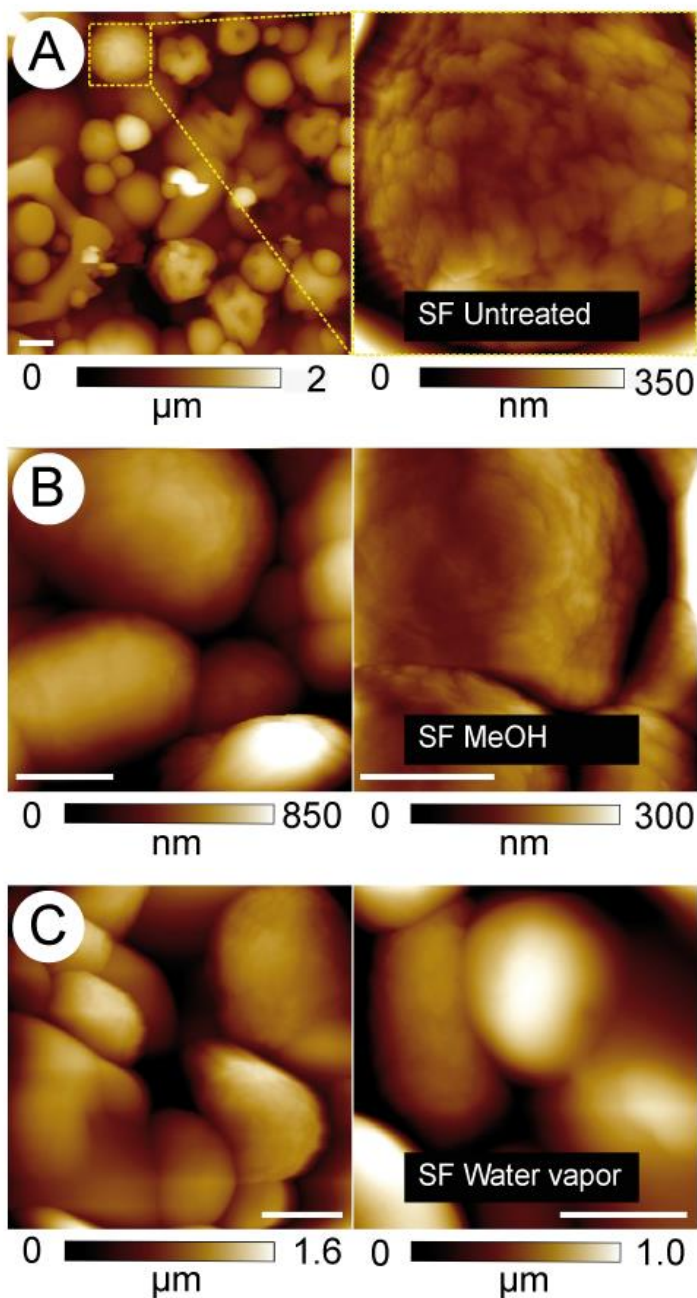


**Figure S1.** AFM images of (A) untreated SF microparticles (left) with respective magnification (right), (B) methanol-treated SF and (C) water vapor-exposed SF microparticles. Color bars represent the surface roughness. Bar length is 1  $\mu\text{m}$ .

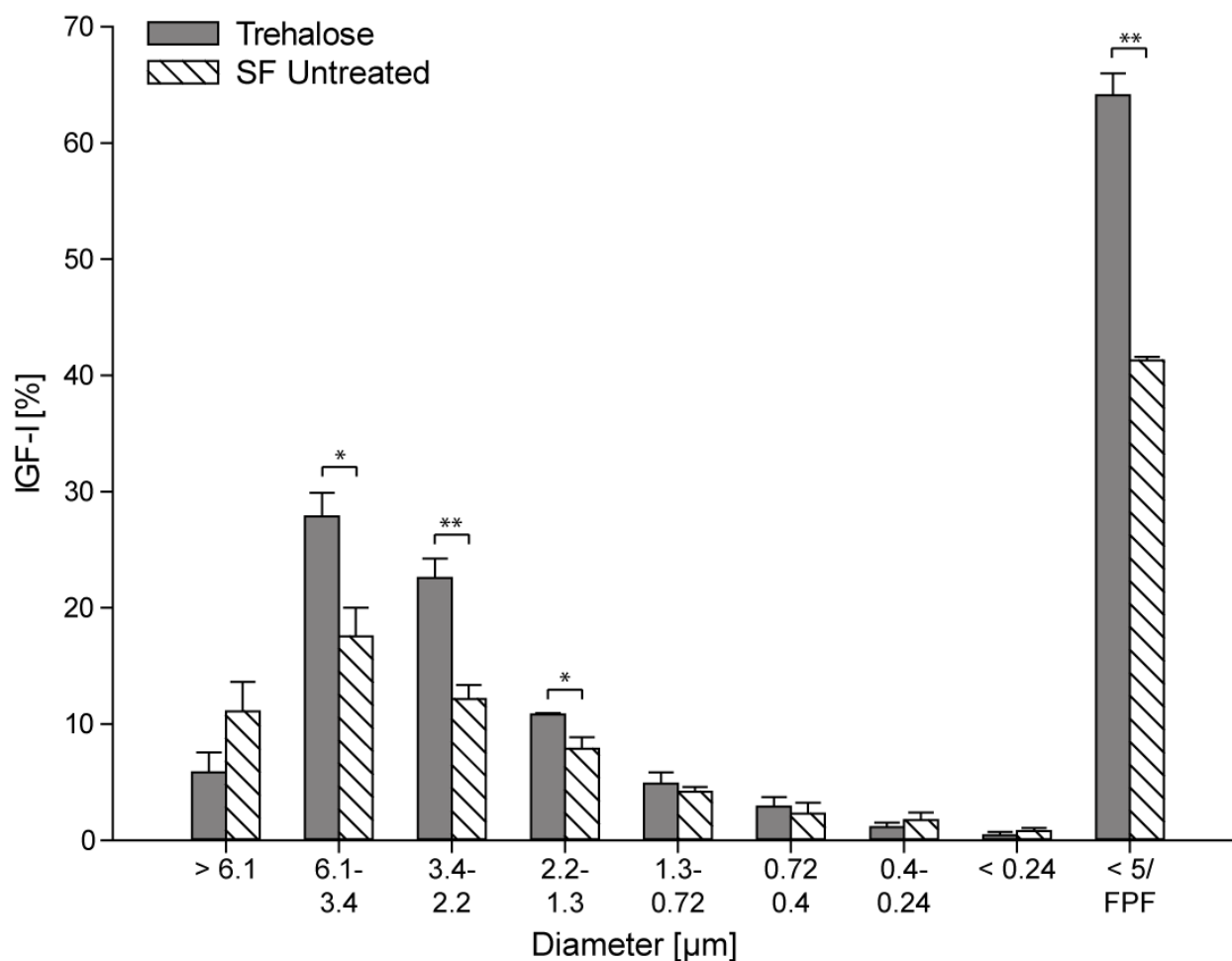


**Figure S2.** Distribution of IGF-I [%] on the different stages of the Next Generation Impactor after aerosolization of trehalose and untreated silk-fibroin microparticles (mean  $\pm$  standard deviation;  $n=3$ ). Asterisks highlight significant difference at  $p < 0.05$  for stage 2 (6.1  $\mu\text{m}$ –3.4  $\mu\text{m}$ ) and 4 (2.2  $\mu\text{m}$ –1.3  $\mu\text{m}$ ) and two asterisks at  $p < 0.01$  for stage 3 (3.4  $\mu\text{m}$ –2.2  $\mu\text{m}$ ) and the FPF (fine particle fraction) of all microparticles. FPF is the sum of particles with a diameter  $\leq 5 \mu\text{m}$ .

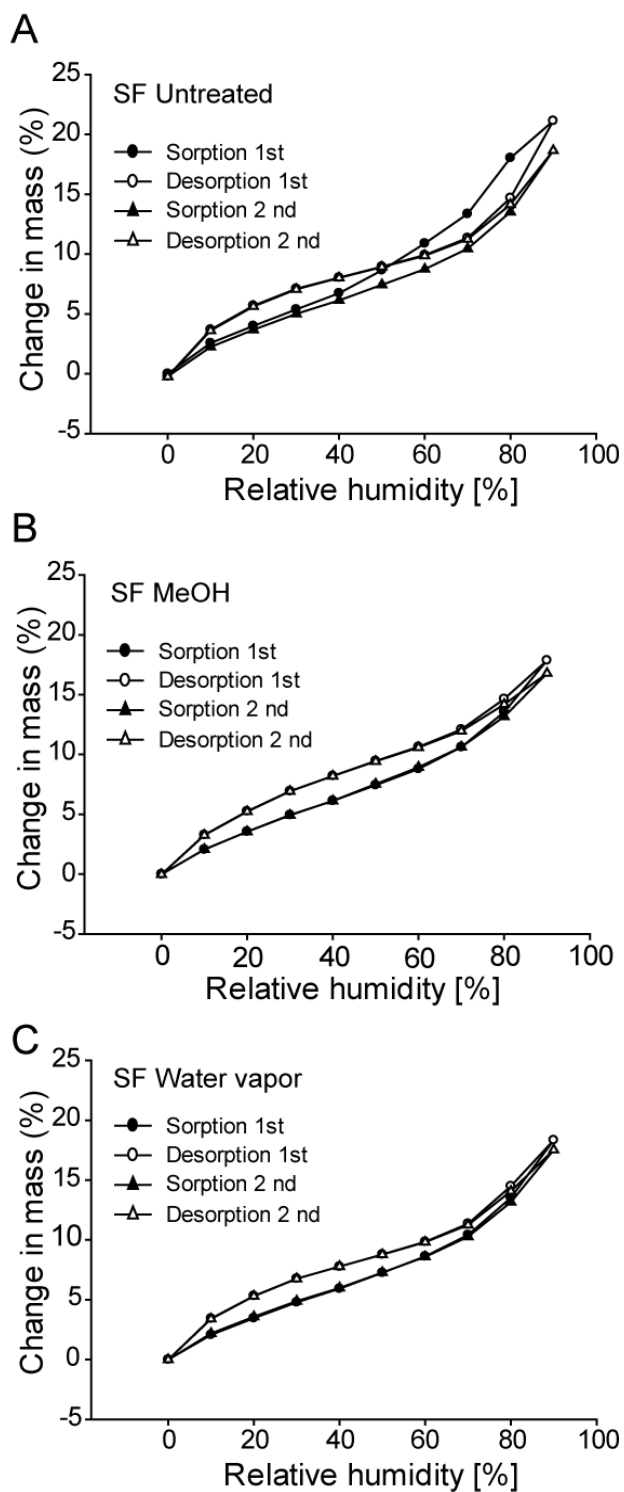


**Figure S3.** Water vapor isotherms of (A) untreated, (B) methanol-treated, and (C) water vapor-exposed microparticles.

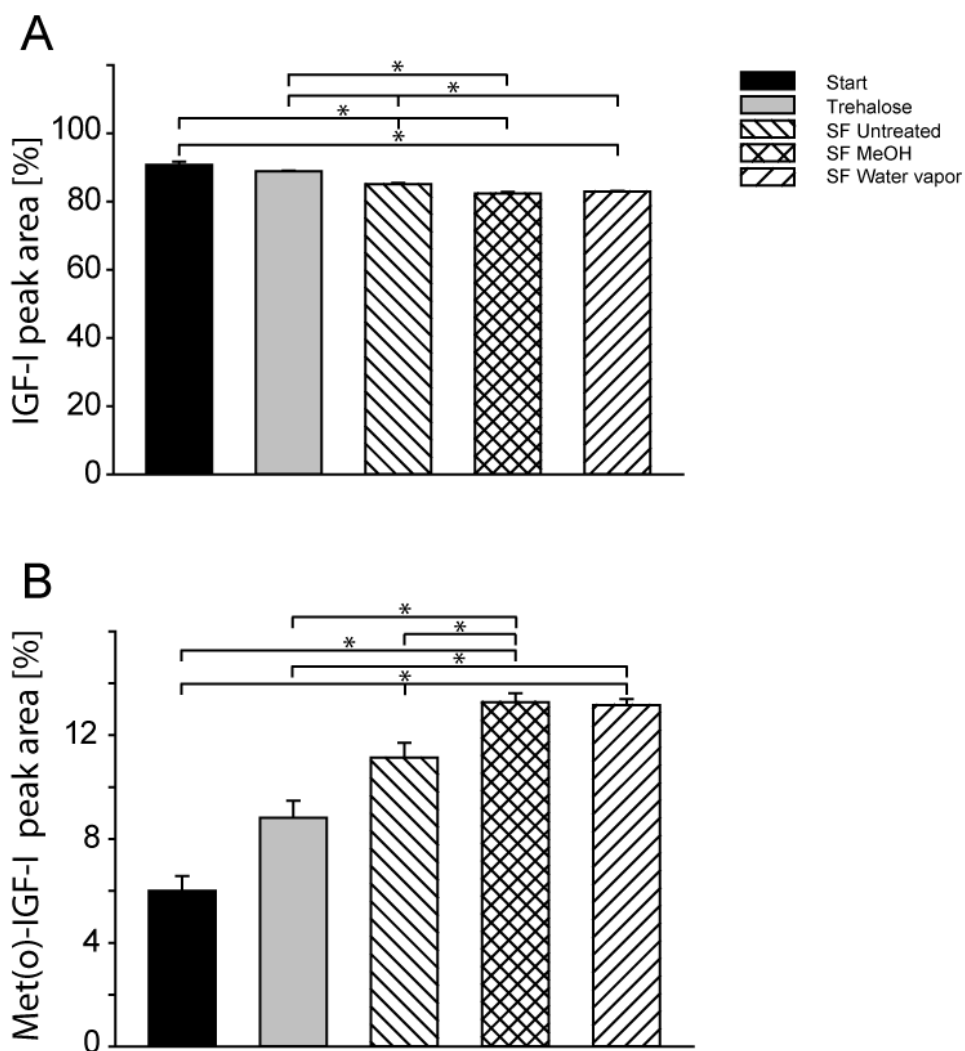


**Figure S4.** IGF-I degradation analysis: (A) IGF-I peak area [%] before spray drying (start) and of IGF-I released from trehalose, untreated, methanol-treated and water vapor-exposed microparticles. (B) Peak area [%] of methionine 59 oxidized IGF-I (Met(o)-IGF-I) from samples collected before spray drying (start) and from trehalose, untreated, methanol-treated and water vapor-exposed microparticles. Asterisks highlight significant difference at  $p < 0.05$ .

### *Copyright*

This chapter is reprinted with permission from Schultz, I., Vollmers, F., Luehmann, T., Rybak, J.-C., Wittmann, R., Stank, K., Steckel, H., Kardziej, B., Schmidt, M., Högger, P., Meinel, L. (2015). Pulmonary Insulin-like growth factor I delivery from trehalose and silk-fibroin microparticles. *ACS Biomaterials Science & Engineering*, 2015, 1(2), pp 119-129. doi: 10.1021/ab500101c. Copyright 2015 American Chemical Society.



## CHAPTER IV

# EXPRESSION OF IGF-I MUTANTS

*Isabel Schultz, Lorenz Meinel\**

Institute for Pharmacy and Food Chemistry, University of Wuerzburg, Am Hubland, DE-97074  
Wuerzburg,

*unpublished*

### **ABSTRACT**

Insulin-like growth factor I is an important regulator of growth and metabolism and, therefore, a valuable agent for musculoskeletal diseases such as sarcopenia. We developed a strategy for safe, reliable and controllable IGF-I delivery. For this purpose we genetically engineered two IGF-I variants containing an unnatural amino acid at two positions, respectively, thereby integrating alkyne functions into the primary sequence of the protein. These allowed linking IGF-I with other molecules in a site specific manner, i.e. via a copper catalyzed azide-alkyne Huisgen cycloaddition (click reaction). In this work we introduce the different IGF-I mutants and the IGF-I delivery concept and describe the optimization of the expression conditions of the IGF-I mutants and initial approaches for the following purification by cation exchange chromatography.

## INTRODUCTION

Insulin-like growth factor-I (IGF-I) is a member of the insulin-like growth factor family as well as insulin and insulin-like growth factor-II. It is a 7649 Da polypeptide and contains 70 amino acids and three intramolecular disulfide bonds [1]. IGF-I is primarily produced in the liver but to some extent in peripheral tissue [2]. The biological actions of IGF-I are mainly mediated by the specific transmembrane IGF-I receptor and include DNA synthesis, cell differentiation and protein synthesis [3]. Thus, possible fields of application are atrophic musculoskeletal diseases such as sarcopenia or dwarfism. Transport of IGF-I is regulated by six IGF-I binding proteins [3]. The IGF-I gene consists of six exons [2] leading to various mRNA transcripts that encode for different IGF-I precursor peptides. These isoforms of IGF-I possess extensions of 35 to 77 amino acids at the C-terminus that are referred to as Ea-, Eb- or Ec-peptides [4]. Biological effects of human E-peptides were shown such as mitogenic, angiogenic and migratory activity and also the regulation of cell differentiation [4]. Posttranslational modification results in the mature IGF-I comprising 70 amino acids by cleaving off the E-peptides. However, other studies demonstrated that prevention of the cleavage of the E-peptide increased the stability of IGF-I in serum and maintained the therapeutic activity [5, 6]. In this work we engineered two IGF-I peptides, one containing its Ea-peptide and another one consisting of the mature IGF-I using *E.coli*. An unnatural amino acid, N<sup>6</sup>-((prop-2-yn-1-yloxy)carbonyl)lysine (pyrrolysine analogue; Plk), was incorporated into the peptides (Plk-IGF-I) at two positions, respectively. By this means, IGF-I was equipped with alkyne functions that provide the opportunity to decorate IGF-I with other molecules carrying an azido group and following formation of a triazol linkage, referred to as Cu(I)-catalyzed Huisgen azide-alkyne cycloaddition (click reaction) [7-9]. Plk could be integrated into the peptide sequence in response to an amber codon (TAG codon) by additionally supplying the genes for the appropriate transfer RNA (tRNA) and pyrrolyl-transfer-RNA-synthetase (pylRS) via two vectors. These genes were naturally found in anaerobic methanogens, the *Methanosarcina barkeri*. Using this strategy is particularly advantageous, since site-specific modification of IGF-I such as PEGylation can be achieved and the problems of product heterogeneity are overcome, as modification will strictly occur only at sites of Plk. PEG modification increases the solubility and half-lives of proteins and reduces their immunogenic potential [10, 11]. Furthermore, Plk-IGF-I can be linked through the click chemistry strategy to short peptides consisting of a protease sensitive sequence, which is

instrumental to yield concepts characterized by the active moiety (here IGF-I) flanked by a bioresponsive element (the protease sensitive sequence), flanked by a surface, a polymer, or any other decoration element. For example, this protease sensitive linker is selectively cleaved by proteolytic enzymes including matrix metalloproteinase (MMP-8) that are upregulated in several diseases. In response to MMP upregulation, cleavage occurs and the active form of IGF-I is generated locally. In this way IGF-I can be released directly at the target tissue and only in case being required. Plk-IGF-I can be linked to other biotherapeutics via a cleavable linker to intensify the therapeutic effect or it can be attached to surfaces such as implants. This work aims at contributing to the development of an innovative IGF-I delivery system with high therapeutic potential and less adverse side effects for musculoskeletal disorders. We mainly describe different approaches to express and purify two IGF-I mutants possessing the unnatural amino acid, the pyrrolysine analogue (Plk), to accomplish the click reaction.

## EXPERIMENTAL DETAILS

### Materials

Recombinant human IGF-I was from Novartis (Basel, Switzerland), ampicillin, kanamycin, bovine serum albumin, bromophenol blue, glycerol, acrylic acid amide, succinic acid, Anti-Insulin-like growth factor-I antibody (produced in goat), Monoclonal Anti-Insulin-like growth factor-I antibody (produced in mouse), sodium hydroxide, tetrahydrofuran, propargylchloroformate, diethyl ether, ethyl acetate, magnesium sulfate, trifluoroacetic acid and poly(propylene glycol) were from Sigma-Aldrich (Schnelldorf, Germany). Boc-Lys-OH was from Merck (Darmstadt, Germany). SuperSignal West Pico Chemiluminescent Substrate was from Thermo Fisher Scientific (Braunschweig, Germany). NucleoSpin Plasmid Miniprep Kit and NucleoBond<sup>®</sup>Xtra Midi kit were from Macherey-Nagel (Düren, Germany). Milli-Q water was from a demineralization system (Millipore, Billerica, MA). All other chemicals were at least of pharmaceutical grade and from Sigma-Aldrich unless otherwise noted. Culture media: Lysogeny Broth (LB) medium (10 g Bacto-Tryptone, 5 g Yeast Extract, 5 g NaCl, 5 g MgSO<sub>4</sub> \* 7 H<sub>2</sub>O, 1 g Glucose (anhydrous) ad 1000 mL Milli-Q water (at pH 7.5) and Terrific Broth (TB) medium (12 g Bacto-Tryptone, 24 g Yeast Extract, 3.2 g glycerol ad 900 mL Milli-Q water).

### ***Introduction of a non-natural amino acid into IGF-I***

A pyrrolysine analogue (Plk) with an alkyne function was introduced into IGF-I.

For this purpose, an amber codon (TAG) was placed on the intended position of the DNA sequence [7-9]. Actually, an amber codon signals the termination of protein synthesis due to the lack of an appropriate transfer RNA (tRNA). But we additionally provided two further genes, a pyrrolysyl-transfer-RNA-synthetase (pyIRS) and its cognate t-RNA (tRNA<sup>PyI</sup>) that naturally occur in *Methanosarcina barkeri*. Consequently; Plk that was added to the culture medium, was recognized by pyIRS, joined to the tRNA<sup>PyI</sup> and incorporated into the protein sequence in response to TAG binding of the Plk loaded tRNA<sup>PyI</sup> at the ribosome and integration into the growing peptide chain, respectively.

### ***DNA Sequence of IGF-I variants:***

The DNA sequence of the modified IGF-I, referred to as Plk-IGF-I, contained two nucleotide triplets substituted to an amber codon (TAG), respectively. At the beginning of the sequence a code standing for glycine (GGC) was added. A recognition sequence of the restriction enzyme NdeI (5'CATATG) was inserted at the 5'-terminus and the 3'-terminus was provided with the recognition sequence of BAmHI (5'GGATCC):

CAT ATG **GGC** GGC CCG **TAG** ACC CTG TGC GGT GCG GAA CTG GTG GAT GCG  
CTG CAG TTT GTG TGC GGC GAT CGC GGC TTT TAT TTT AAC AAA CCG ACC GGC  
TAT GGC AGC TCA AGC CGC CGT GCG CCG CAG ACC GGC ATT GTG GAT GAA  
TGC TGC TTT CGC AGC TGC GAT CTG CGC CGC CTG GAA ATG TAT TGC GCG CCG  
CTG **TAG** CCG GCG AAA AGC GCG TAA GGA TCC.

The DNA sequence of the modified IGF-I, referred to as Plk-IGF-I-Ea, consisted of the IGF-I sequence and additionally an extension that encoded the Ea peptide. Two nucleotide triplets were substituted to an amber codon (TAG), respectively and a code standing for glycine (GGC) was added. Similarly, the recognition sequence of the restriction enzyme NdeI (5'CATATG) was inserted at the 5'-terminus and the 3'-terminus was provided with the recognition sequence of BAmHI (5'GGATCC):

CAT ATG **GGC** GGC CCG **TAG** ACC CTG TGC GGT GCG GAA CTG GTG GAT GCG  
CTG CAG TTT GTG TGC GGC GAT CGC GGC TTT TAT TTT AAC AAA CCG ACC GGC

TAT GGC AGC TCA AGC CGC CGT GCG CCG CAG ACC GGC ATT GTG GAT GAA  
TGC TGC TTT CGC AGC TGC GAT CTG CGC CGC CTG GAA ATG TAT TGC GCG CCG  
CTG AAA CCG GCG AAA AGC GCG GTG CGC GCG CAG CGC CAT ACC GAT ATG  
CCG AAA ACC CAG AAA GAA GTG CAT CTG AAA AAC GCG AGC CGC GGC AGC  
GCG GGC AAC **TAG** AAC TAT CGC ATG TAA GGA TCC.

### *DNA vectors*

Both DNA constructs were cloned into pUC57 vector via multiple cloning site EcoRV by GenScript (Piscataway, New Jersey, USA). The pUC57 vector consisted of 2710 bp and was isolated from *E.coli*. For the expression of the IGF-I variants, each IGF-I sequence was cloned into pET11a vector, respectively. The pET11a vector is a bacterial plasmid with a length of 5677 bp. It contains a T7 promoter which is only recognized by the bacteriophage T7 RNA polymerase. This T7 system enables the high level transcription of cloned genes and consequently the production of high amounts of proteins. An ampicillin resistance gene, a lac operator and a lacI gene are also located on the pET11a vector. The lacI gene codes for the lac repressor protein that regulates the gene expression by binding to the lac operator and thereby preventing the transcription. Isopropyl  $\beta$ -D-1thiogalactopyranoside (IPTG) can interfere in this procedure and the addition of IPTG induces the protein expression, accordingly. The gene of the indispensable T7 RNA polymerase existed on the chromosome of the host cells (*BL(DE3)*), as well as a lac promoter and a lac operator. Hence, the expression of the T7 polymerase was induced by IPTG and thereby the expression of the target protein as well. Furthermore, the gene for the tRNA<sup>Pyl</sup>, the appropriate constitutive lipoprotein promoter lpp and the rrnC terminator were cloned into the pET11a vector. The pRSFduet vector consists of 3829 bp and was co-transformed into the host cells. The pRSFduet vector comprised a kanamycine resistance gene and the pyrrolysyl-tRNA synthetase (PylRS) gene.

### ***Subcloning***

The pUC57 plasmids were transformed into competent bacteria such as *JM 109* and *DH5 $\alpha$*  for the purpose of amplification. After the overnight culture, the plasmid DNA was extracted and purified by Midipreparation according to the instruction manual. A *restriction digestion* of pUC57 vectors with its IGF-I inserts and pET11a vectors was performed and the resulting fragments were analyzed by *agarose gel electrophoresis*. Subsequently, the *ligation* between the insert DNA and the pET11a vector was accomplished. The associated pET11a vectors were *transformed* into competent *E. Coli cells (BL21(DE3))* to amplify the plasmid DNA following purification by Minipreparation. DNA sequence analysis was performed by Eurofins Genomics GmbH (Ebersberg, Germany). Concurrently, a second *restriction digest* and *agarose gel electrophoresis (II)* were done to control the ligation. The verified pET11a plasmids and the pRSFduet plasmids were *cotransformed* into *E. coli cells (BL21(DE3))* and subsequently used for protein expression.

The details of *transformation*, *restriction digestion* and *ligation* following *agarose gel electrophoresis* are described below.

### ***Transformation***

After thawing of 100  $\mu$ L of competent cells on ice, 0.5  $\mu$ L DNA was added and gently mixed (without pipetting up and down). The tubes were incubated on ice for 20 minutes. Subsequently, the cells were heat shocked for 30 seconds at 42 °C without shaking and then again placed on ice for 2 minutes. 250  $\mu$ L of pre-warmed Super Optimal Broth (SOC) medium was added to each tube and incubated at 37 °C for 1 hour at 300 rpm. 100  $\mu$ L of each transformation was spread on prewarmed, selective agar plates following incubation at 37 °C overnight. Subsequently, a single colony from the agar plate was selected and transferred into liquid LB medium, supplemented with antibiotics. The bacterial culture was incubated at 37 °C in a shaking incubator overnight (overnight culture).

### ***DNA purity and concentration***

For plasmid DNA purification the NucleoBond<sup>®</sup>Xtra Midi kit (Macherey-Nagel, Düren, Germany) was used according to the instruction manual. The DNA purity was assessed using the ratio of absorbance at 260 nm and 280 nm (1.8 – 2.0). The DNA concentration was determined by measuring the absorbance at 260 nm.

### ***Restriction digestion (I)***

The DNA substrates were digested with two restriction enzymes simultaneously. The following reactions were set up:

**Table 1. Restriction digestion reactions.**

Attempt	pET11a	Plk - IGF-I	Plk - IGF-I-Ea	BamHI	NDEI	NE Buffer 3	BSA	Water
1	4 µg	-	-	1 µL	1 µL	3 µL	0.3 µL	ad 30 µL
2	-	4 µg	-	1µL	1 µL	3 µL	0.3 µL	ad 30 µL
3	-	-	4 µg	1µL	1 µL	3 µL	0.3 µL	ad 30 µL

Subsequently, the recipient plasmid (pET11a) was additionally treated with a phosphatase to prevent re-circularization: 2 µL Antarctic Phosphatase (New England BioLabs GmbH, Frankfurt, Germany), 3.6 µL Antarctic Phosphatase Reaction Buffer (New England BioLabs GmbH, Frankfurt, Germany) and 0.4 µL water were added. The samples were heated at 37 °C for 15 minutes and at 65 °C for 5 minutes.

### ***Agarose gel electrophoresis (I)***

DNA fragments were isolated due to their size by agarose gel electrophoresis. Therefore, 1.54 g agarose powder was dissolved in 75 mL TAE-buffer under heating. After cooling 3.75 µL Midori Green was added. The lukewarm gel solution was poured into the gel tray and a gel comb was inserted to form wells. The cast was placed into the casting apparatus. Samples were mixed with 6X MassRuler DNA Loading Dye (Thermo Fisher Scientific, Braunschweig, Germany) and loaded



into the wells of the agarose gel. A GeneRuler 1 kb Plus DNA Ladder (Thermo Fisher Scientific, Braunschweig, Germany) and a GeneRuler Low Range DNA Ladder (Thermo Fisher Scientific, Braunschweig, Germany) were applied. The gel was run at 80 V. The resulting DNA fragments were cut out and purified by the use of the GeneJET Gel Extraction Kit (Thermo Fisher Scientific, Braunschweig, Germany) according to the instruction manual.

### ***Ligation***

The DNA ligase was used to join the DNA inserts and the pET11a vector in an aqueous milieu using 10 x buffer. The following ratios were mixed in an Eppendorf tube, respectively and incubated at 22 °C for three hours:

**Table 2. Different ratios of vector DNA and insert DNA for the ligation.**

Attempt	pET11 a vector	Plk-IGF-I/ Plk-IGF-I-Ea	10 x buffer	Ligase	nuclease free water
1	1 µL	10 µL	2.5 µL	0.5 µL	11 µL
2	1 µL	20 µL	2.5 µL	0.5 µL	1 µL
3	2 µL	5 µL	2.5 µL	0.5 µL	15 µL
4	2 µL	10µL	2.5 µL	0.5 µL	10 µL

Afterwards, the samples were transformed into *BL21(DE3) E.coli cells* (see above) and were grown overnight on agar plates containing ampicillin. Several colonies were randomly picked and each was grown in liquid media (Lysogeny Broth (LB) with ampicillin) overnight (overnight culture, OVC), following plasmid DNA purification by means of NucleoSpin Plasmid Miniprep Kit according to the instruction manual.

### ***Restriction digestion (II) to control ligation***

The incorporation of the DNA inserts (Plk-IGF-I, Plk-IGF-I-Ea) into the pET11a vector was controlled by digestion with two restriction enzymes (BamHI, SapI)

The following reactions were set up at 37 °C overnight:

**Table 3. Restriction digestion reactions.**

pET11a-Plk-IGF-I	pET11a-Plk-IGF-I-Ea	pET11a vector	Buffer 4	BamHI	SapI	Nuclease free water
10 µL	-	-	2 µL	1 µL	0.5 µL	6.5 µL
-	-	6 µL	2 µL	1 µL	0.5 µL	10.5 µL
-	10 µL	-	2 µL	1 µL	0.5 µL	10.5 µL

### *Agarose gel electrophoresis (II)*

A 1 % agarose gel was used (1.25 g agarose powder in 125 mL TAE buffer) with 6.25 µL Midori Green and electrophoresis was performed as described above (agarose gel electrophoresis (I)).

### *Cotransformation*

pET11a vector (ampicillin) containing either Plk-IGF-I or Plk-IGF-I-Ea insert and the pRSF vector (kanamycin) were cotransformed as described above (*transformation*). Different ratios were set up including a calculation that has been described before [12].

**Table 4. Different ratios of pET11a and pRSF vector for co-transformation.**

pET11a – Plk-IGF-I	pET11a – Plk-IGF-I-Ea	pRSF	BL21(DE3)
26.5 ng	-	404.5 ng	50 µL
50.0 ng	-	235.3 ng	50 µL
100.0 ng	-	200.0 ng	50 µL
-	46.9 ng	186.8 ng	50 µL
-	25.0 ng	117.0 ng	50 µL
-	83.0 ng	152.7 ng	50 µL

After culturing cells and centrifugation (4500 rpm, 4 °C, 15 min.), a pellet was resuspended in 1.5 ml LB-glycerol-medium and frozen in a cryovial at -80 °C (glycerol stock).

## ***Plk Synthesis***

Plk was synthesized as previously described [7]. 3.1 g Boc-Lys-OH((tert-butyloxycarbonyl)-protected l-lysine) was dissolved in 30 mL 1 M sodium hydroxide and 30 mL tetrahydrofuran and cooled to 0 °C using an ice bath. Subsequently, 980µL propargylchloroformate were added dropwise over 5 min. This reaction was stirred overnight at room temperature. The solution was cooled to 0 °C and washed with 150 mL ice-cold diethylether (Et<sub>2</sub>O). The solution was acidified with 150 mL ice-cold 1 M hydrochloric acid and then extracted with 150 mL ice-cold ethyl acetate twice. The organic layers were combined and 20 g magnesium sulfate (MgSO<sub>4</sub>) was added to dry the solution. After stirring for 5 min. at room temperature, the MgSO<sub>4</sub> was filtered off. The solvent was removed using a rotary evaporator and the Boc-protected Plk was yielded and dissolved in 26 mL dry dichloromethane. 26 mL trifluoroacetic acid was dropwise added and stirred for 1 hour at room temperature. The solvent was removed using a rotary evaporator and the residue was dissolved in 200 mL Et<sub>2</sub>O. Plk was precipitated and dried under vacuum.

## ***Overnight culture***

Some of the frozen *E.coli BL21(DE3)* containing the pRSF vector and the pET11a vector (either with Plk-IGF-I or Plk-IGF-I-Ea insert) were transferred into liquid LB medium, supplemented with carbenicillin and kanamycin. The bacterial culture was incubated at 37 °C in a shaking incubator overnight.

## ***Protein expression***

Protein expression was done as described before [7]. Briefly, 500 mL TB medium (Terrific Broth) containing 500 mg carbenicillin and 170 mg kanamycin was inoculated with 1% overnight culture and the cells were grown at 37 °C and during shaking at 220 rpm. At OD<sub>600</sub> = 0.3 4 mM Plk was added and at OD<sub>600</sub> = 0.8 the protein expression was induced using 1mM IPTG. The cells were harvested by centrifugation (30 min, 4500g) after 16 hours and stored at – 80 °C until further usage. Several modifications of the protein expression were tried to optimize the procedure: (i) the temperature was varied (30 °C / 37 °C), (ii) the concentration of Plk was increased to 20 mM, (iii) the TB medium was supplemented with 1 mM magnesium sulfate and

2-3 drops of propylene glycol and baffled flasks were used, (iv) the duration of protein expression was varied and (v) another cell line, the *ArcticExpress (DE3)* cells, was used.

### ***Inclusion body purification***

Different methods were performed to isolate the protein from inclusion bodies [13, 14].

(I) The pellet was resuspended in 30 mL buffer consisting of Tris/HCL at pH 8, 50 mM NaCl, 1 mM EDTA and 0.1 mM phenylmethylsulphonyl fluoride (buffer A) [13]. After ultrasonication, the suspension was centrifuged at 25,000 g for 15 min. at 4 °C. The pellet was resuspended in buffer A with 5 M guanidine hydrochloride and 2 mM reduced and 0.2 mM oxidized glutathione. For 1 g pellet, 9 mL buffer was used and the suspension was incubated for 1 h at room temperature. Subsequently it was slowly mixed with 9 vol. buffer A without phenylmethylsulphonyl fluoride, but with 2 mM reduced and 0.2 mM oxidized glutathione and incubated for 2.5 hour at room temperature. After centrifugation at 2,500 g for 15 min at 4 °C, the acquired supernatant was dialyzed against phosphate-buffered saline pH 7.4 at 4 °C.

(II) The pellet was resuspended in 50 mL buffer consisting of 20 mmol Tris and 50 mmol NaCl at pH 8.5 [14]. After ultrasonication, the suspension was centrifuged at 10,000 rpm for 15 min. The pellet was resuspended in 50 mL buffer consisting of 20 mmol Tris and 5 mmol EDTA at pH 8. Then, 0.02% lysozyme was added and the suspension was incubated for 3 hours at room temperature. The suspension was centrifuged at 10,000 rpm for 15 min and resuspended in 50 mL buffer consisting of 20 mmol Tris, 5 mmol EDTA at pH 8 and 2% Triton X – 100. After centrifugation at 10,000 rpm for 15 min, two wash steps using 50 mL buffer containing 20 mmol Tris at pH 7.5 were done, respectively. This method was also used adjusting the pH of 6.5 (data not shown).

### ***Sodium dodecyl sulfate polyacrylamide gel electrophoresis (SDS-PAGE)***

SDS-PAGE was performed as described before. In Brief, the stacking gel was a 3.9% polyacrylamide gel at pH 6.8 adjusted by a Tris-HCl buffer and the separating gel was 15% polyacrylamide at pH 8.8 using a Tris-HCl buffer as well. Samples were mixed with SDS sample buffer 6x, heated at 95 °C for 15 min. and applied into the wells of the stacking gel. A protein

ladder was loaded onto the gel (Bio-Rad Laboratories GmbH, München, Germany) and the electrophoresis was run at 120 V.

### ***Western blot***

After SDS-PAGE, the proteins on the gel were transferred in an electrical field to a nitrocellulose membrane. The membrane was blocked with 5% (m/V) skim milk powder in PBS (smp-PBS) for 1 hour at room temperature and during shaking. Then, the membrane was incubated with polyclonal anti-IGF-I antibody (goat IgG1 isotype) in 5% (m/V) smp-PBS at 4 °C overnight and under agitation. The membrane was three times washed with 0.2% (m/V) polysorbate 20 in PBS for 15 min. and following three times with PBS for 15 min. Incubation with an second antibody, rabbit anti-goat IgG, was for 1 hour at room temperature and under agitation. The wash steps were repeated and subsequently the bound antibodies were detected using the SuperSignal West Pico Chemiluminescent Substrate kit. For documentation the FluorChem FC2 imaging system (Protein Simple, Santa Clara, CA) was used.

For evaluation of non-specific antibody binding, a membrane was not incubated in the primary, but in the secondary antibody. Another western blot was done with a sample containing *BL21(DE3)* cells, but not an IGF-I epitop. Furthermore, a monoclonal anti-IGF-I antibody was tested.

### ***In-gel tryptic digestion and mass spectrometric characterization***

Protein samples were applied to SDS-PAGE and subsequently visualized by Coomassie Blue staining [15].

In-gel reduction, acetamidation, and tryptic digestion were done as described before [16]. After elution of the peptides, solutions were desalted using a Millipore C18 Zip Tip according to the manufacturer's instructions.

Electrospray Ionization Mass Spectrometry Analysis (ESI-MS) was performed using an APEX-II FT-ICR (Bruker Daltonic GmbH, Bremen) equipped with a 7.4 T magnet and an Apollo ESI ion source in positive mode.

The samples were injected into the ion source using a Hamilton syringe at a speed of 2  $\mu$ L per minute with a capillary voltage of 160 V. The detection range of the

mass spectrometer was typically set to 300-2100 m/z. An accumulation of 256 scans was combined at a resolution of 256 K. For evaluation, the mass spectra were deconvolved to the single protonated ion formate using the Bruker Xmas software. The monoisotopic signal was selected for mass determination.

### ***Protein purification***

Cation exchange chromatography (CEX) was used to separate the expressed IGF-I mutant from other proteins. Therefore, an Äkta purifier system (GE, Munich, Germany) with a HiTrap SP XL column (GE, Munich, Germany) was applied. A linear gradient was run, starting with a 50 mM succinate buffer pH 4.5 (binding buffer) and shifting to 50 mM succinate buffer with 1 M sodium chloride pH 4.5 (elution buffer). The protein peak was collected in 5 mL fractions and analyzed by western blot analysis.

## **RESULTS**

### ***IGF-I mutants***

Two different IGF-I mutants were engineered. One IGF-I mutant (Plk-IGF-I) contained the unnatural amino acid, a pyrrolysine analogue (Plk) at position 3 (E → Plk) and at position 65 (K → Plk). The N-terminus was extended by a further amino acid (aa), a glycine. The molecular weight of Plk-IGF-I was 8.1 kDa [17]. The other IGF-I mutant (Plk-IGF-I-Ea) contained a carboxy-terminal extension of 33 amino acids, the Ea-peptide. Two amino acids of the Ea-peptide, the arginine (R1) and serine (S2) were excluded to prevent cleavage of the Ea-peptide from IGF-I by proteases [18]. Plk was introduced at position 3 (E → Plk) of IGF-I and at position 29' of the Ea-peptide (K → Plk, Figure 1). A glycine was inserted at the N-terminus. The molecular weight of Plk-IGF-I-Ea was 11.8 kDa [17].

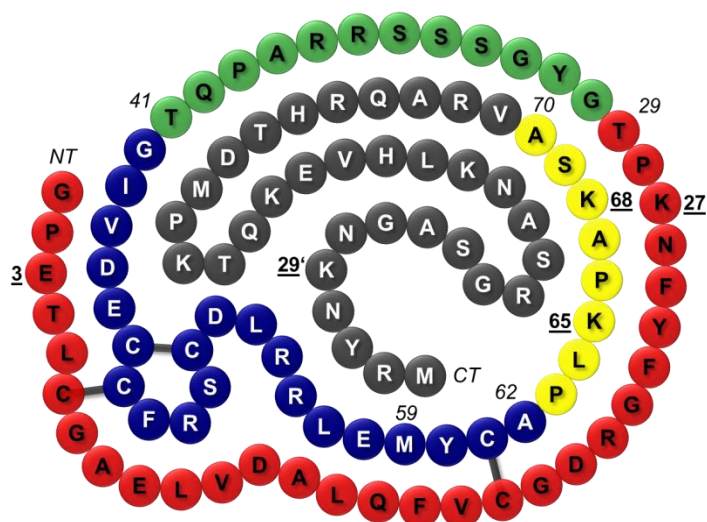


**Figure 1.** Amino acid sequence of Insulin-like growth factor I (aa 1 -70) containing a Ea-peptide (1'-33', gray coloured). The four domains of IGF-I were highlighted with colours: A-domain in red, B-domain in green, C-domain in blue and D-domain in yellow. The three intramolecular disulfide bonds are depicted in grey lines.

### *Agarose gel electrophoresis (I)*

After restriction digestion (I) of pUC57-Plk-IGF-I-Ea, pUC57-Plk-IGF-I and pET11a with BamH and NdeI, DNA fragments of different sizes were detected on the agarose gel (**Figure 2**). The digested pET11a vector (5637 bp) was visible in the range of 5000 and 6000 bp. In the second line, the Plk-IGF-I insert (228 bp) was detected between 200 and 300 bp (highlighted by an arrow) and the rest of the vector (2482 bp) at approximately 2000 bp. In the third line the Plk-IGF-I-Ea insert (327 bp) was detected between 300 and 400 bp and the other part of the vector (2383 bp) ran at approximately 2000 bp. The bands marked with an arrow - digested pET11a (1), Plk-IGF-I (5) and Plk-IGF-I-Ea (4)- were cut and the DNA fragments were extracted from the gel.

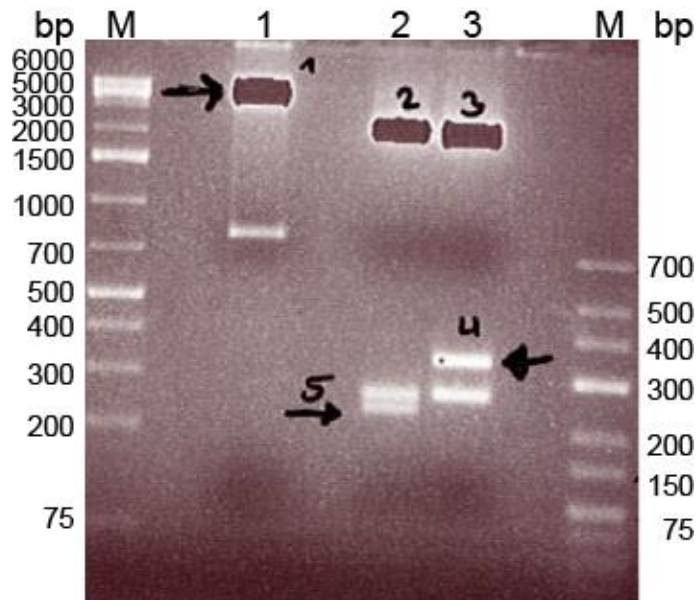


**Figure 2.** Agarose gel electrophoresis I: On the left a DNA ladder (M = Marker) in the range of 75 to 20000 bp (base pairs) and on the right a low range DNA ladder (25 bp – 700 bp) was used. In the first line (1) the sample of the digested pET11a vector was applied, then (2) digested pUC57-Plk-IGF-I and finally (3) digested pUC57-Plk-IGF-I-Ea.

### *Agarose gel electrophoresis (II)*

After the restriction digestion (II) with BamH and SAP I to control the ligation of pET11a vector and the Plk-IGF-I-Ea insert, the associated vector was cleaved into two DNA fragments: One, containing the Plk-IGF-I-Ea insert (3681 bp) ran at approximately 4000 bp on the agarose gel and the other part of the vector (2323 bp) at > 2000 bp (**Figure 3 A**). The DNA fragment between 5000 and 6000 bp was the uncut pET11a vector (5677 bp).

After the restriction digestion of pET11a-Plk-IGF-I, the signal of the fragment containing Plk-IGF-I (3582 bp) was at approximately 4000 bp on the agarose gel, and the other part of the vector was at > 2000 bp. The uncut pET11a vector (5677 bp) was detected at approximately 6000 bp.



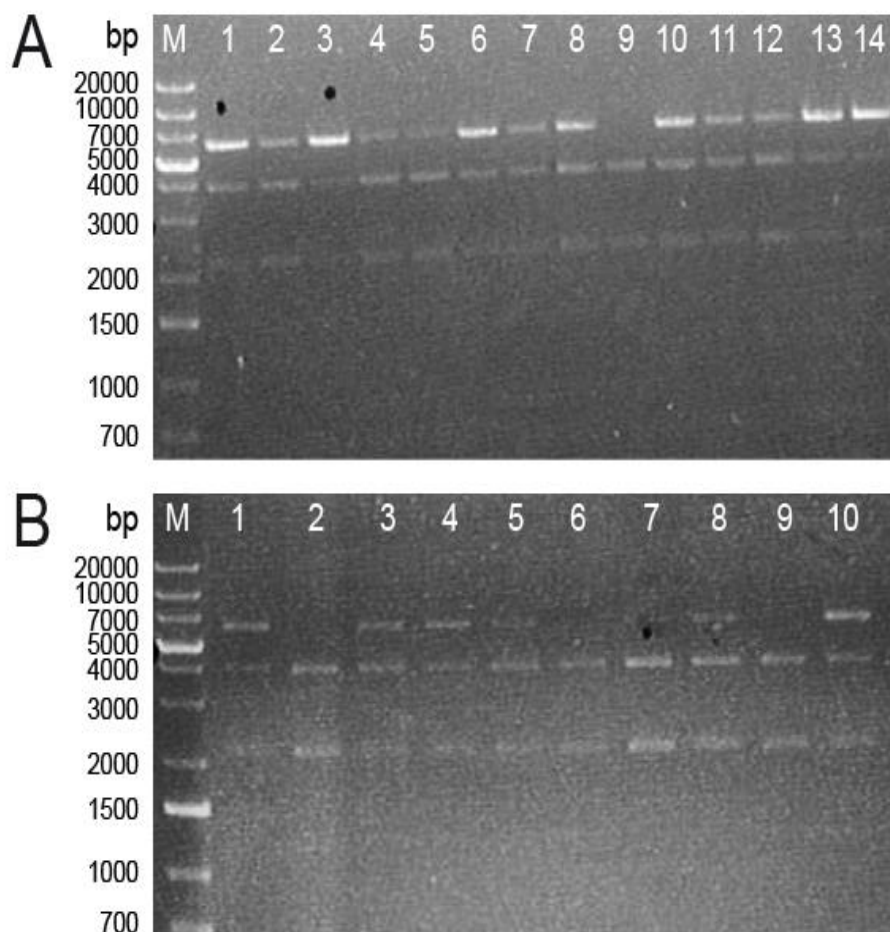


**Figure 3.** Agarose gel electrophoresis II: (A) 14 different samples of digested pET11a-Plk-IGF-I vectors, extracted from 14 different picked and grown up clones, were applied in a row from 1 – 14. A DNA ladder (M = Marker) in the range of 75 to 20000 bp (base pairs) ran on the left. (B) 10 different samples of digested pET11a-Plk-IGF-I-Ea vectors, extracted from 10 different picked and grown up clones, were applied in a row from 1 – 10. A DNA ladder (M = Marker) in the range of 75 to 20000 bp (base pairs) ran on the left.

### *Western blot analysis*

The western blot analysis after the expression of Plk-IGF-I-Ea at 37 °C resulted in a strong band between 10 and 15 kDa (**Figure 4 A**). This is a hint for the presence of Plk-IGF-Ea, since the molecular weight of this IGF-I mutant is about 11.8 kDa. Faint bands were observed between 25 – 60 kDa. IGF-I reference was detected at ~

10 kDa. The blot of Plk-IGF-I showed weak signals between 35 and 60 kDa (**Figure 4 A**). The expression of IGF-I mutants at 30 °C and a higher concentration of Plk, 20 mM, lead to clearly visible protein bands between 25 and 60 kDa on the blot for both, Plk-IGF-I-Ea and Plk-IGF-I (**Figure 4 B**). Additionally, the Plk-IGF-Ea samples, taken 12, 13 and 16 h after the expression was induced by IPTG, showed again a clear signal between 10 and 15 kDa, respectively. This signal was not detected before Plk and IPTG were added (**Figure 4 B**). Consequently, this finding corroborated the assumption of a successful expression of Plk-IGF-I-Ea. The expression of IGF-I mutants at low temperatures using ArcticExpress cells resulted faint bands at 35 and 55 kDa on the western blot, but a band in the size range of the expected proteins was not detected (**Figure 4 C**). The monitoring of the time period of the expression of Plk-IGF-Ea at 37 °C and using baffled flasks and additives such as propylenglycol and magnesium sulfate revealed a strong band after 1 h that tailed off with each passing hour and was barely visible after 8 h (**Figure 4 D**). This protein was not detected before the expression was induced by IPTG, indicating again that Plk-IGF-Ea was expressed. Applying this procedure to Plk-IGF-I yielded in a band between 10 and 15 kDa (**Figure 4 F**). Furthermore, carrying out the whole process, but without adding Plk to the bacterial culture (blank) resulted in faint signals between 35 and 55 kDa, but not between 10 and 15 kDa (**Figure 4 F**). The findings showed that the formation of the band between 10 and 15 kDa only occurred if the plasmid with the IGF-I insert was present and Plk and IPTG were supplemented into the medium, thereby providing evidence of expressed IGF-I mutants.

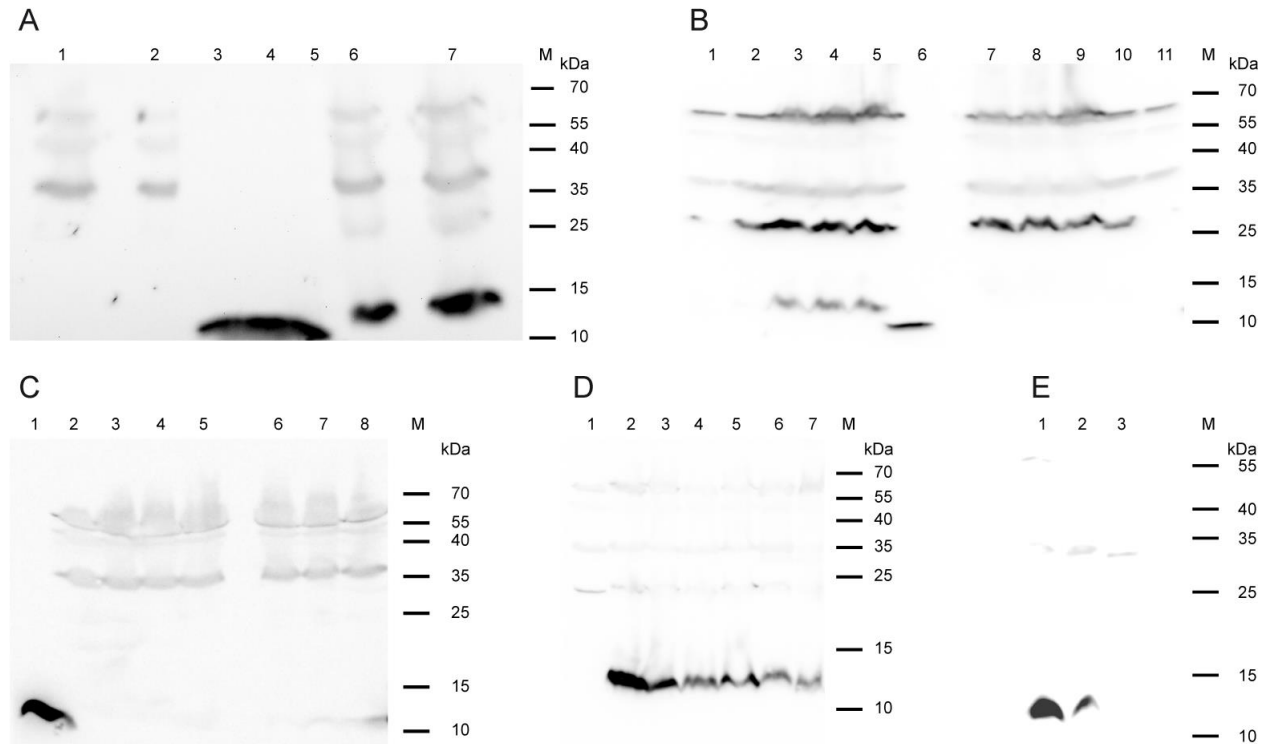


**Figure 4.** Western blot analysis after expression of IGF-I mutants under different conditions. Temperature (T), Plk concentration (c) and the time period (t) of the expression were varied:

(A) T = 37 °C, c = 2 mM, t = 16 h, lane 1: Plk-IGF-I (20  $\mu$ L), lane 2: Plk-IGF-I (10  $\mu$ L), lane 3,4: IGF-I reference (20  $\mu$ L), lane 5: Plk-IGF-I-Ea (10  $\mu$ L), lane 6: Plk-IGF-I-Ea (20  $\mu$ L).

(B) T = 30 °C, c = 20 mM, t = 12, 13, 16 h, lane 1: Plk-IGF-I-Ea (20  $\mu$ L) before Plk was added, lane 2: Plk-IGF-I-Ea (20  $\mu$ L) before IPTG was added, lane 3: Plk-IGF-I-Ea (20  $\mu$ L), t = 12 h, lane 4: Plk-IGF-I-Ea (20  $\mu$ L), t = 13 h, lane 5: Plk-IGF-I-Ea (20  $\mu$ L), t = 16 h, lane 6: IGF-I reference (10  $\mu$ L), lane 7: Plk-IGF-I (20  $\mu$ L), t = 12 h, lane 8: Plk-IGF-I (20  $\mu$ L), t = 13 h, lane 9: Plk-IGF-I (20  $\mu$ L), t = 16 h, lane 10: Plk-IGF-I (20  $\mu$ L) before IPTG was added, lane 11: Plk-IGF-I (20  $\mu$ L) before Plk was added.

(C) T = 10 °C (using ArticExpress cells), c = 15 mM, t = 14.5 h, 18.5 h, 24 h, lane 1: IGF-I reference (15  $\mu$ L), lane 2: Plk-IGF-I-Ea (20  $\mu$ L) before IPTG was added, lane 3: Plk-IGF-I-Ea (20  $\mu$ L), t = 14.5 h, lane 4: Plk-IGF-I-Ea (20  $\mu$ L), t = 18.5 h, lane 5: Plk-IGF-I-Ea (20  $\mu$ L), t = 24 h, lane 6: Plk-IGF-I (20  $\mu$ L), t = 24 h, lane 7: Plk-IGF-I (20  $\mu$ L), t = 18.5 h, Lane 8: Plk-IGF-I (20  $\mu$ L), t = 14.5 h.

(D) T = 37 °C, c = 10 mM , t = 1- 6 h, lane 1: Plk-IGF-I-Ea ( 10 µL) before IPTG was added, lane 2: Plk-IGF-I-Ea (10 µL), t = 1h, lane 3: Plk-IGF-I-Ea (10 µL), t = 2 h, lane 4: Plk-IGF-I-Ea (10 µL), t = 4 h, lane 5: Plk-IGF-I-Ea (10 µL), t = 5 h, lane 6: Plk-IGF-I-Ea (10 µL), t = 6 h, lane 7: Plk-IGF-I-Ea (10 µL), t = 8 h.

(E) T = 37 °C, c = 10 mM, t = 1 - 2 h, lane 1: Plk-IGF-I-Ea (10 µL), t1 h , lane 2: Plk-IGF-I (10 µL), t= 2 h, lane 3: Blank ( 10 µL, without Plk)

### *Antibody specificity*

No proteins were detected on the membrane, when it was not incubated with the primary, but with the secondary antibody only for western blot analysis (data not shown). Accordingly, unspecific binding of the secondary antibody was not observed. In contrast, the western blot of the sample without an IGF-I epitope showed protein bands at 25 -60 kDa (**Figure 5 A, line 10**) and consequently unspecific binding of the primary antibody has to be considered. The use of a monoclonal Anti-IGF-I antibody resulted in several bands between 15 and 70 kDa in each lane (**Figure 5 B**)

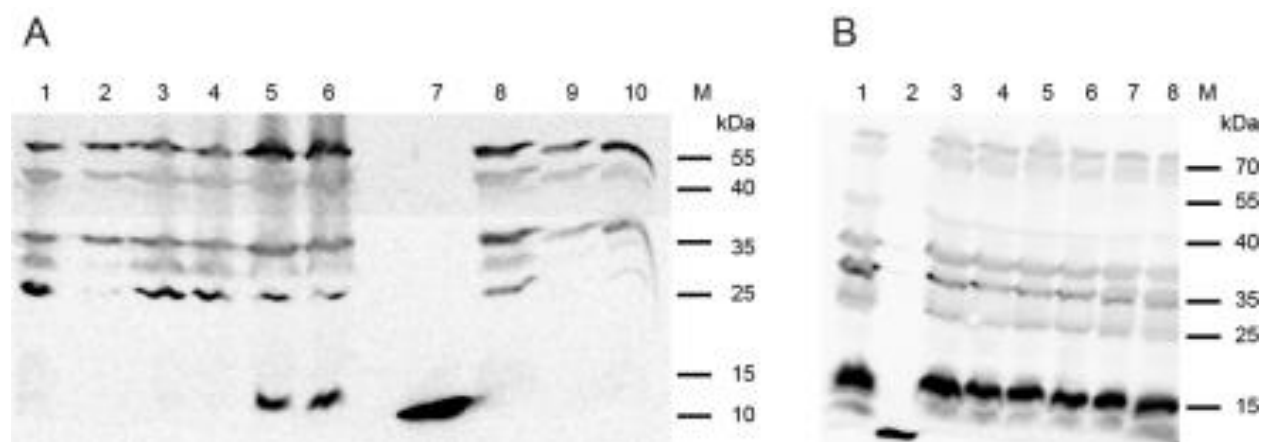


**Figure 5.** Western blot analysis: (A) Expression of IGF-I mutants using *BL21(DE3)*, lane 1: Plk-IGF-I-Ea before IPTG was added, lane 2:Plk-IGF-I-Ea before Plk was added, lane 3, 4:Plk-IGF-I, lane 5,6: Plk-IGF-I-Ea, lane 7: IGF-I reference, lane 8: Plk-IGF-I before IPTG was added, lane 9: Plk-IGF-I before Plk was added, lane 10: *BL21(DE3)* cells containing pET11a without IGF-I epitope, M: protein ladder [kDa]. (B) Expression of IGF-I mutants using *ArcticExpress* cells at different time points (t) and a monoclonal Anti-IGF-I antibody for western blot: lane 1: Plk-IGF-I-Ea before IPTG was added, lane 2: IGF-I reference, lane 3: Plk-IGF-I-Ea, t = 14.5 h, lane 4: Plk-IGF-I-Ea, t = 18.5 h, lane 5: Plk-IGF-I-Ea, t = 24 h, lane 6: Plk-IGF-I, t = 24 h, lane 7:Plk-IGF-I, t = 18.5 h, lane 8: Plk-IGF-I, t = 14.5 h, M = protein ladder [kDa].

### ***Inclusion body purification***

The previously detected protein bands in the western blot analysis mostly vanished after the extraction of protein aggregates from the cells [13]. Only a single band at 35 kDa was shown in each sample in the blot after the inclusion body purification (**Figure 6 A**). Another procedure to purify the Plk-IGF-I-Ea pellet [14] resulted in a distinct band between 10 and 15 kDa and a faint bands between 35 - 55 kDa (**Figure 6 B**). The applied supernatants did not show any signals.

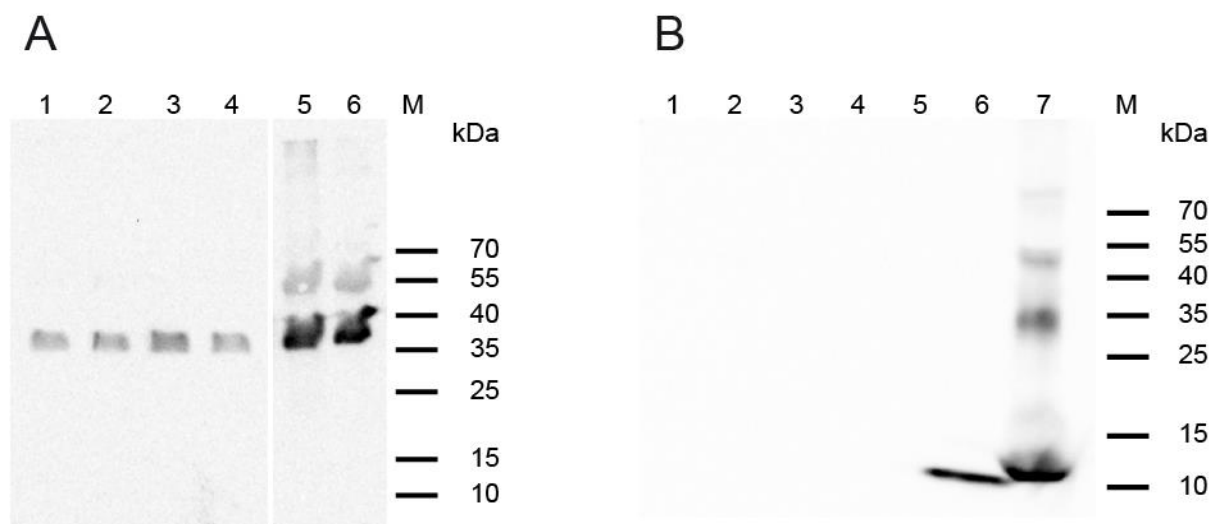


**Figure 6.** (A) Western blot analysis of Plk-IGF-I-Ea and Plk-IGF-I during inclusion body purification[13]: 1, 2: Plk-IGF-I-Ea, 3,4: Plk-IGF-I, 5: supernatant Plk-IGF-I-Ea, 6: supernatant Plk-IGF-I, M: protein ladder [kDa] (B) Western blot analysis of Plk-IGF-I-Ea during inclusion body purification[14] 1: supernatant 1, 2: supernatant 2, 3: supernatant 3, 4: supernatant 4, 5: supernatant 5. 6: IGF-I reference, 7: Plk-IGF-I-Ea, M: protein ladder [kDa].

### *Mass spectrometric characterization*

The mass spectrum of IGF-I reference, recorded after trypsin digest, showed mainly four peptide fragments (**Figure 7 B**): from aa 24 to 38 ( $m/z = 1667.783$ ), from aa 39 to 52 ( $m/z = 1592.733$ ), from aa 40 to 52 ( $m/z = 1436.629$ ) and from aa 58 to 70 ( $m/z = 1519.816$ ). The same peptides were also found in the mass spectrum of Plk-IGF-Ea (**Figure 7 A**). This provided evidence that Plk-IGF-I-Ea was successfully expressed.

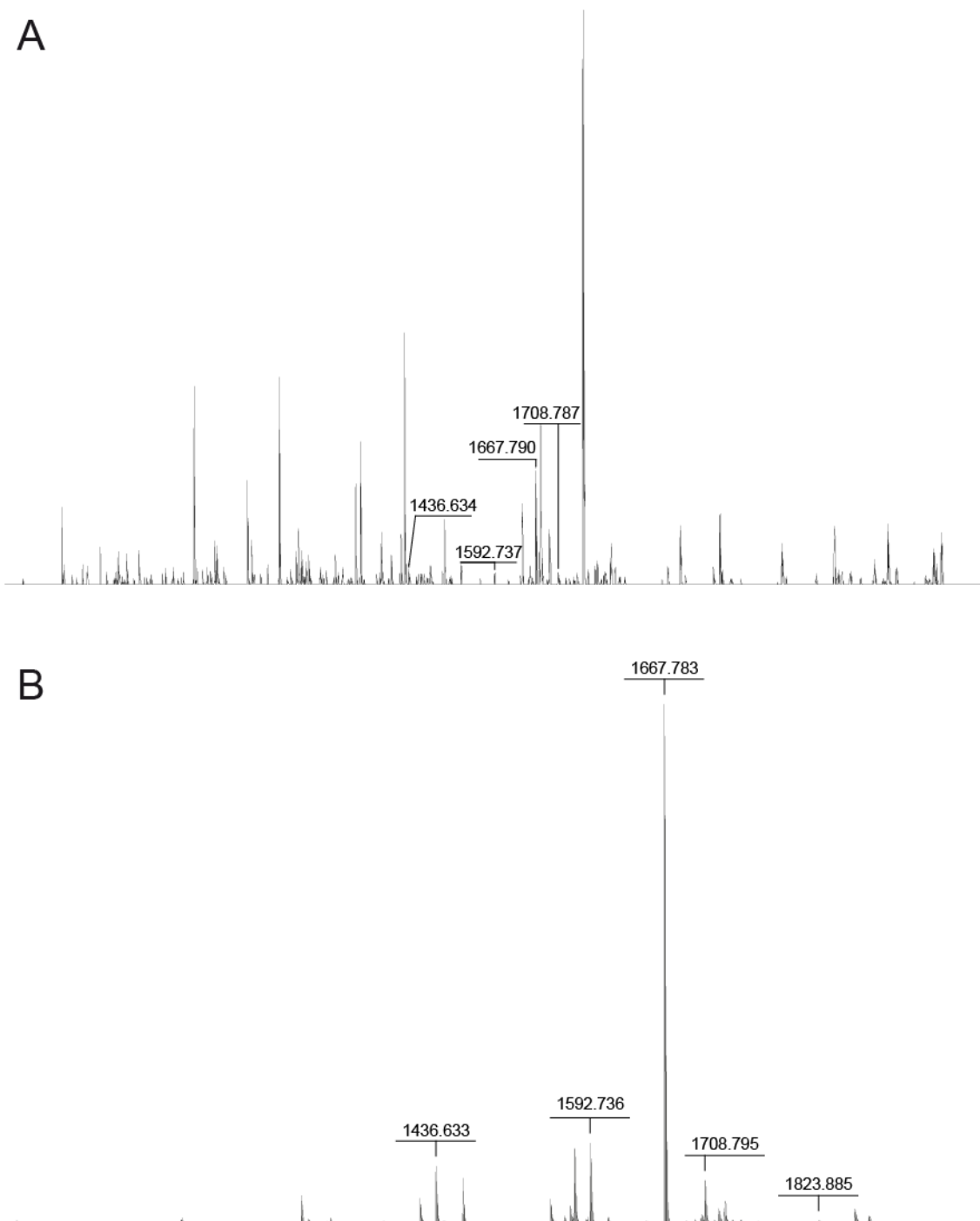


**Figure 7.** Mass chromatogram of (A) Plk-IGF-I-Ea and (B) IGF-I reference after in-gel tryptic digestion and ESI-MS.

## Protein purification

During cation exchange chromatography protein was eluted with buffer containing 50 mM succinate and 1 M sodium chloride at pH 4.5 and collected in a row of fractions from 40 to 49 (**Figure 8 A**). The analysis of the fractions by western blot resulted in a single band between 10 and 15 kDa (**Figure 7 B**).

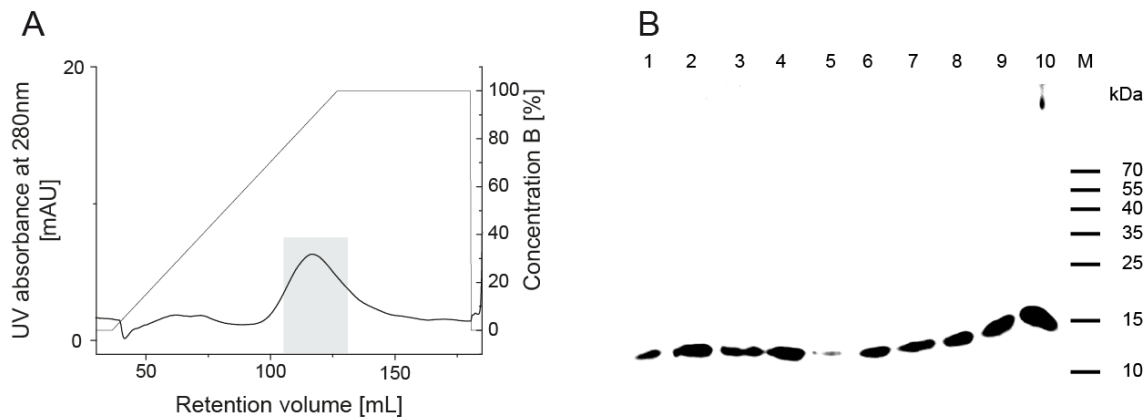


**Figure 8.** (A) Cation exchange chromatogram after the expression and inclusion body purification [14] of Plk-IGF-I-Ea. The collected fractions (40 – 49) are highlighted in grey. (B) Western blot of the collected fractions after CEX. The fractions (40-49) were sequentially applied onto to the gel from line 1-10. M: protein ladder [kDa].



## DISCUSSION

We designed two IGF-I mutants with an incorporated unnatural amino acid. Therefore, in one variant the Glu3 and Lys65 were exchanged for a Plk, respectively. Glu3 is not crucial for IGF-I receptor binding [19] and several examples of IGF-I with deletion or mutation of Glu3 have already been reported [20]. The substitution of Glu3 by either Gly or Arg resulted in a higher potency, but reduced binding to bovine IGFBP-2 and reduced affinity to type-1 receptor on rat L6 myoblasts compared to IGF-I [21]. Similarly, there are several studies reporting on modifications of Lys65. Mutation of Lys65 to Ala reduced the IGF-I receptor affinity 10 fold [19, 22] and pegylation of Lys65 resulted in a 2 fold decrease of receptor phosphorylation [23]. Furthermore, Lys65 was mutated to arginine [24]. According to other studies the D domain of IGF-I on which Lys65 is located was only slightly involved in receptor binding [19, 25].

The other IGF-I mutant with the extension of an Ea-peptide is actually the precursor protein of IGF-I. We prevented the naturally protease cleavage of the Ea-peptide by deleting its first two amino acids, Arg1 and Ser2, following previous studies [6]. Thereby, we provided IGF-I with an increased stability in the presence of serum for which previous studies demonstrated a maintained bioactivity [6, 26, 27]. Likewise, the Glu3 was mutated to Plk and additionally the Lys29 of the Ea-peptide. The decoration of IGF-I with alkyne groups allows the conjugation to other molecules or surfaces by the click reaction [7].

The protein expression at 37 °C and over 16 hours resulted in a signal between 10 and 15 kDa, implying Plk-IGF-I-Ea (**Figure 4 A**). However, the yield was too low arguably as the protein got lost in part during the extraction of inclusion bodies (**Figure 6 A**). Another strategy to enhance the yield of soluble protein and avoid inclusion body formation is the reduction of the temperature during the expression [28, 29]. Inclusion bodies constitute intracellular aggregates of mostly misfolded proteins and commonly form during high-level expression [28]. Lowering the temperature resulted in less hydrophobic interactions and thereby less incorrectly folded proteins. Furthermore, the transcription and translation rate were decreased allowing sufficient time for correct folding [28]. Hence, we expanded the experiments and performed protein expression at 30 °C and even at 12 °C using ArcticExpress cells that co-express cold-adapted chaperonins to support protein folding. Surprisingly, western blot analysis after the expression at 12 °C showed that IGF-I mutants were not formed (**Figure 4 C**) within 24 hours. However, expression at 30 °C lead to formation of Plk-IGF-Ea (**Figure 4 B**). This presumption is supported by the fact that the

protein was not detected before Plk and IPTG was added. Strong bands of byproducts were also detected. The band at 25 kDa may be assigned to aggregated IGF-I (e.g. dimer) or more likely unspecific binding of the antibody, since this band has already been detected before the expression was induced by IPTG. Similarly, the band at 55 kDa seems not to represent IGF-I but rather the pyrrolysyl-tRNA synthetase having a molecular weight of ~ 50 kDa. This is corroborated by the results of the antibody specificity testing, since the signal at 55 kDa was also detected in a sample of *BL21(DE3) cells*, but without an IGF-I epitope (**Figure 5 A**). These results warranted further strategies in an effort to optimize protein expression. Low protein yields can be attributed to low cell density and detrimental effects caused by foam for example. Shaking in combination with surface active agents such as proteins leads to foam formation and bursting bubbles can induce shear forces harming cells and secreted proteins [30]. Furthermore, foam decreases the gas exchange and cells or medium can pass over into the foam phase thereby affecting the efficiency of the process [30]. Indeed, supplementation of the culture medium with antifoams raised the yield of protein production [31, 32]. Hence, we pursued a new strategy and added an antifoam agent to the culture medium (TB medium), the poly(propylene glycol). Additionally, we used baffled flasks to generate a turbulent flow and increase the gas exchange and the oxygen intake. Besides, magnesium sulfate was supplemented to the medium, since it promotes the cell growth to achieve higher densities [33], as well as high temperatures (37 °C). As a result of these changes, we detected a strong signal between 10 and 15 kDa in the western blot of the sample that was taken 1 hour after the expression was induced with IPTG (**Figure 4 D, E**). Western blot analysis do not allow a quantitative assessment, despite we postulate raising the yield of Plk-IGF-I-Ea, since we halved the applied sample volume onto SDS-PAGE, but got this strong signal along with less byproducts. Additionally we measured the four peptides assignable to IGF-I fragments in mass spectrometric analyses (**Figure 7**).

Even a signal of the Plk-IGF-I sample was detected in the western blot for the first time using this procedure (**Figure 4 E**). However, Plk-IGF-I-Ea was not stable under these conditions, since the band intensity diminished over the time (**Figure 4 D**). After 8 hours the signal is only faintly visible. It is probable that the expression yielded in a fairly large quantity of target protein, but cellular proteases degraded IGF-I in this unprotected environment [34, 35]. Different approaches to overcome low yields of IGF-I in *E. coli* were described such as the fusion of the IGF-I gene with a truncated lacZ gene that encodes for  $\beta$ -galactosidase [36]. A hydroxylamine cleavage site

enabled the recovery of the mature IGF-I. A strong enhancement of the production of the IGF-I fusion protein in *E.coli* was achieved by coexpression of the genes that were significantly down-regulated after the induction of the target protein expression [37]. Another strategy for improved IGF-I fusion protein production was the suppression of cell filamentation by coexpression of two *E. coli* genes that are involved in cell division processes [38]. For optimization of the production and purification of IGF-I, it was also linked to LH through a methionine and cyanogen bromide degradation yielded in the mature IGF-I [34]. Furthermore, IGF-I was fused to a portion of interferon  $\gamma$  through a methionine and cleaved with cyanogen bromide [39] and the growth conditions were improved regarding the composition of the culture medium and its additives such as yeast, glucose and amino acids [40].

Another efficient system was developed by fusing IGF-I with an N-terminal extension of the first 46 amino acids of methionyl porcine GH and a dipeptide (Val-Asn). Cleavage was done at the Asn-Gly linkage using hydroxylamine [21]. The expression of IGF-I linked to a IgG-binding peptide had the advantage of a convenient protein purification using an IgG-Sepharose column [41, 42]. An alternative possibility for a successful IGF-I production was the usage of yeast [43, 44]. A common procedure to purify IGF-I is cation exchange chromatography [36, 39]. We achieved small signals in the chromatogram after CEX and an insufficient separation and yield of Plk-IGF-I-Ea. A well-established strategy for facilitated protein purification is the fusion of the protein with a polyhistidine-tag that enables affinity chromatography [45] and could also afford an opportunity for Plk-IGF-I-Ea. While we still have to focus – on an improvement on the yield and the purification of IGF-I, we have successfully expressed Plk-IGF-I-Ea and presumably of Plk-IGF-I for the first time.

## CONCLUSION

We engineered two different IGF-I mutants containing a pyrrolysine analogue (Plk) at two positions, respectively. The decoration with Plk provides the possibility of linking molecules through click reaction. The expression of IGF-I mutants was demonstrated by western blot and corroborated by mass spectrometry for Plk-IGF-I-Ea. Hence, we showed the feasibility of the production of IGF-I mutants, an important requirement for our innovative IGF-I delivery concept.

# REFERENCES

- [1] E. Rinderknecht, R.E. Humbel, The Amino Acid Sequence Of Human Insulin-Like Growth Factor I And Its Structural Homology With Proinsulin, *The Journal of biological chemistry*, 253 (1978) 2769-2776.
- [2] D.R. Clemmons, *Insulin-Like Growth Factors: Their Binding Proteins And Growth Regulation*, Lippincott Williams and Wilkins, 530 Walnut Street, Philadelphia, PA, 19106-3261, USA 2-6 Boundary Row, London, SE1 8HN, UK, 2000.
- [3] J.I. Jones, D.R. Clemmons, *Insulin-Like Growth-Factors And Their Binding-Proteins - Biological Actions*, *Endocrine Reviews*, 16 (1995) 3-34.
- [4] A. Philippou, M. Maridaki, S. Pneumaticos, M. Koutsilieris, The Complexity Of The IGF1 Gene Splicing, Posttranslational Modification And Bioactivity, *Molecular Medicine*, 20 (2014) 202-214.
- [5] D.J. Glass, *Modified IGF1 Polypeptides With Increased Stability And Potency*, in: US 7355018 B2, Regeneron Pharmaceuticals Inc, United States, 2008.
- [6] D.J. Glass, M. Fornaro, *Stabilized Insulin-Like Growth Factor Polypeptides*, in: WO2007141309 A3, Google Patents, United States, 2007.
- [7] S. Eger, M. Scheffner, A. Marx, M. Rubini, Formation Of Ubiquitin Dimers Via Azide-Alkyne Click Reaction, *Methods in molecular biology*, 832 (2012) 589-596.
- [8] W. Wan, J.M. Tharp, W.R. Liu, *Pyrolysyl-tRNA Synthetase: An Ordinary Enzyme But An Outstanding Genetic Code Expansion Tool*, *Biochimica et biophysica acta*, 1844 (2014) 1059-1070.
- [9] D.P. Nguyen, H. Lusic, H. Neumann, P.B. Kapadnis, A. Deiters, J.W. Chin, *Genetic Encoding and Labeling of Aliphatic Azides and Alkynes in Recombinant Proteins via a*

---

Pyrrolysyl-tRNA Synthetase/tRNA(CUA) Pair and Click Chemistry, *J. Am. Chem. Soc.*, 131 (2009) 8720-+.

[10] J.M. Harris, R.B. Chess, Effect Of Pegylation On Pharmaceuticals, *Nat. Rev. Drug Discov.*, 2 (2003) 214-221.

[11] F.M. Veronese, G. Pasut, Pegylation, Successful Approach To Drug Delivery, *Drug Discov. Today*, 10 (2005) 1451-1458.

[12] R.M. Cranenburgh, An Equation For Calculating The Volumetric Ratios Required In A Ligation Reaction, *Appl. Microbiol. Biotechnol.*, 65 (2004) 200-202.

[13] A. Vankimmenade, M.W. Bond, J.H. Schumacher, C. Laquoi, R.A. Kastelein, Expression, Renaturation And Purification Of Recombinant Human Interleukin-4 From *Escherichia-Coli*, *Eur. J. Biochem.*, 173 (1988) 109-114.

[14] B.K.O.N. Norbert D. Wangsa-Wirawan, \*,† and Anton P. J. Middelberg‡, Physicochemical Characteristics of LR3-IGF1 Protein Inclusion Bodies: Electrophoretic Mobility Studies, (2001).

[15] V. Neuhoff, N. Arold, D. Taube, W. Ehrhardt, Improved Staining Of Proteins In Polyacrylamide Gels Including Isoelectric-Focusing Gels With Clear Background At Nanogram Sensitivity Using Coomassie Brilliant Blue G-250 And R-250, *Electrophoresis*, 9 (1988) 255-262.

[16] M. Wilm, A. Shevchenko, T. Houthaeve, S. Breit, L. Schweigerer, T. Fotsis, M. Mann, Femtomole Sequencing Of Proteins From Polyacrylamide Gels By Nano-Electrospray Mass Spectrometry, *Nature*, 379 (1996) 466-469.

[17] E. Gasteiger, A. Gattiker, C. Hoogland, I. Ivanyi, R.D. Appel, A. Bairoch, ExPASy: the proteomics server for in-depth protein knowledge and analysis, *Nucleic Acids Res.*, 31 (2003) 3784-3788.

## CHAPTER IV

---

- [18] D.J. Glass, M. Fornaro, Stabilized Insulin-Like Growth Factor Polypeptides, in: US8343918 B2, Google Patents, United States, 2013.
- [19] A. Denley, L.J. Cosgrove, G.W. Booker, J.C. Wallace, B.E. Forbes, Molecular Interactions Of The IGF System, *Cytokine & growth factor reviews*, 16 (2005) 421-439.
- [20] D.J. Glass, G.D. Yancopoulos, T.J. Daly, N.J. Papadopoulos, IGF-I Fusion Polypeptides And Therapeutic Uses Thereof, in: US7396918 B2, Google Patents, United States, 2008.
- [21] R. King, J.R.E. Wells, P. Krieg, M. Snoswell, J. Brazier, C.J. Bagley, J.C. Wallace, F.J. Ballard, M. Ross, G.L. Francis, Production And Characterization Of Recombinant Insulin-Like Growth Factor-I (IGF-I) And Potent Analogs Of IGF-I, With Gly Or Arg Substituted For Glu3, Following Their Expression In Escherichia-Coli As Fusion Proteins, *Journal of Molecular Endocrinology*, 8 (1992) 29-41.
- [22] W.G. Zhang, T.A. Gustafson, W.J. Rutter, J.D. Johnson, Positively Charged Side-Chains In The Insulin-Like Growth-Factor-I C-Regions And D-Regions Determine Receptor-Binding Specificity, *Journal of Biological Chemistry*, 269 (1994) 10609-10613.
- [23] M. Sivaramakrishnan, A.S. Kashyap, B. Arnrein, S. Saenger, S. Meier, C. Staudenmaier, Z. Upton, F. Metzger, PEGylation Of Lysine Residues Reduces The Pro-Migratory Activity Of IGF-I, *Biochimica Et Biophysica Acta-General Subjects*, 1830 (2013) 4734-4742.
- [24] F. Metzger, W. Sajid, S. Saenger, C. Staudenmaier, C. van der Poel, B. Sobottka, A. Schuler, M. Sawitzky, R. Poirier, D. Tuerck, E. Schick, A. Schaubmar, F. Hesse, K. Amrein, H. Loetscher, G.S. Lynch, A. Hoeflich, P. De Meyts, H.J. Schoenfeld, Separation Of Fast From Slow Anabolism By Site-Specific Pegylation Of Insulin-Like Growth Factor I (IGF-I), *The Journal of biological chemistry*, 286 (2011) 19501-19510.

- 
- [25] M.L. Bayne, J. Applebaum, D. Underwood, G.G. Chicchi, B.G. Green, N.S. Hayes, M.A. Cascieri, The C-Region Of Human Insulin-Like Growth-Factor (IGF)-I Is Required For High-Affinity Binding To The Type-1 IGF Receptor, *Journal of Biological Chemistry*, 264 (1989) 11004-11008.
- [26] D.J. Glass, <Modified IGF1 polypeptides with increased stability and potency.pdf>, (2005).
- [27] D.J. Glass, M. Fornaro, Stabilized Insulin-like Growth Factor Polypeptides, in: Patent Application Publication US 2010/0234290 A1, NOVARTIS AG, United States, 2010.
- [28] F. Baneyx, M. Mujacic, Recombinant Protein Folding And Misfolding In Escherichia Coli, *Nat. Biotechnol.*, 22 (2004) 1399-1408.
- [29] D.L. Wilkinson, R.G. Harrison, Predicting The Solubility Of Recombinant Proteins In Escherichia-Coli, *Bio-Technology*, 9 (1991) 443-448.
- [30] W. Holmes, R. Smith, R. Bill, Evaluation Of Antifoams In The Expression Of A Recombinant Fc Fusion Protein In Shake Flask Cultures Of Saccharomyces Cerevisiae & Pichia Pastoris, *Microb. Cell. Fact.*, 5 (2006).
- [31] S.J. Routledge, C.J. Hewitt, N. Bora, R.M. Bill, Antifoam Addition To Shake Flask Cultures Of Recombinant Pichia Pastoris Increases Yield, *Microb. Cell. Fact.*, 10 (2011) 11.
- [32] S.J. Routledge, R.M. Bill, The effect of antifoam addition on protein production yields, *Methods in molecular biology* (Clifton, N.J.), 866 (2012) 87-97.
- [33] F.W. Studier, Protein Production By Auto-Induction In High-Density Shaking Cultures, *Protein expression and purification*, 41 (2005) 207-234.
- [34] Y. Saito, H. Yamada, M. Niwa, I. Ueda, Production And Isolation Of Recombinant Somatomedin-C, *Journal of Biochemistry*, 101 (1987) 123-134.

- [35] G. Buell, M.F. Schulz, G. Selzer, A. Chollet, N.R. Movva, D. Semon, S. Escanez, E. Kawashima, Optimizing The Expression In Escherichia-Coli Of A Synthetic Gene Encoding Somatomedin-C (IGF-I), *Nucleic Acids Res.*, 13 (1985) 1923-1938.
- [36] S.O. Kim, Y.I. Lee, High-Level Expression And Simple Purification Of Recombinant Human Insulin-Like Growth Factor I, *Journal of biotechnology*, 48 (1996) 97-105.
- [37] J.H. Choi, S.J. Lee, S.J. Lee, S.Y. Lee, Enhanced Production of Insulin-Like Growth Factor I Fusion Protein in Escherichia coli by Coexpression of the Down-Regulated Genes Identified by Transcriptome Profiling, *Applied and Environmental Microbiology*, 69 (2003) 4737-4742.
- [38] K.J. Jeong, S.Y. Lee, Enhanced production of recombinant proteins in Escherichia coli by filamentation suppression, *Applied and Environmental Microbiology*, 69 (2003) 1295-1298.
- [39] H. Yamada, Y. Saito, T. Fujimoto, Y. Noguchi, T. Mori, T. Miura, M. Kobayashi, K. Shimomura, Large Scale Purification Of Recombinant Insulin-Like Growth Factor I (IGF-I, Mecasermin) From A Fused Protein Produced In Escherichia Coli, *Journal of Fermentation and Bioengineering*, 82 (1996) 134-139.
- [40] S.S. Y. Noguchi, M. Yamaguchi, K. Watanabe, M. Hayashi, H. Yamada, Y. Saito, M. Kobayashi, K. Shimomura, An approach to high-level production of a mecasein (somatomedin C) fused protein in Escherichia coli HB101, (1996).
- [41] T. Moks, L. Abrahmsen, E. Holmgren, M. Bilich, A. Olsson, M. Uhlen, G. Pohl, C. Sterky, H. Hultberg, S. Josephson, A. Holmgren, H. Jornvall, B. Nilsson, Expression Of Human Insulin-Like Growth Factor-I In Bacteria - Use Of Optimized Gene Fusion Vectors To Facilitate Protein-Purification, *Biochemistry*, 26 (1987) 5239-5244.
- [42] G. Forsberg, G. Palm, A. Ekebacke, S. Josephson, M. Hartmanis, Separation And Characterization Of Modified Variants Of Recombinant Human Insulin-Like Growth Factor-I



Derived From A Fusion Protein Secreted From Escherichia-Coli, *Biochemical Journal*, 271 (1990) 357-363.

[43] M.L. Bayne, J. Applebaum, G.G. Chicchi, N.S. Hayes, B.G. Green, M.A. Cascieri, Expression, Purification And Characterization Of Recombinant Human Insulin-Like Growth Factor-I In Yeast, *Gene*, 66 (1988) 235-244.

[44] P. Gellerfors, K. Axelsson, A. Helander, S. Johansson, L. Kenne, S. Lindqvist, B. Pavlu, A. Skottner, L. Fryklund, Isolation And Characterization Of A Glycosylated Form Of Human Insulin-Like Growth Factor-I Produced In *Saccharomyces-Cerevisiae*, *Journal of Biological Chemistry*, 264 (1989) 11444-11449.

[45] E. Hochuli, W. Bannwarth, H. Dobeli, R. Gentz, D. Stuber, Genetic Approach To Facilitate Purification Of Recombinant Proteins With A Novel Metal Chelate Adsorbent, *Bio-Technology*, 6 (1988) 1321-1325.



## **CONCLUSION AND OUTLOOK**

IGF-I is an influential and versatile growth factor and a forceful stimulator of protein synthesis [1, 2]. Consequently, a benefit of IGF-I treatment is indicated in many different diseases such as muscle atrophy, growth failure, cartilage lesions, fracture repair, osteoporosis or neurodegenerative disorders [3-11]. The therapy can be carried out both locally or systemically. Systemic administration is typically performed by means of subcutaneous injections that are already available commercially (e.g. Increlex) [12]. Localized IGF-I delivery is favoured in the field of tissue engineering or fracture repair. For this purpose, depot dosage forms are preferably applied avoiding frequent administrations and overcoming the challenge of the short half-life of free IGF-I [1, 13]. Depot delivery systems such as implants or microparticles have been reported releasing IGF-I over several days and it may be assumed that constant and efficient plasma levels can be achieved bypassing peaks and strong side effects such as severe hypoglycaemia using these IGF-I delivery systems. Microparticles based on PLGA or the biopolymer silk-fibroin have been widely used for successful IGF-I delivery [3, 5, 7-10, 14-16]. Also immediate IGF-I delivery systems have been developed for administration via the pulmonary route [17]. Hence, different routes of administration and various delivery systems for IGF-I, solid and liquid dosage forms are summarized in this work. We outline advice regarding formulation and process parameters (e.g. pH, buffer, excipients) for stable and efficient IGF-I delivery systems. In addition, IGF-I delivered in a complex with IGFBP-3 (Iplex) was a successful approach to reduce the administration to a single dose once a day [18, 19]. Interesting biotechnological modifications such as PEGylation [20-24] or the extension of IGF-I with an E-peptide, as it is naturally expressed, improved the pharmacokinetic properties of IGF-I as for instance demonstrated by a prolonged half-life of IGF-I in the blood circulation [25]. Furthermore, IGF-I decoration was instrumental to achieve IGF-I targeting to certain tissues [26, 27]. Briefly, we review different strategies of IGF-I modification and decoration showing an improved pharmacokinetic pattern of IGF-I.

This PhD thesis also demonstrates the suitability of IGF-I for pulmonary delivery [6, 17]. We developed liquid IGF-I formulations preserving IGF-I integrity over several months and revealing beneficial nebulization performances. Nebulization of aqueous solutions is a common procedure to deliver proteins to the deeper regions in the lung. The droplet size was a decisive

## CONCLUSION AND OUTLOOK

---

factor for a successful deposition and greatly influenced by formulation parameters and nebulizers [28]. The nebulization of IGF-I formulated in 50 mM histidine buffer and 150 mM NaCl at pH 6.5 using an air-jet or a vibrating-mesh nebulizer was comparable with the nebulization of a 0.9% sodium chloride reference regarding fine particle fraction, mass median aerodynamic diameter, and aerosol output rate. Proteins may be harmed by air jet or ultrasonic nebulizer, but we did not detect formation of covalent aggregates in non-reducing SDS-PAGE after the nebulization, respectively. However, a slight increase in oxidized IGF-I was observed after the experiment regardless of the device used. All in all, the data suggested that the delivery through this mode of administration is feasible. The stability testing of liquid IGF-I formulations varying in buffer type, sodium chloride concentration (50 – 150 mM) and pH value (4.5 – 6.5) showed that IGF-I integrity was influenced by the buffer type. Furthermore Met(o) IGF-I formation along with reducible dimers and trimers were observed in acetate buffer after 4 month storage and the formation of aggregates was more pronounced at low pH value. Accordingly, a loss of IGF-I bioactivity was assessed under these conditions. However, IGF-I stability and bioactivity was fully preserved in histidine buffer over the entire pH range. The stability testing should be expanded to defined conditions regarding temperature and humidity and over a prolonged time period. In addition, further tests have to be performed to make a clear statement of the lung deposition of IGF-I in humans, but the experiments that have already been done, encouraged us to follow up on the strategy of pulmonary IGF-I delivery. Thus, in the third chapter of this thesis *in vitro* transport of IGF-I through a lung epithelial cell monolayer (Calu-3 model) was studied and resulted in kinetics comparable with insulin that was already successfully applied via the pulmonary route. Furthermore, we embedded IGF-I in microparticles based on both trehalose and silk-fibroin by nano spray drying. Trehalose is a well-established excipient in spray drying and pulmonary protein delivery. It has low chemical reactivity, a high glass transition and is not hygroscopic [29]. Additionally it shows advantageous properties in aerolization of dry powder, associated with an increased fine particle fraction [29]. Silk-fibroin is a protein polymer and a favored carrier for drug delivery owing to its properties as biocompatibility and biodegradability [30, 31]. Furthermore we have the possibility to embed sensitive growth factors into silk-fibroin under mild and aqueous conditions. Silk-fibroin is widely used and well-studied for several biomedical applications. It has extensively been reported that silk-fibroin stabilized formulations with sensitive biologics as for instance the

preservation of integrity of growth factors, particularly IGF-I. Hence, we decided to evaluate the potential of silk-fibroin to deliver IGF-I through the lung and in comparison to the common excipient trehalose. Both kinds of microparticles possessed shapes and properties allowing alveolar deposition as demonstrated by next generation impactor measurements. IGF-I integrity was completely maintained in trehalose microparticles including the antioxidant methionine. IGF-I was also protected in silk-fibroin (no methionine was added) except for a slight oxidation. Silk-fibroin microparticles were further analyzed by FTIR and XRPD regarding crystallinity and by DVS. However, other analytical techniques for the characterization of silk-fibroin are needed for a better understanding of interactions between silk-fibroin and IGF-I to clarify for instance the lower loading or outcome of IGF-I during release compared to IGF-I/trehalose microparticles. The systemic availability of IGF-I after pulmonary application was demonstrated in an *ex vivo* human lung lobe model. The use of both carriers, trehalose or silk-fibroin, resulted in identical uptake kinetics of IGF-I through the epithelial barrier of the lung into the blood circulation. This work shows the promising potential of IGF-I for pulmonary delivery and the option of silk-fibroin for pulmonary use. However, *in vivo* studies have to be performed in the future, since the deposition of the drug is also influenced by the anatomy of the respiratory tract (e.g. mouth cavity, epiglottis, and pharynx) and the consistency of mucosa [32]. Similarly, toxicological studies are unavoidable to clarify that there are no harmful effects of IGF-I on the lung tissue or interference with the natural IGF-I signaling in the lung.

In the last part of the thesis, the focus was shifted from solutions or carriers with dissolved or physically absorbed IGF-I to advanced IGF-I analogues allowing for a site specific decoration at predetermined sites within the biologic. Thereby, polymers modulating the pharmacokinetics could be site specifically tagged to IGF-I, resulting in homogenous product outcome and an overall improvement of pharmaceutical quality standards. Therefore, we followed another interesting approach for IGF-I delivery through the targeted decoration of IGF-I by engineering an IGF-I variant including a pyrrolysine analogue (Plk) and thereby introducing an alkyne function. This modification provides the opportunity to link IGF-I with other molecules possessing an azido group following a Cu (I) catalyzed (Huisgen azide-alkyne cycloaddition) strategy yielding a decoration in a site-specific manner [33-37]. As demonstrated by western blot and mass spectrometry, we expressed an IGF-I variant containing Plk on two different positions of the protein sequence and with improved pharmacokinetic properties. These promising results

## CONCLUSION AND OUTLOOK

---

indicated, that IGF-I analogues with the desired functionality may be obtained through genetic engineering. However, the work is still at a preliminary state. Further work is to be devoted for the optimization to up- and downstream processes alike with the ultimate goal to increase the protein yield. Afterwards Plk-IGF-I can be linked with other molecules or surfaces such as cells or implants. The immobilization of growth factors is an attractive strategy for tissue repair and regeneration [38]. Another promising approach is the PEGylation via click reaction using an azido-PEG polymer. This site-specific PEGylation results in strictly homogenous conjugated products. Furthermore, a bioresponsive (e.g. protease sensitive) linker could be placed between the biologic and the polymer. Providing an upregulated protease can serve as a reliable proxy for a disease flare, systemically given “IGF-I – bioresponsive linker – PEG” conjugates shuttle to the site of need, at which these are effectively cleaved by the target protease. Thereby, IGF-I is liberated from the complex and exerting its anabolic role in a strictly confined manner. Such targeted IGF-I delivery deploying bioresponsive linkers form an attractive strategy, since inflammatory diseases are usually associated with upregulated protease activity. Thus, the linker get selectively cleaved by proteases such as matrix metalloproteinase (MMP-8) and the active form of IGF-I is released locally from the conjugate. Thereby, active IGF-I is located to the seat of the disease while otherwise shuttling systemically as part of the conjugate. Plk-IGF-I can also be connected with other biopharmaceutics via protease sensitive or otherwise cleavable linkers. An interesting option is the conjunction of Plk-IGF-I and a myostatin antagonist, possibly in terms of a necklace. Using this strategy combines the anabolic effect of IGF-I and the anti-catabolic effect of a myostatin antagonist and may result in an enhanced and synergistic activity, e.g. in sarcopenia. Certainly, the bioactivity of IGF-I after the incorporation of the two Plks and after the click reaction and protease cleavage has to be demonstrated. Similarly, we have to focus on the accomplishment and selectivity of the click reaction and cleavage of the linker by proteases. Furthermore different ratios of the participating biopharmaceutics have to be analysed to find appropriate conditions for the click reaction and following therapeutic effect. Therefore, the performance of *in vivo* studies is absolutely essential following thorough *in vitro* characterisation. It might also be the question whether free alkyne groups are able to react with other groups in the human bodies and induce thereby harmful effects, e.g. nucleophilic thiol groups of cysteines. In this thesis we laid the first stone for an innovative IGF-I delivery system

by demonstrating feasibility of the expression of Plk-IGF-I using E.coli, but still much work has to be done for the implementation of this strategy and to answer the arising questions.

In conclusion, in this thesis we demonstrate various strategies for IGF-I delivery and contribute to a better knowledge of a successful and safe IGF-I therapy. IGF-I was aerolized for pulmonary use and, extending from these studies, advanced particle carriers with physically entrapped IGF-I were developed and characterized. Lastly, novel IGF-I analogues with functional groups at specific sites of the primary sequence were genetically engineered, which are primed for covalent coupling of polymers, to surfaces, or of other molecules with unmatched spatial control.

## REFERENCES

- [1] J.I. Jones, D.R. Clemmons, Insulin-Like Growth-Factors And Their Binding-Proteins - Biological Actions, *Endocrine Reviews*, 16 (1995) 3-34.
- [2] D.R. Clemmons, Metabolic Actions Of Insulin-Like Growth Factor-I In Normal Physiology And Diabetes, *Endocrinol. Metabol. Clin. North Amer.*, 41 (2012) 425-+.
- [3] V. Luginbuehl, E. Zoidis, L. Meinel, B. von Rechenberg, B. Gander, H.P. Merkle, Impact Of IGF-I Release Kinetics On Bone Healing: A Preliminary Study In Sheep, *European journal of pharmaceutics and biopharmaceutics : official journal of Arbeitsgemeinschaft fur Pharmazeutische Verfahrenstechnik e.V.*, 85 (2013) 99-106.
- [4] V. Luginbuehl, E. Wenk, A. Koch, B. Gander, H.P. Merkle, L. Meinel, Insulin-Like Growth Factor I-Releasing Alginate-Tricalciumphosphate Composites For Bone Regeneration, *Pharmaceutical research*, 22 (2005) 940-950.
- [5] L. Meinel, E. Zoidis, J. Zapf, P. Hassa, M.O. Hottiger, J.A. Auer, R. Schneider, B. Gander, V. Luginbuehl, R. Bettschart-Wolfisberger, O.E. Illi, H.P. Merkle, B.v. Rechenberg, Localized Insulin-Like Growth Factor I Delivery To Enhance New Bone Formation, *Bone*, 33 (2003) 660-672.
- [6] O. Germershaus, I. Schultz, T. Luhmann, M. Beck-Broichsitter, P. Hogger, L. Meinel, Insulin-Like Growth Factor-I Aerosol Formulations For Pulmonary Delivery, *European journal of pharmaceutics and biopharmaceutics : official journal of Arbeitsgemeinschaft fur Pharmazeutische Verfahrenstechnik e.V.*, 85 (2013) 61-68.
- [7] E. Wenk, A.J. Meinel, S. Wildy, H.P. Merkle, L. Meinel, Microporous Silk Fibroin Scaffolds Embedding PLGA Microparticles For Controlled Growth Factor Delivery In Tissue Engineering, *Biomaterials*, 30 (2009) 2571-2581.



- [8] X. Wang, E. Wenk, X. Zhang, L. Meinel, G. Vunjak-Novakovic, D.L. Kaplan, Growth Factor Gradients Via Microsphere Delivery In Biopolymer Scaffolds For Osteochondral Tissue Engineering, *Journal of controlled release : official journal of the Controlled Release Society*, 134 (2009) 81-90.
- [9] L. Uebersax, H.P. Merkle, L. Meinel, Insulin-Like Growth Factor I Releasing Silk Fibroin Scaffolds Induce Chondrogenic Differentiation Of Human Mesenchymal Stem Cells, *Journal of controlled release : official journal of the Controlled Release Society*, 127 (2008) 12-21.
- [10] L. Meinel, O.E. Illi, J. Zapf, M. Malfanti, H.P. Merkle, B. Gander, Stabilizing Insulin-Like Growth Factor-I In Poly(D,L-Lactide-Co-Glycolide) Microspheres, *Journal of Controlled Release*, 70 (2001) 193-202.
- [11] S. Perrini, L. Laviola, M.C. Carreira, A. Cignarelli, A. Natalicchio, F. Giorgino, The GH/IGF1 Axis And Signaling Pathways In The Muscle And Bone: Mechanisms Underlying Age-Related Skeletal Muscle Wasting And Osteoporosis, *Journal of Endocrinology*, 205 (2010) 201-210.
- [12] [http://www.ema.europa.eu/docs/en\\_GB/document\\_library/EPAR\\_-\\_Product\\_Information/human/000704/WC500032225.pdf](http://www.ema.europa.eu/docs/en_GB/document_library/EPAR_-_Product_Information/human/000704/WC500032225.pdf).
- [13] H.P. Guler, J. Zapf, C. Schmid, E.R. Froesch, Insulin-Like Growth Factor-I And Factor-II In Healthy Man - Estimations Of Half-Lives And Production-Rates, *Acta Endocrinologica*, 121 (1989) 753-758.
- [14] A. Clark, T.A. Milbrandt, J.Z. Hilt, D.A. Puleo, Retention Of Insulin-Like Growth Factor I Bioactivity During The Fabrication Of Sintered Polymeric Scaffolds, *Biomedical Materials*, 9 (2014).

## CONCLUSION AND OUTLOOK

---

- [15] M. Singh, B. Shirley, K. Bajwa, E. Samara, M. Hora, D. O'Hagan, Controlled Release Of Recombinant Insulin-Like Growth Factor From A Novel Formulation Of Polylactide-Co-Glycolide Microparticles, *Journal of Controlled Release*, 70 (2001) 21-28.
- [16] E. Wenk, A.J. Wandrey, H.P. Merkle, L. Meinel, Silk Fibroin Spheres As A Platform For Controlled Drug Delivery, *Journal of controlled release : official journal of the Controlled Release Society*, 132 (2008) 26-34.
- [17] I. Schultz, F. Vollmers, T. Lühmann, J.-C. Rybak, R. Wittmann, K. Stank, H. Steckel, B. Kardziej, M. Schmidt, P. Högger, L. Meinel, Pulmonary Insulin-Like Growth Factor I Delivery From Trehalose And Silk-Fibroin Microparticles, *ACS Biomaterials Science & Engineering*, (2015) 150129161644009.
- [18] R.M. Williams, A. McDonald, M. O'Savage, D.B. Dunger, Mecasermin Rinfabate: RhIGF-I/RhIGFBP-3 Complex: Iplex (TM), *Expert Opinion on Drug Metabolism & Toxicology*, 4 (2008) 311-324.
- [19] S.F. Kemp, K.M. Thrailkill, Investigational Agents For The Treatment Of Growth Hormone-Insensitivity Syndrome, *Expert Opin. Investig. Drugs*, 15 (2006) 409-415.
- [20] F. Metzger, W. Sajid, S. Saenger, C. Staudenmaier, C. van der Poel, B. Sobottka, A. Schuler, M. Sawitzky, R. Poirier, D. Tuerck, E. Schick, A. Schaubmar, F. Hesse, K. Amrein, H. Loetscher, G.S. Lynch, A. Hoeflich, P. De Meyts, H.J. Schoenfeld, Separation Of Fast From Slow Anabolism By Site-Specific Pegylation Of Insulin-Like Growth Factor I (IGF-I), *The Journal of biological chemistry*, 286 (2011) 19501-19510.
- [21] F. Metzger, W. Sajid, S. Saenger, C. Staudenmaier, C. van der Poel, B. Sobottka, A. Schuler, M. Sawitzky, R. Poirier, D. Tuerck, E. Schick, A. Schaubmar, F. Hesse, K. Amrein, H. Loetscher, G.S. Lynch, A. Hoeflich, P. De Meyts, H.J. Schoenfeld, Separation Of Fast From

Slow Anabolism By Site-Specific Pegylation Of Insulin-Like Growth Factor I (IGF-I), *Journal of Biological Chemistry*, 286 (2011) 19501-19510.

[22] S. Saenger, B. Holtmann, M.R. Nilges, S. Schroeder, A. Hoeflich, H. Kletzl, W. Spooren, S. Ostrowitzki, T. Hanania, M. Sendtner, F. Metzger, Functional Improvement In Mouse Models Of Familial Amyotrophic Lateral Sclerosis By PEGylated Insulin-Like Growth Factor I Treatment Depends On Disease Severity, *Amyotroph. Lateral. Scler.*, 13 (2012) 418-429.

[23] K.J. Martins, S.M. Gehrig, T. Naim, S. Saenger, D. Baum, F. Metzger, G.S. Lynch, Intramuscular Administration Of PEGylated IGF-I Improves Skeletal Muscle Regeneration After Myotoxic Injury, *Growth hormone & IGF research : official journal of the Growth Hormone Research Society and the International IGF Research Society*, 23 (2013) 128-133.

[24] M. Sivaramakrishnan, A.S. Kashyap, B. Arnrein, S. Saenger, S. Meier, C. Staudenmaier, Z. Upton, F. Metzger, PEGylation Of Lysine Residues Reduces The Pro-Migratory Activity Of IGF-I, *Biochimica Et Biophysica Acta-General Subjects*, 1830 (2013) 4734-4742.

[25] D.J. Glass, M. Fornaro, Stabilized Insulin-like Growth Factor Polypeptides, in: Patent Application Publication US 2010/0234290 A1, NOVARTIS AG, United States, 2010.

[26] R.S. Khan, M.D. Martinez, J.C. Sy, K.D. Pendergrass, P.-l. Che, M.E. Brown, E.B. Cabigas, M. Dasari, N. Murthy, M.E. Davis, Targeting Extracellular DNA To Deliver IGF-1 To The Injured Heart, *Scientific Reports*, 4 (2014).

[27] F.S. Loffredo, J.R. Pancoast, L. Cai, T. Vannelli, J.Z. Dong, R.T. Lee, P. Patwari, Targeted Delivery To Cartilage Is Critical For In Vivo Efficacy Of Insulin-Like Growth Factor 1 In A Rat Model Of Osteoarthritis, *Arthritis & Rheumatology*, 66 (2014) 1247-1255.

[28] H. Steckel, F. Eskandar, Factors Affecting Aerosol Performance During Nebulization With Jet And Ultrasonic Nebulizers, *Eur. J. Pharm. Sci.*, 19 (2003) 443-455.

## CONCLUSION AND OUTLOOK

---

- [29] X. Li, H.M. Mansour, Physicochemical Characterization and Water Vapor Sorption of Organic Solution Advanced Spray-Dried Inhalable Trehalose Microparticles and Nanoparticles for Targeted Dry Powder Pulmonary Inhalation Delivery, *Aaps Pharmscitech*, 12 (2011) 1420-1430.
- [30] S. Hofmann, C.T. Foo, F. Rossetti, M. Textor, G. Vunjak-Novakovic, D.L. Kaplan, H.P. Merkle, L. Meinel, Silk Fibroin As An Organic Polymer For Controlled Drug Delivery, *Journal of controlled release : official journal of the Controlled Release Society*, 111 (2006) 219-227.
- [31] E. Wenk, H.P. Merkle, L. Meinel, Silk Fibroin As A Vehicle For Drug Delivery Applications, *Journal of controlled release : official journal of the Controlled Release Society*, 150 (2011) 128-141.
- [32] H.C. Yeh, R.F. Phalen, O.G. Raabe, Factors Influencing Deposition Of Inhaled Particles, *Environ. Health Perspect.*, 15 (1976) 147-156.
- [33] S. Eger, M. Scheffner, A. Marx, M. Rubini, Formation Of Ubiquitin Dimers Via Azide-Alkyne Click Reaction, *Methods in molecular biology*, 832 (2012) 589-596.
- [34] V.D. Bock, H. Hiemstra, J.H. van Maarseveen, Cu-I-catalyzed alkyne-azide "click" cycloadditions from a mechanistic and synthetic perspective, *Eur. J. Org. Chem.*, (2006) 51-68.
- [35] J.F. Lutz, 1,3-dipolar cycloadditions of azides and alkynes: A universal ligation tool in polymer and materials science, *Angew. Chem.-Int. Edit.*, 46 (2007) 1018-1025.
- [36] J.E. Moses, A.D. Moorhouse, The Growing Applications Of Click Chemistry, *Chem. Soc. Rev.*, 36 (2007) 1249-1262.
- [37] D.P. Nguyen, H. Lusic, H. Neumann, P.B. Kapadnis, A. Deiters, J.W. Chin, Genetic Encoding and Labeling of Aliphatic Azides and Alkynes in Recombinant Proteins via a

Pyrrolysyl-tRNA Synthetase/tRNA(CUA) Pair and Click Chemistry, *J. Am. Chem. Soc.*, 131 (2009) 8720-+.

[38] K.S. Masters, Covalent Growth Factor Immobilization Strategies For Tissue Repair And Regeneration, *Macromol. Biosci.*, 11 (2011) 1149-1163.



## DOCUMENTATION OF AUTHORSHIP

This section contains a list of the individual contribution for each author to the publications reprinted in this thesis. Unpublished manuscripts are handled, accordingly.

<b>P1</b>	<b>Germershaus O, Schultz I, Lühmann T, Beck-Broichsitter M, Högger P, Meinel L (2013) Insulin-like Growth Factor-I aerosol formulation for pulmonary delivery. European Journal of Pharmaceutics and Biopharmaceutics 85: 61-68</b>					
<b>Author</b>	<b>1</b>	<b>2</b>	<b>3</b>	<b>4</b>	<b>5</b>	<b>6</b>
Sample preparation and stability study		X				
Determination of IGF-I content and purity		X				
Reducing and non-reducing SDS-PAGE		X				
IGF-I bioassay		X				
Nebulization experiments	X	X		X		
Statistical analysis	X	X				X
Study design/concept development	X	X	X		X	X
Data analysis and interpretation	X	X	X	X	X	X
Manuscript planning	X	X			X	X
Manuscript writing	X	X			X	X
Correction of manuscript	X				X	X
Supervision of Isabel Schultz						X

<b>P2</b>	<b>Schultz I, Vollmers F, Lühmann T, Rybak J-C, Wittmann R, Stank K, Steckel H, Kardziev B, Schmidt M, Högger P, Meinel L (2015) Pulmonary Insulin-like Growth Factor I Delivery from Trehalose and Silk-Fibroin Microparticles. ACS Biomaterials Science &amp; Engineering 1: 119-129</b>										
<b>Author</b>	<b>1</b>	<b>2</b>	<b>3</b>	<b>4</b>	<b>5</b>	<b>6</b>	<b>7</b>	<b>8</b>	<b>9</b>	<b>10</b>	<b>11</b>
Silk-Fibroin processing	X										
IGF-I purification	X										
IGF-I microparticle preparation and physical characterization	X										
Aerodynamic properties of spray-dried microparticles	X					X					
DVS of SF microparticles					X						
Wide-angle X-ray scattering (WAXS)	X			X							
IGF-I microparticle visualization	X										
Determination of IGF-I content and purity	X										

## DOCUMENTATION OF AUTHORSHIP

IGF-I bioassay and transepithelial transport	X	X	X								
Human lung perfusion model		X									
Study design/concept development	X	X					X	X	X	X	X
Data analysis and interpretation	X	X								X	X
Manuscript planning	X									X	X
Manuscript writing	X	X								X	X
Correction of manuscript										X	X
Supervision of Isabel Schultz											X

<b>P3</b>	<b>Schultz I, Wurzel J, Meinel L (2015) Drug delivery of Insulin-like Growth Factor-I. European Journal of Pharmaceutics and Biopharmaceutics, in press</b>		
<b>Author</b>	<b>1</b>	<b>2</b>	<b>3</b>
Manuscript planning	X		X
Manuscript writing	X		X
Design of the graphics	X	X	
Correction of manuscript			X
Supervision of Isabel Schultz			X

	<b>Schultz I, Meinel L Expression of IGF-I mutants, unpublished</b>	
<b>Author</b>	<b>1</b>	<b>2</b>
Subcloning	X	
Plk synthesis	X	
Protein expression	X	
Inclusion body purification	X	
SDS-PAGE	X	
Western blot	X	
Protein purification	X	
Study design/concept development	X	X
Data analysis and interpretation	X	X
Manuscript planning	X	X
Manuscript writing	X	X
Correction of manuscript		X
Supervision of Isabel Schultz		X



**Erklärung zu den Eigenanteilen des Doktoranden sowie der weiteren Doktoranden als Koautoren an Publikationen und Zweitpublikationsrechten bei einer kumulativen Dissertation.**

Für alle in dieser kumulativen Dissertation verwendeten Manuskripte liegen die notwendigen Genehmigungen der Verlage („reprint permission“) für die Zweitpublikation vor, außer das betreffende Kapitel ist noch gar nicht publiziert. Dieser Umstand wird einerseits durch die genaue Angabe der Literaturstelle der Erstpublikation auf der ersten Seite des betreffenden Kapitels deutlich gemacht oder die bisherige Nichtveröffentlichung durch den Vermerk „unpublished“ oder „nicht veröffentlicht“ gekennzeichnet.

Die Mitautoren der in dieser kumulativen Dissertation verwendeten Manuskripte sind sowohl über die Nutzung als auch über die oben angegebenen Eigenanteile informiert.

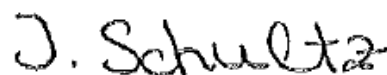
Die Beiträge der Mitautoren an den Publikationen sind in den vorausgehenden Tabellen aufgeführt.

Würzburg, Mai 27th, 2015



(Prof. Dr. Dr. Lorenz Meinel)

Würzburg, Mai 27th, 2015



(Isabel Schultz)



# CURRICULUM VITAE

*Isabel Schultz*

*born December 1, 1982 in Dahn, Germany*

## EDUCATION

Since 2015

**Post doc**

Abbvie GmbH & Co. KG

NCE formulation sciences

Since 2011

**Postgraduate training**

Fachapotheker für Pharmazeutische Technologie

2011-2015

**PhD candidate**

Chair of Pharmaceutics and Biopharmacy

Director Prof. Dr. Dr. Lorenz Meinel

University of Würzburg

2010

**Pharmacist license**

2005-2010

**Study of Pharmacy**

Johannes Gutenberg University Mainz

State examination

2002-2005

**Pharmacy technician**

Naturwissenschaftliches Technikum Dr. Künkele

Landau

1993-2002

Otfried-von-Weißenburg-Gymnasium Dahn

A level

## SCIENTIFIC CONTRIBUTIONS

### *Journal contributions*

**Schultz I**, Wurzel J, Meinel L (2015). Drug delivery of Insulin-like Growth Factor-I. European Journal of Pharmaceutics and Biopharmaceutics, in press

**Schultz I**, Vollmers F, Lühmann T, Rybak J-C, Wittmann R, Stank K, Steckel H, Kardziej B, Schmidt M, Högger P, Meinel L (2015). Pulmonary Insulin-like Growth Factor I Delivery from Trehalose and Silk-Fibroin Microparticles. ACS Biomaterials Science & Engineering **1**: 119-129.

Germershaus O, **Schultz I**, Lühmann T, Beck-Broichsitter M, Högger P, Meinel L (2013). Insulin-like Growth Factor-I aerosol formulation for pulmonary delivery. European Journal of Pharmaceutics and Biopharmaceutics **85**: 61-68.

### *Oral and poster presentations/workshop*

Schultz, I. et al. Pharmaceutical development of Insulin-like growth factor-I delivery systems. **Fraunhofer-Institute**, Stuttgart, 2014.

Schultz I. et al. Dry powder formulations for pulmonary IGF-I delivery. **Controlled Release Society** – Germany local chapter, Kiel, Germany, 2014.

**2<sup>nd</sup> Galenus workshop** 2013: Pulmonary Drug Delivery, Dublin, Irland, 2013.

Schultz I. Silk fibroin as a vehicle for pulmonary drug delivery of IGF-I. **North-Bavaria Biomaterials Alliance**, Würzburg, Germany, 2013 (oral).

Schultz I. et al. Dry powder for pulmonary IGF-I administration deploying silk-fibroin. **North-Bavaria Biomaterials Alliance**, Würzburg, Germany, 2013 .

Schultz I. et al. Development and stability assessment of Insulin like Growth Factor-I formulation for pulmonary drug delivery. **Controlled Release Society – Germany local chapter**, Ludwigshafen, Germany, 2013.

Schultz I. et al. Development of a liquid formulation of Insulin-like growth factor-I for pulmonary application. **Chemie-Symposium der Studierenden Mainfrankens**, Würzburg, Germany, 2012.

**Controlled Release Society – Germany local chapter**, Würzburg, Germany, 2012.



## ACKNOWLEDGMENTS

My sincerest thank is meant to Prof. Dr. Dr. Lorenz Meinel for the opportunity to perform my thesis in his group. Throughout my doctorate, I was attended by his valuable and wide scientific skills, his encouragement, helpful guidance and constructive feedback. Furthermore he provided a great laboratory equipment in the group.

I thank Prof. Dr. Sottriffer and Prof. Dr. Högger for being my referee. Additionally, I am very grateful to Prof. Dr. Högger and Frederic Vollmers for their contributions to chapter II/III and the great cooperation. I thank Prof. Dr. Steckel, Dr. Katharina Stank and Dr. Ronja Wittman for their support concerning NGI and DVS experiments, Dr. Vladimir Stephanenko for the SEM and AFM measurements and Dr. Werner Schmitz for the mass spectrometry measurements. I really appreciate the help of Prof Dr. Oliver Germershaus, especially in chapter II. My gratitude is also directed to Dr. Tessa Lühmann for her kind assistance.

I am very grateful to all my colleagues of the group and particularly Gabriel Jones for the mutual support and inspiring conversations.

Finally, I thank my mother Dagmar, my sister Katharina and my brother Matthias for constant caring.